UNIVERSITÄT ZU LÜBECK

From the Institute of Nutritional Medicine
of the University of Lübeck
Director: Prof. Dr. Christian Sina

Regulation of the alpha2,6-sialyltransferase and IgG Fc glycosylation in immunization-induced germinal center reactions

Dissertation
for Fulfillment of
the Requirements
for the Doctoral Degree
of the University Lübeck

From the Department of Natural Science

Submitted by
Hanna Bele Lunding
from Henstedt-Ulzburg

Lübeck 2021

First referee: Prof. Dr. Marc Ehlers

Second referee: PD Dr. Kai-Uwe Kalies

Date of oral examination: February 2, 2022

Approved for printing: Lübeck, February 9, 2022

I List of content

II List of figures

III List of tables

IV List of abbreviations

Abs	antibodies
AF488	Alexa Fluor 488
AF647	Alexa Fluor 647
AF700	Alexa Fluor 700
AID	Activation-induced cytidine deaminase
APC	antigen presenting cell
Asn-297	Asparagine 297
BCR	B cell receptor
BSA	Bovine serum albumin
BV421	Brilliant violet 421
BV786	Brilliant violet 786
CFA	complete Freunds adjuvant
CTLA-4	cytotoxic T-lymphocyte-associated protein 4
CNBr	Cyanogen bromide
dKO	double knock-out
DZ	dark zone
eCFA	enriched complete Freunds adjuvant
F	Fucose, fucosylated residue
Fab	Fragment antigen-binding
Fc	Fragment crystallizable
FDC	Follicular dendritic cell
G	Galactose, galactosylated residue
G0	agalctosylated residue
HIV	Human immune-deficiency virus
HRP	Horse radish peroxidase
IC	Immune complex
IFNγRI	Interferon gamma receptor I
IFA	Incomplete Freunds adjuvant
Ig	Immunoglobulin
IL-10	Interleukin-10
IL-27R	Interleukin-27 receptor
i.p.	Intraperitoneally
IFN-γ	Interferon-gamma
KO	Knock-out
LC-MS	Liquid chromatography-mass spectrometry
LPS	Lipopolysaccharide
LZ	Light zone
mAb	monoclonal Antibody
MHC	Major histocompatibility complex
MFI	median fluorescence intensity
MPLA	Monophosphoryl Lipid A
Mtb	*Mycobacterium tuberculosis*

Ova	Ovalbumin
P	Probability, p-value
PBS	Phosphate buffered saline
PD-1	programmed cell death protein 1
PE	Phycoerythrin
PRR	Pattern recognition pattern
PerCP/Cy5.5	Peridinin chlorophyll protein-Cyanine5.5
RA	Rheumatoid arthritis
RT	room temperature
S	sialic acid, sialylated residue
SEM	standard error of the mean
SHM	somatic hypermutation
St6gal1	α2,6-Sialyltransferase
TCR	T cell receptor
TDB	Trehalose-6,6-dibehenat
TLR	Toll-like receptor
TNFα	Tumor necrosis factor alpha
Tr1	T regulatory type 1
WT	wildtype
w/v	weight per volume

V List of units

°C	degree Celsius	ng	nanogram
g	gram	u	unit(s)
h	hour	xg	acceleration of gravity
mg	milligram	µg	microgram
min	minute	µL	microliter
mL	milliliter	%	percent
mM	millimolar		

Summary

The effector function of an IgG antibody is influenced by its subclass and type of Fc *N*-glycosylation pattern. A lack of fucose has been linked to pro-inflammatory conditions. A short glycan structure lacking galactose and terminal sialic acid residues is associated with the disease severity in inflammatory autoimmune disorders. In contrast, IgG glycan structures with terminal sialylation are correlated with autoimmune disease remission and have been shown to mediate anti-inflammatory functions. Currently, the glycan structure of IgG antibodies is also discussed in the context of vaccine-induced protection. However, the regulatory mechanism influencing the IgG Fc glycosylation are not entirely clear.

In this thesis I investigated the effect of different adjuvants on the IgG Fc glycosylation and the role of the germinal center (GC) reaction in the IgG Fc sialylation programming after immunization with different adjuvants. T follicular cells, GC B cells and PCs as well as IgG antibodies were analyzed in a mouse immunization model using different adjuvants plus the soluble protein antigen Ovalbumin.

Different adjuvants induced distinct antigen-specific IgG^+ GC B cell responses with distinct expression levels of the α2,6-sialyltransferase responsible for IgG Fc sialylation that correlated with specific serum IgG Fc galactosylation and sialylation patterns. Afucosylated IgG Abs were hardly induced through the immunization with a soluble protein antigen. Inflammatory IgG Fc glycosylation patterns with low galactosylation and sialylation levels correlated with enhanced $Foxp3^-$ T follicular helper cells (T_{FH}) cells, the induction of IL-27R-depndent IFN-γ^+ T_{FH1} cells, T_{FH17} cells as well as high ratios between T_{FH} cells and $Foxp3^+$ T follicular regulatory (T_{FR}) cells. The latter three were most potently induced by water-in-oil adjuvants like CFA, IFA and Montanide as well as *Mycobacterium tuberculosis* (*Mtb*) and its cord factor. Additionally, immune regulatory mechanisms on the IgG Fc glycosylation pattern were linked to follicular IL-10^+ IFN-γ^+ T regulatory type 1 (Tr1) cells in the GC.

The results of this thesis suggest that a certain GC-dependent IgG Fc *N*-glycosylation programming can be favored by the induction of distinct mechanisms by the choice of adjuvant. The findings of this thesis improve the understanding of the regulation of the IgG Fc galactosylation and sialylation within the GC reaction and might help to develop new vaccination strategies for the induction of IgG antibodies with high affinity and defined IgG Fc glycosylation patterns.

Zusammenfassung

Die Effektorfunktion von IgG Antikörpern wird beeinflusst durch deren Subklasse und Fc *N*-Glykosylierung. Afucosylierte Glykane werden mit erhöhter Inflammation verbunden. Eine kurze Glykanstruktur ohne Galactose und terminale Sialinsäure wird mit einem schweren Verlauf von inflammatorischen autoimmunen Krankheiten assoziiert. Im Gegensatz korrelieren terminal sialylierte Glykane mit der Remission von Autoimmunkrankheiten. Unterschiedliche IgG Glykosylierungen werden zusätzlich im Zusammenhang mit dem Schutz durch Impfungen diskutiert. Allerdings ist nur wenig bekannt über die regulatorischen Mechanismen, die die Fc Glykosylierung bestimmen.

In dieser Thesis wurde der Effekt unterschiedlicher Adjuvanzien auf die IgG Fc Glykosylierung, sowie die Rolle des Keimzentrums in der Programmierung der IgG Fc Sialylierung nach Immunisierung mit unterschiedlichen Adjuvanzien untersucht. In einem murinen Vakzinierungsmodel mit dem löslichen Proteinantigen Ovalbumin in Kombination mit unterschiedlichen Adjuvanzien wurden follikuläre T Zellen, Keimzentrums-B Zellen und Plasmazellen, sowie IgG Antikörper analysiert.

Die unterschiedlichen Adjuvanzien induzierten definierte Antigen-spezifische IgG^+ B Zell-Antworten im Keimzentrum, mit definierten Expressionsleveln der für die IgG Fc Sialylierung verantwortlichen α2,6-Sialyltransferase. Diese stimmten mit der IgG Fc Galaktosylierung und Sialylierung von Serumantikörpern überein. Afucosylierte IgG Antikörper wurden nur schwach durch das lösliche Proteinantigen induziert. Inflammatorische IgG Fc Glykosylierungen mit niedriger Galaktosylierung und Sialylierung korrelierten mit erhöhten $Foxp3^-$ T follikulären Helferzellen (T_{FH}), der IL-27R-abhängige Induktion von IFN-γ^+ T_{FH1} Zellen sowie T_{FH17} Zellen und mit einer erhöhten Ratio zwischen T_{FH} Zellen und $Foxp3^+$ follikulären T regulatorischen (T_{FR}) Zellen. Diese Faktoren wurden vor allem von Wasser-in-Öl Adjuvanzien, wie eCFA, IFA und Montanide, als auch von *Mycobacterium tuberculosis* (*Mtb*) und dessen Cordfaktor stark induziert. Zusätzlich konnten immunregulierende Wirkungen auf die IgG Fc *N*-Glykosylierung mit IL-10^+ IFN-γ^+ T regulatorische Typ 1 (Tr1) Zellen in Zusammenhang gebracht werden.

Die Ergebnisse dieser Thesis zeigen, dass eine Keimzentrums-abhängige Programmierung der IgG Fc Glykosylierung über bestimmte Mechanismen durch die Wahl des Adjuvans bestimmt werden kann. Das gewonnene Verständnis über die Regulierung der IgG Fc Galaktosylierung und Sialylierung im Keimzentrum könnte die Entwicklung neuer Vakzinierungsstrategien, mit dem Ziel IgG Antikörper mit hoher Affinität und definierter Fc Glykosylierung zu induzieren, unterstützen

1 Introduction

1.1 Vaccination

One of the leading causes for morbidity and mortality worldwide are infectious diseases and the consequences and complications they implicate. There are four categories of pathogens causing infectious disease: viruses, bacteria, fungi and parasites. Invasion and extra- or intracellular persistence can lead to acute or chronic infections, which in turn can result in inflammation, organ failure, cancer or death. Even though improved hygiene standards as well as the introduction of antibiotic treatment and vaccination have managed to reduce infections as a cause of death, there are still uncontrolled human infectious diseases for which there is no effective treatment or vaccination worldwide. The possibility of new emerging pathogens and the increasing antibiotic-resistance emphasize the need for improved vaccination strategies that meet the immunological requirements to cope with different pathogens (Khabbaz et al., 2014; Murphy et al., 2012).

1.1.1 The inception and milestones of vaccination

The first observations of an immunological memory were already made in ancient times, when survivors of an infection did not suffer from the same infectious disease again. The practice of variolation, in which fresh infectious matter containing the disease-causing pathogen (e.g., liquid of a pustule) were administered at low doses to healthy individuals, was initially performed in China, India and Africa and spread to Europe and the world in the 18th century. Even though variolation had its attendant risks and often, instead of the intended mild infection, disease was caused, it was a widely used procedure against smallpox in Europe (Riedel, 2005).

In 1796 Edward Jenner, a country physician and scientist, performed the first vaccination, which later has been turned out to be a groundbreaking event in the field of immunology and vaccination. Based on his awareness of the variolation procedure and his observation that dairy maids were in some way naturally protected from smallpox after suffering from cow pox, Edward Jenner inoculated an 8-year-old boy with cow pox matter from a fresh pustule. The boy developed a mild fever, chills, loss of appetite and pain in the axillae, but did not suffer from the disease itself. When Jenner inoculated the boy ~1 month later with

fresh matter of smallpox, the boy was protected from the disease. This was the first-time, protection was successfully achieved by the inoculation of an attenuated agent without the risk of a significant disease. Jenner later called this procedure vaccination (from *vacca*, latin for cow). In 1840 variolation was replaced by vaccination (Riedel, 2005).

In the following years the research on immunology gained attention and was greatly pushed on by the work of Robert Koch, who discovered the relation between microorganisms and disease, and Louis Pasteur, who proofed that pathogens can be attenuated or even inactivated for vaccination (Murphy et al., 2012; Plotkin, 2005).

The greatest success in the history of vaccination is the global vaccination campaign against smallpox which succeeded in the eradication of smallpox, which was officially announced by the WHO in 1979 (WHO, 1980). Since then, polio and measles disease incidents were decreased by >99.9% by the introduction of an appropriate vaccine. Similar accomplishments were achieved against diphtheria, pertussis, mumps, rubella and *H. influenzae*, varying between 94% to 99% reduction of disease incidents (Ada, 2005).

1.1.2 Vaccination principle, vaccine types and adjuvants

The goal of vaccinations is the induction of a long-lasting and protective immunity to a reinfection with the same infectious agents. Therefore, non-infected individuals are inoculated with an attenuated disease-related agent to induce an immune response providing a protective effect (e.g., neutralizing and opsonizing antibodies, immunological memory) without taking the risk of significant disease. The vaccination procedure benefits from the immune systems natural specificity and inducibility (Murphy et al., 2012).

Even persons that under some circumstances, e.g. due to immune suppression or allergy (Bonilla, 2018; McNeil and DeStefano, 2018), cannot be immunized, are protected by the herd immunity. By vaccination of the majority of the population, susceptible persons have a lower probability to get in contact with an infected person and thus are passively protected (Rashid et al., 2012).

Today, vaccines for the prevention of over 20 infectious diseases are available, and new vaccines against other pathogens are in the pipeline (WHO, 2021). Additionally, vaccination strategies for the prevention and/or treatment of cancer and autoimmune diseases are under investigation (Chiang et al., 2011; Pardoll, 1998; Petrovsky et al., 2003).

Different types of vaccination that have been developed to counter the existing diversity of pathogens are introduced in the following.

1.1.2.1 Live attenuated and inactivated vaccines

Live attenuated vaccines are based on the application of complete, living organisms that are equally immunogenic but less pathogenic than the pathogen in its normal form. For inactivated vaccines dangerous pathogens are e.g. heat inactivated and subsequently dead.

One approach for a live attenuated vaccine is the use of a virus that naturally occurs in another mammalian host. One example is Edward Jenner's use of cowpox to vaccinate against smallpox. Also, a naturally occurring attenuated strain of the same pathogen is possible to use. Polio type 2 was successfully used, and an attenuated rotavirus strain could be extracted from former infected children. Some other examples exist in nature, yet for most diseases there is a lack of proper counterparts (Ada, 2005). Thus, an artificial generation of attenuated vaccines is performed by passaging the wild-type strain in animal cell cultures until balance between retained immunogenicity and loss of virulence is reached, or by the adaption of the pathogen to 'sub-optimal' conditions (e.g., low temperature) so that survival in a human host becomes unlikely. These procedures are especially effective for viral pathogens due to short generation times and high mutation rates (Ada, 2005). Furthermore, attenuated microorganisms can be genetically engineered by the selective deletion or inactivation of a target gene (Ada, 2005; Plotkin, 2005). Another way to decrease pathogenicity is the inactivation of a pathogen. The resulting vaccine induces generally required immune responses, especially neutralizing antibodies, but has shown reduced induction of cytotoxic T cells over the MHC I pathway (Ada, 2005).

Live attenuated vaccines are most effective, but some immunosuppressed individuals might not be able to generate a proper immune response and adverse side effects can appear and lead to death. Inactivated vaccines generally carry a lower risk but need to be applied in larger doses and sometimes given more frequently. Genetically engineered attenuation and inactivation are considered more safely (Ada, 2005; Murphy et al., 2012).

1.1.2.2 Adjuvanted soluble protein or polysaccharide vaccines

For many pathogens, the development of attenuated or inactivated vaccines was not successful, or turned out to be impracticable, like it is seen for influenza vaccines, which fail to provide protective immunity (Coffman et al., 2010). Due to ongoing discoveries in the field of molecular biology, it became possible to separate subunits like capsular polysaccharides and proteins from microorganisms or to produce recombinant antigens of these subunits (Ada, 2005). There is increasing evidence that protein-based vaccines have a better outcome compared to polysaccharide vaccines and there is a clear trend to protein-based vaccines. Highly purified protein antigens have an improved safety but insufficient immunostimulatory capabilities. To overcome this poor immunogenic potential, adjuvants are applied. Adjuvants are substances of different origin that have direct effect on the innate immunity, such as enhanced immunogenicity, and eventually direct the type of adaptive immune response (Pasquale et al., 2015; Plotkin, 2005). The word adjuvant is derived from the Latin word for help, *adjuvare* (Coffman et al., 2010).

The most prominent adjuvant is Alum, forming precipitates of aluminum salts that adsorb antigens (Coffman et al., 2010). It is applied in multiple anti-bacterial and anti-viral vaccines (Marrack et al., 2009; Petrovsky and Aguilar, 2004) and has been the only adjuvant to be licensed in human for a long time, starting in the 1930th (Pasquale et al., 2015). Until today its mechanism of action is not completely understood (Marrack et al., 2009), but can be attributed to the initiation of innate immune responses, resulting in a profound T_H2 immune response in mice, (in humans T_H1 responses are also partially triggered). Also, there is a discussed depot effect releasing protein antigen over an elongated time (Coffman et al., 2010).

In 1937, Jules Freund introduced the oil-based adjuvant complete Freund's adjuvant (CFA), consisting of paraffin oil mixed with inactivated *Mycobacterium tuberculosis* (*Mtb*) (Freund et al., 1937). Emulsified with an aqueous protein antigen it induces a strong T_H1 and T_H17 response. A similar effect was observed for liposome-encapsulated TDB (a subunit derivate of *Mtb*) (Coffman et al., 2010). The effect of oil-based adjuvants is not entirely understood. It is speculated that endogenous signals during the necrotic cell death, that is induced by the cellular damage upon injection, contribute to the adjuvant effect (Coffman et al., 2010). Water-in-oil adjuvants have long been considered too toxic for the use in human, yet Montanide is broadly used in animal models and humans for cancer, HIV and malaria treatment, in which side effects are more tolerated (Petrovsky and Aguilar,

2004). Squalene-based water-in-oil adjuvants are considered less pathogenic. The adjuvant MF59 induces increased cell and antibody responses, without shifting the antigen-specific T_H1/T_H2 balance. It is licensed in Europe e.g., for the use in flu vaccines in the elderly (Coffman et al., 2010).

Another possible way to trigger the innate immune system is the activation of pattern recognition receptors (PRRs) or cytokine receptors. A broad group of Toll-like receptor (TLR) agonists is under extensive research for the use as adjuvant. Polysaccharides have long been recognized as immune activators (Plotkin, 2005) and MPLA, a less pathogenic derivate of lipopolysaccharide (LPS) of gram negative bacteria, targeting the TLR4 has been licensed in human (Petrovsky and Aguilar, 2004). TLR3, TLR4, TLR7, TLR8 and TLR9 adjuvants were reported to induce T_H1 responses (Coffman et al., 2010).

Adjuvanted vaccines are highly promising for the future. They enable the use of smaller doses of vaccine and antigen, reduce the number of required doses to gain protection and improve the immune response in individuals with an impaired response (infants, elderly, immunosuppressed people) (Coffman et al., 2010; Pasquale et al., 2015). The H5N1 influenza vaccine for example has improved immunogenicity and efficacy in the adjuvanted form, than being applied without adjuvant (Pasquale et al., 2015). The choice of adjuvant might depend on the type of adaptive immune response that is most effective against a specific pathogen. The use of adjuvant combinations, activating multiple innate responses, is under development with promising progress reaching late preclinical and early clinical stages (Coffman et al., 2010).

1.1.2.3 Newly arising vaccine types

Besides extensive research efforts on the improvement of attenuated or adjuvanted vaccines, new vaccination approaches are on the rise. Licensed one year ago, mRNA vaccines are a promising technique in the field of vaccination. The genetic information for an antigenic protein, in the form of mRNA, is packed into lipid nanoparticles (LNPs). Via endocytosis the mRNA is introduced to the cell cytoplasm where the human translational machinery is expressing the antigen-protein. From here, the protein gets either degraded and subsequently presented by the major histocompatibility complex (MHC) class I, or the protein is secreted, taken up by antigen presenting cells (APCs) and subsequently presented via the MHC II on the hosts cell surface. Consequently, B cell and T cell responses are

initiated (Noor, 2021). Two mRNA vaccines from BioNTech/Pfizer and Moderna, coding for the SARS-CoV-2 spike protein, were successfully used in the vaccination campaign against SARS-CoV-2 to prevent COVID-19. Both vaccines induced high titers of neutralizing antibodies as well as $CD8^+$ and $CD4^+$ T cell responses and proofed to ensure high efficacy, whilst side effects were mostly restricted to mild-to-moderate local reactions (Jackson et al., 2020; Polack et al., 2020).

Similar to mRNA vaccines are DNA vaccines. In this technique, the coding gene for the antigen protein is cloned into a vector which is introduced to the cell nucleus. Using a human promoter, the gene gets transcribed into mRNA and translated into the protein antigen. The initiation of the immune response equals the one of the mRNA vaccines (Noor, 2021).

Another new approach is the use of vector-based vaccines. The gene for the appropriate antigen is cloned into a replication-defective virus vector. After viral cell invasion the antigen gets expressed alongside with the immunogenic viral antigens and eventually targeted by the immune system (Lasaro and Ertl, 2009). The ChAdOx1 nCoV-19 vaccine from AstraZeneca against SARS-CoV-2 is based on this technique using an adenovirus vector. Additional to common vaccine side effects, in very rare cases ChAdOx1 nCoV-19 was associated with cross-reactivity to platelet factor 4 in young women and youth (Pai et al., 2021). The vaccine reached sufficient efficacy to prevent COVID-19.

In DNA/mRNA as well as vector-based vaccines the genetic information of multiple antigens with different epitopes can be cloned into the vector or packed into LNPs and transferred into the cell, allowing a simple combination vaccine targeting different pathogens (Noor, 2021).

1.2 Vaccine-induced immune responses

The immune system is classically divided into the innate and the adaptive immunity. Upon primary antigen encounter due to infection or immunization the relatively non-specific innate immunity is immediately activated to ensure a fast, direct response against the pathogen or applied antigen. The adaptive immune system instead acts by the means of highly specific antigen receptors on B and T lymphocytes that need to be acquired (Iwasaki and Medzhitov, 2010; Murphy et al., 2012).

1.2.1 Innate immune response

The mechanisms of the innate immunity are genetically programmed and non-specific. Immediately activated, the innate immune system reacts to invariant molecular patterns, such as pathogen-associated molecular patterns (PAMPs) or danger-associated molecular patterns (DAMPs), that are found on most microorganisms or are generated by the host cell, respectively (Murphy et al., 2012). These widely distributed structures are recognized by PRRs. PRRs are represented by different receptor families, including TLRs and C-type lectins (Iwasaki and Medzhitov, 2010). Secreted receptors, located for example in the blood or in extracellular fluids, can bind to the surface of pathogens and activate antimicrobial enzymes, such as lysozymes, inflammasomes or complement proteins, which target the pathogen cell for lysis or phagocytosis (Murphy et al., 2012). The interaction of PAMPs with membrane bound PRRs on the surface of innate immune cells, including dendritic cells (DCs), macrophages and neutrophiles, leads to their activation and following phagocytosis or destruction. Antigen presenting cells (APCs), e.g., DCs, can engulf the pathogen upon recognition and, after antigen processing, antigens are presented to $CD4^+$ T helper cells via MHC II resulting in the activation of these T cells. Similarly, infected cells can process and present antigens over the MHC I to $CD8^+$ T cells, which in turn kill the infected cell (Iwasaki and Medzhitov, 2010). This presentation is a crucial mechanism by which the innate immune system takes part in the activation of the adaptive immune system.

The highly purified protein antigens in subunit vaccines are not capable to activate an innate immune response due to their lack of immunogenicity through co-stimulation. At this point, the indispensability of adjuvants becomes clear. The activation of the innate immunity and the eventual antigen presentation to the adaptive immune system is ensured by the use of adjuvants and its co-stimulatory function (Coffman et al., 2010).

1.2.2 Adaptive immune response

The adaptive immunity depends on the activation and generation of highly specific antigen receptors of B and T lymphocytes. Antigen presentation via MHC I or MHC II activates $CD8^+$ and $CD4^+$ T cells, respectively (Iwasaki and Medzhitov, 2010). The initial B cell activation occurs by BCR clustering through the binding of antigen and can be further

triggered by $CD4^+$ T cells, leading to a vast production of antigen-specific antibodies (Kurosaki et al., 2015).

The importance of antibodies was first observed in 1890 by von Behring and Kitasato. In the context of their research on the prevention and treatment of diphtheria and tetanus they proposed the existence of an essential neutralizing factor (von Behring and Kitasato, 1890) that was later identified as antibody. Even though different mechanisms of the immune system can contribute to the protective immunity – e.g., the clearance of virus particles by $CD8^+$ T cells or by caspase-1 inflammasome activation (Ichinohe et al., 2009) – the induction of antigen-specific antibodies is a key feature of the protective effect, and vaccination success is measured by the level of antigen-specific antibodies (Plotkin, 2005). In the following the activation of the B cell response and the induction of antibody production are described in more detail.

1.2.2.1 T cell-independent B cell response

Non-protein antigens cannot be presented on the MHC II to the TCR. Hence, a T cell-induced activation is not possible. Nevertheless, there are T cell-independent (TI) antigens that can stimulate a humoral antibody response without additional T cell help (Endres et al., 1983). TI antigens are large, multivalent antigens, e.g., polysaccharides. The high density of epitopes enables massive crosslinking of membrane-bound Ig molecules (mIg) and subsequent B cell activation (Mond, 1995). TI antigens need help of other activating factors, such as TLRs (Martin et al., 2001) or cytokines (Endres et al., 1983; Mond, 1995).

The generated protective response is relatively fast compared to the complex T cell-dependent (TD) immune response (Mond, 1995). The fast induction of IgM-producing plasma cells (PCs) within the first three days of the primary response (Martin et al., 2001) is effective as a first line of defense. Nevertheless, to gain the full vaccination goal, the generation of highly-specific antigen receptors and a powerful immunological memory is vital (Ada, 2005; Murphy et al., 2012) and in need of T cell help. Accordingly, there is a strong trend in the development of protein-based vaccines.

1.2.2.2 T cell-dependent B cell response

For the T cell - B cell interaction, both cells need to be initially primed with a protein antigen, whose processed peptides can be presented on the MHC II of the B cell. B cell priming occurs by BCR clustering through antigen binding. The B cell eventually presents the processed protein antigen in a peptide-MHC II complex (Kurosaki et al., 2015). For the priming of naïve T cells, a prolonged antigen peptide-MHC II presentation by APCs e.g. DCs is essential. The following contact between cognate T and B cell takes place at the T:B border, an area where the T cell zone and B cell follicle meet (Mesin et al., 2016). Several signals between the cells lead to activation, proliferation and/or differentiation of both cell types (McHeyzer-Williams et al., 2012; Vinuesa et al., 2016). These signals include the interaction between peptide-MHC II and the T cell receptor (TCR) of $CD4^+$ T helper cells, different co-stimulatory signals, like the interaction between CD28 on T cells and CD80 or CD86 on B cells (June et al., 1994), as well as the release and recognition of cytokines (McHeyzer-Williams et al., 2012).

At this point, the B cell can follow three different fates: The B cells can differentiate into (a) short-lived extrafollicular PCs, (b) extrafollicular memory B cells or (c) enter the germinal center (GC) (Fig. 1-1) (Kurosaki et al., 2015). The selection to the one or the other fate depends mainly on the affinity of the BCR. B cells with low and high affinity compete for the present antigen at the T:B border. It is supposed that B cells with high affinity receptors dominate the binding of antigen and present more peptide-MHC II. The eventual prolonged contact to cognate T cells favors the differentiation into GC B cells. A rather short contact leads to the differentiation of GC-independent memory B cells (Kurosaki et al., 2015). Also, the selection into the extrafollicular PC fate depends on the affinity. It was shown, that BCR with high specificity and affinity are prevalently chosen to differentiate into extrafollicular PCs, when the affinity to the antigen is substantially higher than the threshold value that is required to enter the GC (Paus et al., 2006).

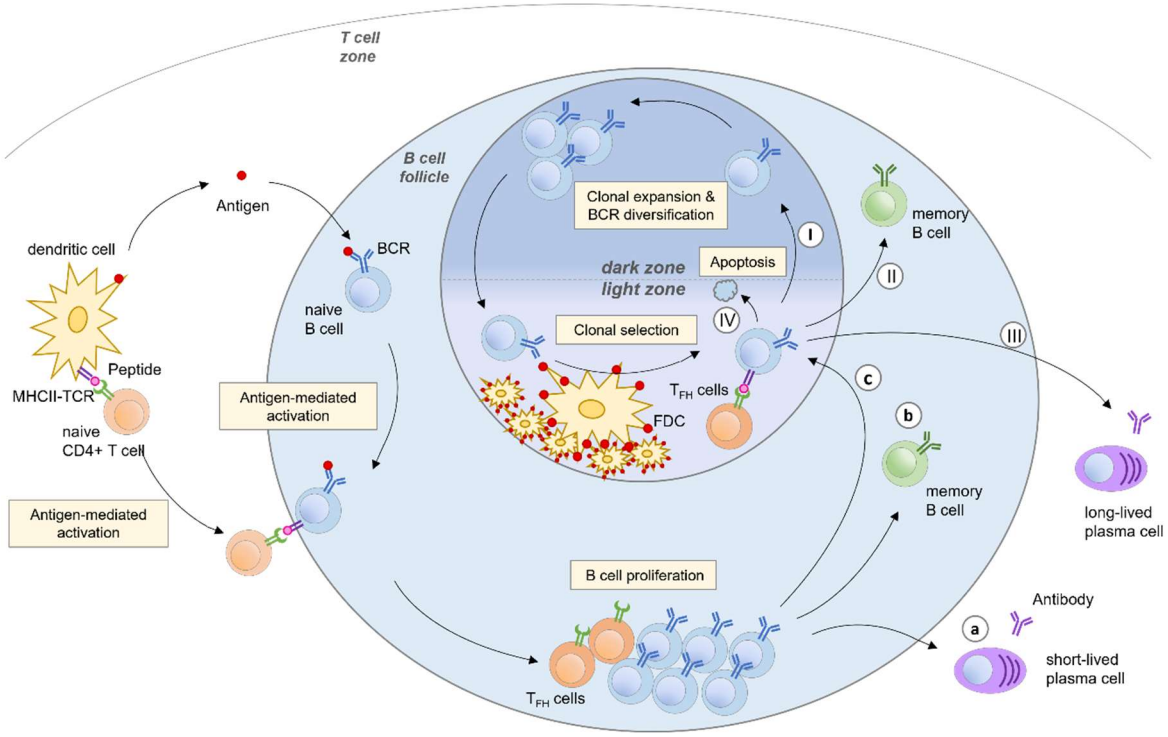

(Kurosaki et al., 2015, modified)

Figure 1-1: B cell response to T cell-dependent antigen

For more detail see text. Briefly, naïve B cells are activated by antigen-mediated BCR clustering in the B cell follicle. Naïve $CD4^+$ T helper cells are activated by APCs in the T cell zone. Interaction of T cell and B cell occurs at the T:B border, leading to proliferation of B cells and differentiation of T helper cells into the T_{FH} subset. The B cell is directed to follow one of three possible pathways: proliferation into (a) an extrafollicular short-lived PC, (b) extrafollicular memory B cell or (c) a GC B cell entering the GC. Within the GC the B cell undergoes iterative cycles of clonal expansion and BCR diversification in the dark zone and clonal selection in the light zone. Once in the LZ there are four different B cell fates: (I) re-enter the dark zone or exit the GC and proliferate into (II) an affinity-matured memory B cell or (III) long-lived plasma cell or (IV) cell death (Kurosaki et al., 2015).

It is important to mention that **class switch recombination**, a process in which the isotype is changed, can occur already in this pre-GC stage (Kurosaki et al., 2015). During this process, an activation-induced cytidine deaminase (AID) -driven enzymatic machinery rearranges the gene segments of the constant heavy chain domains by connecting two gene segments whilst others get excised (Stavnezer et al., 2008). Thus, extrafollicular PCs, that emerge three to four days after infection or immunization, can produce antibodies of the IgM and IgG isotype, contributing to an early TD antibody response (Paus et al., 2006).

The **germinal center** is a microanatomical structure that is formed within in the B cell follicle of secondary lymphoid tissues (such as spleen or lymph nodes) around six days upon immunization (Mesin et al., 2016; Victora and Nussenzweig, 2012). It is predominated by B cells, $CD4^+$ T cells and DCs (Shlomchik et al., 2019) and essential for antibody diversification and affinity maturation (Mesin et al., 2016). The GC can be divided into two compartments: the dark zone and the light zone - designated based on their appearance in histology staining (Mesin et al., 2016). The dark zone (DZ) is located proximal to the T cell zone and almost entirely occupied by densely packed, extensively proliferating GC B cells. The light zone (LZ), located distal to the T cell zone, is rich of follicular dendritic cells (FDCs) forming a network that is interspersed with GC B cells and follicular T cells (Mesin et al., 2016; Victora and Nussenzweig, 2012).

Concerning the function, the DZ is the site of clonal expansion and diversification of the antigen receptor (Victora and Nussenzweig, 2012). The diversification occurs on gene level by the introduction of somatic hyper mutations (SHM) by an enzymatic machinery, including the enzyme AID and the error-prone DNA polymerase η (Murphy et al., 2012). As a consequence, the clonal variants exhibit V(D)J regions with changed antigen affinity (Shlomchik et al., 2019). In addition, class switching occurs resulting in antibody clones of different isotypes. The newly generated B cell clones leave the DZ and enter the LZ.

In the LZ, antigen-driven clonal selection of the somatic hyper mutated B cell variants takes place. The positive selection of B cell clones requires antigen-dependent signals (Mesin et al., 2016). One important signal is the binding of the BCR to antigen. The FDC network retains intact antigen immune complexes (ICs) on the surface, which plays a key role in this interaction (Mesin et al., 2016; Shlomchik et al., 2019; Victora and Nussenzweig, 2012). The access of antigen is the limiting factor in positive selection. Further selectively signals are provided by $CD4^+$ $Foxp3^-$ follicular T helper (T_{FH}) cells upon contact between peptide-MHC II and the TCR. The precise signals are not clear but supposedly include survival and/or differentiation signals. B cells with high affinity receptors outcompete low B cells with low BCR. Consequently, they express more peptide-MHCs on their surface that get recognized by T cells. In this way a relative threshold is set for clonal selection (Victora and Nussenzweig, 2012). At this point one B cell clone can be selected (I) to re-enter the DZ for another round of diversification, (II) to exit the GC as memory B cell, (III) to exit the GC as long-lived PC, or (IV) to be eliminated (Fig. 1-1).

Most B cells follow the first path several times. The migration between the DZ and the LZ is called cyclic re-entry. The repeating improvement of the affinity of the antigen receptor and clonal selection of high affinity clones is called **affinity maturation** (Mesin et al., 2016).

B cells that were not sufficiently provided with survival signals go into apoptosis. Negative selection can be a consequence of low affinity, defective or autoreactive BCR clones that originate from the random process of SHM (Shlomchik et al., 2019).

The mechanisms that drive the selection between cyclic re-entry and GC exiting are not fully understood (Vinuesa et al., 2016). The selection might depend on transcriptional factors or on stochastically events (Kurosaki et al., 2015; Shinnakasu et al., 2016). Moreover, a T cell dependent selection towards the memory B cell fate was proposed, in which weak T cell help, due to low affinity BCRs, correlated with the memory B cell fate (Shinnakasu et al., 2016). A switched isotype to IgG was observed to guide the B cell towards the PC cell fate and against the memory B cell fate (Mesin et al., 2016). Despite many unclarities, affinity-matured memory B cells and PCs exit the GC eventually and persist in the spleen or the bone marrow, respectively (Manz, 1998; Slifka et al., 1998).

During the TD B cell response generated cells ensure immunological memory against re-infection with the same pathogen. In case of re-exposure, the humoral response will be faster and of a higher magnitude, compared to the first response (Kurosaki et al., 2015). Long-lived plasma cells continually produce antigen-specific antibodies that can act as a first line of defense (Manz et al., 1997). Pathogen-experienced memory B cells proliferate rapidly in response to re-exposure, giving a second line of defense. If T cell help through a cognate (memory) T cell is provided, memory B cells can re-enter the GC reaction and undergo further affinity maturation and class switching, resulting in the production of antibodies with extremely high specificity and affinity (McHeyzer-Williams et al., 2012). This natural improvement of the immunological memory and protection against pathogens is induced in booster vaccinations (re-injection of the same antigen). In general, IgG^+ memory B cells rapidly proliferate into antibody-producing PCs, whereas IgM^+ memory B cells are prone to enter the GC reaction. The GC-independent memory B cell pool is assumed to possess a broader range of antigen-specificity, compared to GC-dependent memory B cell pool (Kurosaki et al., 2015). This might be beneficial in case of an infection with another variant of the same pathogen.

1.2.2.3 Immune regulatory components

During the germinal center reaction several molecular effectors support inflammation. To protect the host from excessive inflammation and following tissue damage, interference through immune regulatory mechanisms takes place. One important self-regulation is accomplished by $Foxp3^+$ follicular T regulatory cells (T_{FR} cells) (Sage and Sharpe, 2016). T_{FR} cells inhibit the T_{FH}-mediated activation of B cells in the GC in an antigen-specific manner and thereby control the extent of the GC reaction. The extent of the inhibitory effect depends on the T_{FH}/T_{FR} ratio (Aloulou et al., 2016; Sage and Sharpe, 2016), and acts through e.g., signaling over inhibitory receptors or the secretion of anti-inflammatory cytokines such as interleukin-10 (IL-10) (Aloulou et al., 2016).

1.3 The structure and function of antibodies

Antibodies are essential glycoproteins of the adaptive immune system. They exist in membrane-bound form – anchored in the membrane building the B cell receptor (BCR) – and in soluble form, secreted by PCs. (Murphy et al., 2012; Pieper et al., 2013). The predominant isotype in serum is IgG. It makes up 75% of all serum Abs, followed by IgA and IgM with 15% and 10%, respectively, and IgE with about 0,01%. IgA is the most present isotype in mucosal tissue. IgE is generally cell-bound and tissue-associated (Shade and Anthony, 2013).

Antibodies are heterodimer, built from two heavy and two light chains linked by a disulfide bond. Antibodies can be functionally separated into two fragments: the N-terminal fragment antigen-binding (Fab) and the C-terminal fragment crystallizable (Fc), which are connected by a flexible hinge region. The heavy chain consists of one variable domain (VH) and three to four constant regions (CH1, CH2, CH3, CH4), the light chain of one variable (VL) and one constant region (CL) (Fig. 1-2)(Porter, 1973; Quast et al., 2017).

The paired variable region (VH + VL) of one heavy and one light chain are responsible for the paratope-epitope binding. Each variable region exhibits three highly variable complementary determining regions (CDRs), which are the result of the conformational structure of the recombined V(D)J regions (Murphy et al., 2012).

The Fc part of an antibody mediates the effector function by its binding to distinct molecular receptors and thereby inducing humoral immunity. The heavy chain constant regions determine the immunoglobulin isotype. Five isotypes are known in mice and men: IgM, IgD, IgG, IgE and IgA (Murphy et al., 2012; Shade and Anthony, 2013).

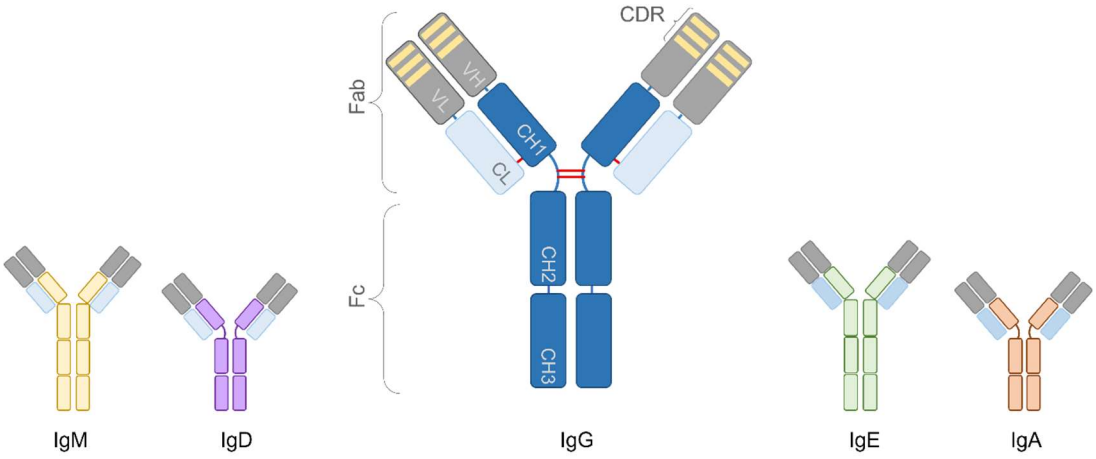

Figure 1-2: Schematic antibody structure and antibody isotypes

Schematic visualization of the different antibody isotypes with IgG exemplary for the detailed antibody structure. The antibody molecule is built of two heavy and two light chains that are connected via disulfide bonds (red lines). Each chain carries one variable region (grey, VH=variable domain of the heavy chain, VL=variable domain of the light chain), within which the complement determining regions (CDRs, yellow) are located. The light chain carries one constant region (CL), the heavy chain comprises three to four constant regions (CH1-CH3 for IgG). The antibody molecule can be functionally separated into the fragment antigen binding (Fab) and the fragment crystallizable (Fc). The constant regions of the heavy chains determine the isotype (different isotypes are represented in different colors).

1.3.1 IgG subclasses and effector functions

The IgG isotype can be differentiated into subclasses. There are four IgG subclasses found in humans, namely IgG1-4, and in mice, namely IgG1, IgG2a (allelic variant to IgG2c in C57BL/6 mice), IgG2b and IgG3 (de Haan et al., 2017; Shade and Anthony, 2013; Steffen et al., 2020; Vidarsson et al., 2014). The subclasses carry ~90% homology with variations in particular in the hinge region and the N-terminal CH2 domain. FcγRs and the C1q complement protein exhibit overlapping binding sites within the CH2 domain most proximal to the hinge region. Correspondingly, variations in the hinge region and CH2 domain between the four IgG subclasses affect the binding to immune receptors and molecules and thus mediate different effector functions (Vidarsson et al., 2014).

To protect the host from pathogens and pathogenic agents, the IgG Abs have three major tasks: neutralization, opsonization and complement activation. In neutralization, antibodies bind to pathogens or toxins and thereby block their cell access for infection or destruction. The success of vaccination is currently measured by the induction of high, pathogen-specific antibody titers. In this way, the protection against the pathogen is mainly associated with the induction of neutralizing antibodies, which are geenrally sufficient to neutralize toxins or prevent viral entry. Yet, additional Fc-mediated effector functions contribute, in particular, to pathogen elimination (Alter et al., 2018; Plotkin, 2005).

Antibodies link the specificity of the adaptive immunity with the destructive mechanisms of the innate immunity (Rosales and Uribe-Querol, 2013; Shade and Anthony, 2013). After opsonization of bacteria, viruses or infected cells, the Fc part of the antibodies can recruit immune cells capable of killing or phagocytosis, resulting in antibody-dependent cell-mediated cytotoxicity (ADCC) or antibody-dependent cell-mediated phagocytosis (ADCP), respectively. Furthermore, complement-dependent cytotoxicity (CDC) (1.3.1.2) can be initiated (Murphy et al., 2012; Quast et al., 2017).

In humans, IgG1 and IgG3 are considered to be most effective. IgG2 is particularly induced to bacterial capsular polysaccharides (Vidarsson et al., 2014), although its role is less clear. IgG4 induces weaker activating effector functions yet has the potential to inhibit the effect of other IgG subclasses by e.g., reducing the activating effect when present in ICs with other IgG subclasses or by their high affinity to inhibitory receptors (James and Till, 2016). In mice, IgG2a/c and IgG2b are the most efficient subclasses. IgG1 shows a relatively weak activating effector function and can be functionally compared to the human IgG4 (Rosales and Uribe-Querol, 2013). The role of murine IgG3, as the one of human IgG2, is less clear.

1.3.1.1 Classical FcγR-mediated effector function

Fc gamma receptors (FcγRs) bind IgG subclasses with different specificities and affinities (Bruhns and Jönsson, 2015; Rosales and Uribe-Querol, 2013). There are three classes of human FcγRs and four classes of FcγR in mice with different subclasses (Tab. 1-1) (Bruhns, 2012). The human and murine FcγRs exhibit highly homolog amino acid sequences (Rosales and Uribe-Querol, 2013). Still, dissimilar expression patterns and binding abilities to the distinct IgG subclasses mediate distinct effector functions dependent on the IgG subclass (Tab. 1-1) (Bruhns, 2012).

Table 1-1: Mouse and human Fc gamma receptors

FcγRs have activating or inhibitory functions. The binding strength to mouse and human IgG subclasses, respectively to the receptors, is separated into high affinity (bold), low affinity (normal), very low affinity (in between brackets) or no binding (-).

		Function	IgG subclass binding			
mouse	**FcγRI**	Activation	-	**2a**	2b	(3)
	FcγRIIB	Inhibition	1	2a	2b	-
	FcγRIII	Activation	1	2a	2b	-
	FcγRIV	Activation	-	**2a**	**2b**	-
human	**FcγRI**	Activation	**1**	-	**3**	**4**
	FcγRIIA	Activation	1	2	3	4
	FcγRIIB	Inhibition	1	(2)	3	4
	FcγRIIC	Activation	1	(2)	3	4
	FcγRIIIA	Activation	1	(2)	3	4
	FcγRIIIB	?	1	-	3	4

FcγRs can have activating or inhibitory function. Intracellular signaling is induced upon FcγR aggregation, by crosslinking the receptors through the binding of antigen-bound immune complexes. Activating FcγRs induce signals over the immunoreceptor tyrosine-based activation motif (ITAM). The FcγRIIB is the only inhibitory FcγR with an intracellular immunoreceptor tyrosine-based inhibitory motif (ITIM), counteracting activating signals. (Bruhns, 2012; Quast et al., 2017; Rosales and Uribe-Querol, 2013; Shade and Anthony, 2013).

FcγRs are expressed by different leucocytes. In general, more than one type of FcγRs is presented on the cell surface at the same time and most times the inhibitory FcγRIIB is co-expressed. Cell activation is accomplished, when the ratio of activating and inhibiting signals (A/I ratio) reaches a threshold for activation. An increase in the A/I ratio indicates an enhanced activating effector function. The possibility that the threshold is reached and a signal is induced depends on the expression level and distribution of FcγRs on the cell surface plus the affinity of the IgG subclasses to the FcγRs (Quast et al., 2017; Rosales and Uribe-Querol, 2013).

1.3.1.2 Complement mediated effector function

Complement-dependent cytotoxicity (CDC) can be initiated through the binding of the C1q complement protein to antigen-bound immune complexes (classical pathway), such as opsonized bacteria or infected cells.

In humans IgG3 is most efficient in C1q binding and complement-dependent cell lysis, followed directly by IgG1. IgG4 does not bind C1q (Tao et al., 1993). In mice IgG2a, IgG2b and IgG3 are all potent to bind C1q and mediate cell lysis, whereas murine IgG1 has only been found capable to induce weak hemolysis (Neuberger and Rajewsky, 1981).

In the following, the complement cascade leads to the formation of the membrane attack complex (MAC), which disrupts the cell membrane and causes cell lysis. In addition, complement-induced inflammation is promoted by produced anaphylatoxins and phagocytic cells are recruited to efficiently engulf and destroy the opsonized pathogen (Kojouharova et al., 2010; Quast et al., 2017).

1.3.2 IgG Fc glycosylation

The induced effector function does not depend on the IgG subclass alone, but also on the type of the attached Fc glycan (Quast et al., 2017).

Immunoglobulins are glycoproteins that are post-translationally glycosylated in their Fab and Fc region. IgM, IgD, IgA and IgE exhibit various glycosylation sites in the constant domains of their heavy chains (Arnold et al., 2007). IgG has one singular conserved *N*-glycosylation site at Asn297 in its CH2 domains of both heavy chains (Howell et al., 1967; Kaneko, 2006). Posed into the interface between the CH2 and CH3 domains, the glycan attributes to the conformation of the Fc part (Arnold et al., 2007; Vidarsson et al., 2014).

The glycan attached to Asn297 features a heptasaccharide core structure built of two *N*-acetylglucosamines (GlcNAc) followed by three mannose residues branching into a biantennary structure with both arms carrying an additional GlcNAc (Fig. 1-3). The core structure can be further modified by a fucose attached to the protein-bound GlcNAc, a bisecting GlcNAc at the branched mannose and/or by the elongation of the two arms by galactose and terminal sialic acid (Kaneko, 2006; Parekh et al., 1985; Vidarsson et al., 2014) (Fig. 1-3). These modifications can be found in various combinations (de Haan et al., 2017) resulting in a highly diverse IgG glycan composition. The majority, >90%, of the

total IgG is fucosylated (Quast et al., 2017; Shade and Anthony, 2013), 20-40% are agalactosylated (G0), ~40% carry one galactose (G1) and 20-40% carry two galactoses (G2) (Quast et al., 2017). Sialylated glycans are rather rare; with 5-15% of the glycans being elongated by one sialic acid (G2S1) and only ~1% by two sialic acids (G2S2) (Quast et al., 2017; Vidarsson et al., 2014). The percentages of the different types of glycans vary between subclasses (de Haan et al., 2017) and depend on the age, sex and inflammatory condition (Shade and Anthony, 2013).

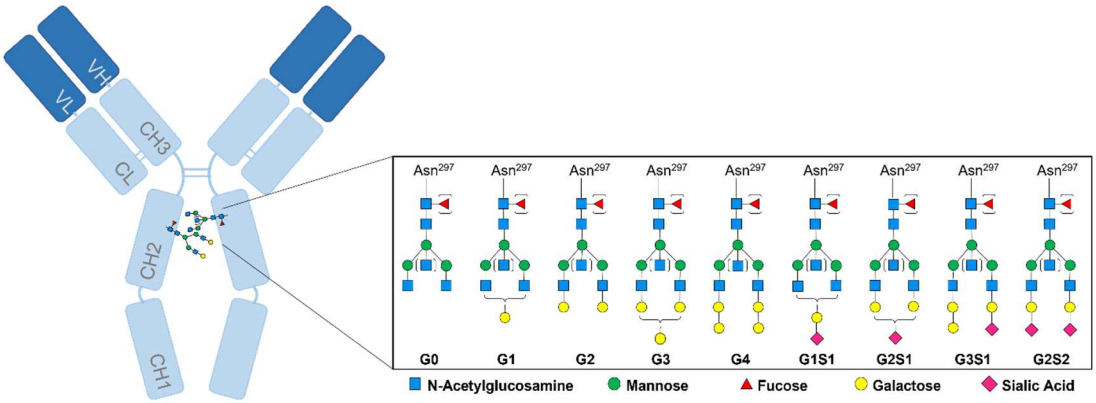

Figure 1-3: IgG Fc *N*-glycosylation patterns

The IgG antibody occupies one conserved Fc *N*-glycosylation site at asparagine-297 (Asn^{297}) in their CH2 domain of the heavy chain. The glycans are placed in the interface of the CH2 and CH3 domains and depending on the glycan structure influencing the conformation of the Fc part. The most frequent glycan structures are shown: The core structure consists of a heptasaccharide consisting of four *N*-Acetylglucosamines (blue square) and three mannoses (green circle), called G0 due to the lack of galactose. The core structure can be elongated with galactose (G, yellow circle) and/or terminal sialic acid (S, pink square). Contingently (depicted in brackets), fucose (red triangle) or one bisecting *N*-Acetylglucosamine can be attached. G3 and G4 forms are quite rare for IgG Abs.

The importance of the Fc *N*-glycosylation is emphasized by the reduced effector function and impaired binding ability to FcγRs of glycan-deficient IgG Abs produced by hybridoma cells (Nose and Wigzell, 1983) or of IgG lacking the glycan, after glycan removal with EndoS (leaving only the protein-bound GlcNAc) (Collin and Ehlers, 2013).

Furthermore, a correlation between the IgG glycosylation pattern and disease severity has been described for inflammatory autoimmune diseases (Alter et al., 2018; Shade and Anthony, 2013). An increase of agalactosylated (G0) total serum IgG was detected in patients with rheumatoid arthritis (RA), systemic lupus erythematosus (SLE), multiple

sclerosis (MS) and inflammatory bowel diseases (IBD) (Parekh et al., 1985; Trbojević Akmačić et al., 2015; Vučković et al., 2015; Wuhrer et al., 2015). This effect was even more pronounced when antigen-specific IgG of RA patients have been investigated and was suggested as a potential indicator for the disease onset (Rombouts et al., 2015). Intriguingly, disease remission in rheumatoid arthritis (RA) patients during pregnancy or anti-TNFα therapy correlated with reduced proportion of agalagctosylated IgGs and elevated proportions of galactosylated and sialylated IgGs that revealed a less inflammatory or even anti-inflammatory activity that provoked post-partum. (Bartsch et al., 2018; Collin and Ehlers, 2013; Epp et al., 2018; Hess et al., 2013; Karsten et al., 2012; van de Geijn et al., 2009).

Additionally, the evidence that the IgG Fc glycosylation plays a role in the immune response against infectious pathogens becomes more concrete but is still incompletely understood. Enhanced IgG G0 levels have been associated with liver necroinflammation and fibrosis in patients with chronic hepatitis B infection (Ho et al., 2015) and with acute tuberculosis infections compared to latent ones (Lu et al., 2016). In these cases, elevated G0 IgG levels seem to indicate a more inflammatory condition with potential pathogenicity.

Furthermore, elevated levels of G0 IgG correlated with enhanced protection against simian immunodeficiency virus in rhesus macaques after immunization (Vaccari et al., 2016) and the protection in HIV controllers (infected individuals without HIV enrichment)(Ackerman et al., 2013).

The same HIV controllers, that showed enhanced G0 IgG levels, showed an additional loss of fucosylation that probably helps to control the disease by enhanced ADCC (Ackerman et al., 2013). Elevated afucosylation was also detected in and correlated with enhanced protection in latent tuberculosis (TB) infections compared to acute infections (Lu et al., 2016). Interestingly, in these patients with latent TB infection the enhanced F0 IgG was in contrast to the G0 IgG Abs.

Whereas F0 IgG Abs can be associated with strong pathogen fighting, the induction and role of different combinations of afucosylated glycans with or without galactose as well as fucosylated glycans with or without galactose are still unclear.

Rergarding IgG sialylation, HIV controllers showed reduced IgG sialylation levels. Nevertheless, IgG Fc sialylation has also been linked to enhanced pathogen clearance, as highly sialylated IgG Abs have been suggested to improve antigen presentation in GC

reactions, and thus, induce enhanced neutralizing IgG Abs in the context of HIV and influenza virus (Lofano et al., 2018; Wang et al., 2015). Different roles of agalactosylated and in particular sialylated IgG Abs at distinct time points upon infection or vaccination have probably been taken into account in this context (Lofano et al., 2018; Wang et al., 2015). In the following the known precise roles of the single monosaccharides of the glycan are described.

1.3.2.1 The role of distinct IgG Fc monosaccharides in the effector function

The IgG Fc glycosylation plays an essential role in the binding to classical FcγRs. Placed between the two CH2 domains in the CH2-CH3 interface modifications of the glycan structure can change the quaternary Fc conformation (Vidarsson et al., 2014). In addition, the type of IgG Fc glycosylation influences the binding to C1q (Lilienthal et al., 2018; Tao et al., 1993) and the activation of further sugar residue binding receptors, for example of the C-type lectin receptors family (type 2 Fc receptors) (Petry et al., 2021; Pincetic et al., 2014).

The lack of **fucose (F0)** results in enhanced affinity of human IgG1and IgG3 to the activating human FcγRIIIA (Shade and Anthony, 2013) with up to 50-fold enhanced binding detected for afucosylated compared to fucosylated IgG (Shields et al., 2002). Accordingly murine IgG2a and IgG2b showed enhanced affinity to the human FcγRIIIA-ortholog mouse FcγRIV (Kao et al., 2017), respectively. The increased affinity is assumed to be based on decreased steric hindrance for glycan-glycan interaction to the corresponding receptor (Shade and Anthony, 2013). F0 IgGs are associated with heightened ADCC and ADPC activity (Quast et al., 2017) and are currently tested in several clinical trials with monoclonal tumor-antigen specific human IgG1 Abs.

IgG **bisecting GlcNAc** has been linked to inflammatory immune conditions. A modest (compared to the afucosylated IgG) 10-20-fold increase of the binding affinity to the FcγRIIIA in humans alongside with increased ADCC has been observed in the presence of bisecting GlcNAc (Shade and Anthony, 2013). IgG bisecting GlcNAc is very rare in mice (de Haan et al., 2017).

Accumulation of **agalactosylated (G0)** IgG has been observed in several inflammatory (autoimmune) diseases as well as in inflammatory infection and cancer conditions. As a consequence, the loss of galactose is linked to increased pro-inflammatory conditions

(Bartsch et al., 2018; Hess et al., 2013; Oefner et al., 2012; Shade and Anthony, 2013). Furthermore, immune complexes of agalactosylated IgG has been identified to activate the lectin pathway of the complement system as a consequence of enhanced binding to mannose-binding lectin (Arnold et al., 2007).

Contradictive observations have been made for **galactosylated (G1, G2)** IgG. Highly galactosylated IgG ICs have been reported to induce enhanced complement activity by binding C1q (Alter et al., 2018). On the contrary, highly galactosylated murine IgG1 ICs (but not IgG2) have been found to facilitate association of FcγRIIB to the sugar-binding C-type lectin receptor dectin-1, which results in the blocking of the anaphylatoxin C5a-dependent effector function and inflammatory response *in vitro* and *in vivo* (Karsten et al., 2012).

Hence, G0 is associated with inflammatory conditions, whereas the final pathogenic or non-pathogenic role of galactose is controversially discussed and still needs to be investigated in different contexts.

Terminal **Sialic acid (S)** connected to galactose has been associated with an anti-inflammatory function. In contrast to the drastic increase of G0 IgGs in inflammatory (auto)immune diseases, which decrease during pregnancy and disease remission, the level of sialylated IgG is reduced under these inflammatory conditions and elevated levels are observed during pregnancy or after anti-TNFα treatment and have been associated with disease remission (Rook et al., 1991; van de Geijn et al., 2009). The attachment of sialic acid to the glycan reduces the binding affinity to the classical FcγRs by a 5-10-fold (compared to asialylated glycoform) resulting in reduced ADCC *in vivo* an *in vitro* (Anthony et al., 2008a; Kaneko, 2006; Shade and Anthony, 2013).

Intriguingly, in mice the anti-inflammatory effect of therapeutical intravenous immuno-globulin (IVIG) has been suggested to depend on the effect of IgG sialylation. IVIG is the pooled total serum IgG of 5,000-10,000 healthy donors. Applied at high doses (1-2 g/kg body weight) it is used to treat inflammatory diseases by balancing a dysregulated total blood IgG glycosylation pattern that seems to act as a buffer system of the inflammatory state (Collin and Ehlers, 2013; Kaneko, 2006). Enzymatic removal of the sialic acid by neuraminidase abrogates the protective effect of IVIG in several autoimmune mouse models (Kaneko, 2006; Shade and Anthony, 2013). IgG enriched for sialic acid revealed a 10-fold increase in protection. Accordingly, only 0.1 g/kg highly sialylated IgG was

sufficient to induce equivalent protection compared to 1 g/kg of IVIG (Anthony et al., 2008a; Kaneko, 2006).

Based on mouse experiments, it has been suggested that the anti-inflammatory effect of IVIG requires the C-type lectin receptor mouse SIGN-RI or the ortholog human DC-SIGN (Bruhns and Jönsson, 2015; Shade and Anthony, 2013). Here the glycan itself takes part in the binding between the receptor and the IgG (Vidarsson et al., 2014). Eventually, activation of SIGN-RI / DC-SIGN leads to the upregulation of the inhibitory FcγRIIB on immune cells and following moderation of immune responses (Samuelsson, 2001), by e.g., counteracting FcγRIII engagement (Samuelsson, 2001) or inhibiting of the B cell activation (Hess et al., 2013; Rosales and Uribe-Querol, 2013). Based on the reduced binding to FcγRs and the upregulation of the FcγRIIB, sialic acid vastly decreases the A/I ratio and is extensively associated with reduced inflammation and pathology.

However, the role of sialic acid in IVIG and its interaction with SIGN-R1 or DC-SIGN is highly discussed (Anthony et al., 2008b; Petry et al., 2021). In addition to SIGN-R1 / DC-SIGN, another C-type lectin receptor has been discovered for IVIG. Binding of sialylated IgG to the dendritic cell immune receptor (DCIR) has been connected to the upregulation of Treg cells (Massoud et al., 2014).

Moreover, the inhibitory effect of sialylation, described for total IgG, has also been linked to the inhibitory effect of antigen-specific IgG (Bartsch et al., 2018; Hess et al., 2013; Oefner et al., 2012; Ohmi et al., 2016; Pfeifle et al., 2017).

Besides, as mentioned above, IgG Fc sialylation has been linked to enhance pathogen clearance in the context of HIV and influenza virus. In this context, highly sialylated IgG Abs have been suggested to improve antigen presentation in GC reactions and thereby induce neutralizing IgG Abs with enhanced affinity (Lofano et al., 2018; Wang et al., 2015).

In summary, enhanced potential to encounter pathogens has been linked to F0 antigen-specific human IgG1 and IgG3 Abs and murine IgG2a and IgG2b Abs that might be enhanced by bisecting GlcNAc. The role of antigen-specific galactosylation and sialylation in the fight against pathogens is still unclear and highly discussed. Different roles of galactosylated and in particular sialylated IgG Abs at different time points, needs to be taken into account (Lofano et al., 2018; Wang et al., 2015).

1.3.3 Regulation of IgG Fc glycosylation

Antibody glycosylation takes place during the vesicular transport from the endoplasmatic reticulum (ER) to the Golgi apparatus and the plasma membrane. Specific enzymes modify the glycan in a hierarchically order (Moremen et al., 2012). The glycosylation is controlled by the availability of enzymes, substrate and acceptor molecules (Shade and Anthony, 2013).

The addition of sialic acid, for example, depends on the access of galactosylated glycans and availability of the α-2,6-sialyltransferase (St6gal1) to transfer cytidine monophosphate (CMP)-activated sialic acid to the galactose. Accordingly, the St6gal1 expression level in PCs is associated with the sialylation level of the produced IgG (Bartsch et al., 2018; Hess et al., 2013; Oefner et al., 2012; Pfeifle et al., 2017). The conditional knock-out of the St6gal1 in case of class switched B cells ($St6gal1^{fl/fl}$ AID-cre mice), lead to reduced sialylation of total IgG, demonstrating the major contribution of St6gal1 to the IgG Fc glycosylation (Ohmi et al., 2016). Furthermore, the enzymes β-1,4-galactosyltransferase (B4galt1) and St6gal1 have been associated with galactosylation and sialylation, respectively, in genome-wide association studies in humans (Lauc et al., 2013; Wahl et al., 2018). Interestingly, there are remarkable differences in the steady-state glycosylation between the subclasses especially in C57BL/6 mice. Whereas sialylated glycoforms make up approximately 20% of IgG1, around 40% of IgG2 antibodies are sialylated (de Haan et al., 2017). Since IgG2 is superior to IgG1 to enhance immune responses in mice, the IgG subclass seems to influence the glycosylation regulation mechanisms in some sort of self-regulating manner (Kao et al., 2017). Furthermore, variants in IgG glycoforms correlate with age, sex, ethnic and hormones (Mahan et al., 2016; Pučić et al., 2011; Vidarsson et al., 2014).

Regulation of the IgG Fc glycosylation has been proposed for the observed changes in autoimmune diseases. The glycosylation level shift towards a pro-inflammatory state (agalactosylated glycans) during disease flare and to a less pro-inflammatory state (galactosylated and sialylated glycans) during remission following monoclonal antibody treatment (e.g. TNFα blocking) or during pregnancy (Collins et al., 2013; Rook et al., 1991; van de Geijn et al., 2009).

Different IgG Fc glycan patterns have also been described in infectious diseases and seem to depend on the type of pathogen (Larsen et al., 2021). For example, as mentioned before,

a reduction of galactosylation and fucosylation has been found in HIV controllers, whereas enhanced G0 was associated with an acute tuberculosis infection but elevated F0 with a latent tuberculosis infection (Lu et al., 2016).

Also, a time-dependent effect has been determined, as highly sialylated IgG Abs occur in the early state (7 days post vaccination), whereas a shift so low sialylation was determined in the later phase (3 weeks post vaccination) in an influenza immunization model (Wang et al., 2015).

Different variations of IgG glycan patterns can be induced by vaccination and depend on different factors (e.g. adjuvant, antigen, number of doses) (Kao et al., 2017; Mahan et al., 2016).

Even though, first studies have been performed to investigate the influence of adjuvants on the development of differently glycosylated IgG, little is known about the mechanisms by which distinct IgG glycosylation patterns are induced. In these studies it was shown that T cell dependent immune response induce a stronger downregulation of the St6gal1 and following less sialylated IgG than T cell independent immune responses upon vaccination (Hess et al., 2013). Also, downregulated St6gal1 expression and an increase of pro-inflammatory G0 IgG could be correlated to the induction of T_H17 cells and the involvement of IL-6 (Bartsch, 2019; Pfeifle et al., 2017). Anyhow, regulating mechanisms are still just barely understood, emphasizing the need of further investigations.

1.4 Aims

Extensive research has been conducted on the induction of different T and B cell responses. Furthermore, first studies have correlated different immunizations with distinct adjuvants with the induction of differently glycosylated IgG Abs in B cells. However, there is still a lack of knowledge regarding the regulation of differentially glycosylated antibodies upon immune activation with distinct adjuvants. A better understanding might help to design suitable vaccines in the future.

In this thesis, an immunization model with the T cell-dependent soluble protein antigen Ovalbumin (Ova), as a foreign model antigen, was used to induce immune responses equally to those induced upon vaccination with a soluble protein, which is used in most recombinant vaccines. In this way, the effect of different adjuvants on the induction of the adaptive immune response was investigated alongside with mechanisms that play an essential role in the regulation of the B cell response and IgG Fc glycosylation.

The first aim was to investigate the influence of a broad panel of different adjuvants combined with Ova on the induced antigen-specific antibody responses with a special regard on the subclass, titer, IgG Fc glycosylation and the corresponding St6gal1 expression in PCs.

Alongside with the first aim, the second aim was to investigate the importance of the germinal center reaction on the induction of different IgG Fc glycosylation patterns. Due to the possibility of class switching and affinity maturation, the germinal center might be an essential step in the production of distinct IgG antibodies with different effector function.

The third aim was to analyze the different T follicular helper cell responses initiated upon the immunization with different adjuvants that support GC B cell responses. In this context, a focus was placed on the determination of the induced cytokine profile, especially the induction of $T_{FH}1$ responses, and the associated influence on the B cell response.

2 Material and Methods

2.1 Material

2.1.1 Mice

C57BL/6 mice were purchased from the Jackson Laboratories or Janvier Labs. IL-17RA-deficient (IL-17R KO) mice were generated as described before (Ye et al., 2001), IFNγRI-deficient mice (IFNgRI KO) (no. 003288) and Vert-X mice (IL-10^{gfp}, IL-10 reporter mice) were purchased from Jackson Laboratories. IFNγRI- and IL-17RA-deficient mice (IFNgRI x IL-17R dKO) were bred, and all strains maintained in our internal facility according to the institutional guidelines. WSX-1-deficient (IL-27R KO) mice were developed as described (Yoshida et al., 2001) and bred in the animal facility of the research center Borstel. All mouse strains were already on or back-crossed at least eight times on the C57BL/6 background. For the *in vivo* experiments female mice, of 8-12 weeks (or otherwise indicated) and for the *in vitro* experiments, cells from 8-16 weeks old female mice were analyzed following the regulatory guidelines and ethical standards of the University of Lübeck. The experiments were approved by the Federal Ministry of Energy, Agriculture, the Environment and Rural Areas Schleswig-Holstein (License numbers: 39_48-6-18; 39_45-4-17).

2.1.2 Consumables

Table 2-1 List of used consumable materials

Material	Manufacturer / Vendor
3-way stopcock, Discofix C	Braun (Melsungen, Germany)
8-well tube strips	Kisker Biotech (Steinfurt, Germany)
96-well PP plate (conical, 450µl/well)	Thermo Fisher (Waltham, MA, USA)
Costar Assay plates (high binding), 96-well	Corning (Kennebunk, ME, USA)
Falcon 70µm cell strainer	Corning (Kennebunk, ME, USA)
Falcon tubes (15, 50 mL)	Greiner Bio-one (Kremsmünster, Austria)

Flow Cytometry tube 5 mL	Sarstedt (Sarstedt, Germany)
MACS LS column	Miltenyi Biotec (Bergisch Gladbach, Germany)
Maxi Column	G Biosciences (St, Louis, MO USA)
MiniCollect Tube (serum)	Greiner Bio-one (Kremsmünster, Austria)
Needle 26G 0.45x13mm	Braun (Melsungen, Germany)
Needle 26G 0.45x25mm	Braun (Melsungen, Germany)
Needle (Eclipse)	BD Bioscience (San Diego, CA, USA)
Neubauer chamber	Assistant (Sondheim vor der Rhön, Germany)
Pipette tips with and without Filter (10, 100, 200, 1000 µL)	Sarstedt (Nümbrecht, Germany)
Reaction tubes (1.5, 2.0 mL)	Sarstedt (Nümbrecht, Germany)
Serological pipettes (5, 10, 25, 50 mL)	Sarstedt (Nümbrecht, Germany)
Single-use syringes (1, 2, 5, 10 mL)	Braun (Melsungen, Germany)
Solofix blood lancets	Braun (Melsungen, Germany)
Tissue culture plate, 12-well, suspension	Greiner Bio-One (Frickenhausen, Germany)
Tissue culture plate, 6-well, suspension	Sarstedt (Nümbrecht, Germany)

2.1.3 Chemicals

Table 2-2 List of used chemicals

Chemical compound	Manufacturer / Vendor
Ammonium chloride (NH_4Cl)	Merck (Darmstadt, Germany)
BD OptEIA (TMB substrate)	BD Bioscience (San Diego, CA, USA)
Brefeldin A (1000x)	Biolegend (San Diego, CA, USA)
BSA (bovine serum albumin)	GE Healthcare (Little Chalfont, UK)
Carbonate-bicarbonate buffer	Sigma-Aldrich (St, Louis, MO, USA)
CNBr-activated SepharoseTM 4 Fast Flow	GE Healthcare (Little Chalfont, UK)
Cytofix/Cytoperm	BD Bioscience (San Diego, CA, USA)
DMSO	Roth (Karlsruhe, Germany)
Dulbecco´s Phosphate buffered saline	Thermo Fisher (Waltham, MA, USA)
EDTA	Sigma-Aldrich (St, Louis, MO, USA)
Ethanol	Carl Roth (Karlsruhe, Germany)
FCS (Fetal calf serum)	Thermo Fisher (Waltham, MA, USA)
Fixable viability dye (eFluor780)	Thermo Fisher (Waltham, MA, USA)
Focusing Fluid	Thermo Fisher (Waltham, MA, USA)
Formaldehyde (4.5%)	Th. Geyer GmbH & Co. KG (Renningen, Germany)
Gelatin	Sigma-Aldrich (St, Louis, MO, USA)
HEPES (N-(2-Hydroxyethyl) piperazin-N'-(2-ethansulfonacid))	Thermo Fisher (Waltham, MA, USA)
Hydrochloric acid (HCl)	Merck (Darmstadt, Germany)
Ionomycin	Biolegend (San Diego, CA, USA)
Ketamin 10 mg/ml	WDT (Garbsen, Germany)

Lipopolysaccharide from E. coli O111:B4	Sigma-Aldrich (St, Louis, MO, USA)
Monensin (1000x)	Biolegend (San Diego, CA, USA)
Ovalbumin AF647 conjugated	Thermo Fisher (Waltham, MA, USA)
Ovalbumin Grade VI	Sigma-Aldrich (St, Louis, MO, USA)
Penicillin Streptomycin	Thermo Fisher (Waltham, MA, USA)
Permeabilisation Buffer 10x	Thermo Fisher (Waltham, MA, USA)
PMA (Phorbol myristate acetate)	InvivoGen (Toulouse, France)
Rompun 2% (Xylazine)	Bayer (Lerverkusen, Germany)
RPMI1640 (L-Glutamine)	Thermo Fisher (Waltham, MA, USA)
Saponin	Sigma-Aldrich (St, Louis, MO, USA)
Sodium acetate ($C_2H_3NaO_2$)	Carl Roth (Karlsruhe, Germany)
Sodium azide (NaN_3)	AppliChem (Darmstadt, Germany)
Sodium bicarbonate ($NaHCO_3$)	Merck (Darmstadt, Germany)
Sodium chloride (NaCl)	Merck (Darmstadt, Germany)
Sodium hydroxide (NaOH)	Merck (Darmstadt, Germany)
Streptavidin BV605 conjugated	Biolegend (San Diego, CA, USA)
Streptavidin BV421 conjugated	Biolegend (San Diego, CA, USA)
Sulfuric acid (H_2SO_4)	Sigma-Aldrich (St, Louis, MO, USA)
Tris-HCl	Sigma-Aldrich (St, Louis, MO, USA)
Trizmabase (Tris)	Sigma-Aldrich (St, Louis, MO, USA)
Trypan blue solution	Sigma-Aldrich (St, Louis, MO, USA)
Tween 20	Sigma-Aldrich (St, Louis, MO, USA)
β-Mercaptoethanol	Sigma-Aldrich (St, Louis, MO, USA)

2.1.4 Buffers

Table 2-3 List of used buffers and their compositions

Buffer	Components	Concentration
Activation buffer (Ova coupling)	Hydrochloric acid (HCl) in pure H_2O	1 mM
Blocking buffer (ELISA)	BSA	3% (w/v)
	Gelatine	0.1% (w/v)
	EDTA	3 mM
	in PBS	
Coating buffer (ELISA)	Carbonate-Bicarbonate in pure H_2O	50 mM
Coupling buffer (Ova coupling)	Sodium bicarbonate ($NaHCO_3$), pH 8.3	100 mM
	Sodium chloride (NaCl)	500 mM
	in pure H_2O	
Red blood cell lysis buffer	EDTA	0.1 mM
	Ammonium chloride (NH_4Cl)	155 mM
	Sodium bicarbonate ($NaHCO_3$)	10 mM
	in pure H_2O	
FACS Buffer	BSA	0.5% (w/v)
	Sodium azide (NaN_3)	0.05% (w/v)
	in PBS	
MACS Buffer	FCS	1.5% (v/v)
	EDTA	1 mM
	in D-PBS	
PBS-T	Tween-20	0.05% (v/v)
	in PBS	
PermWash	PBS	0.05x
	BSA	0.1% (w/v)
	Saponin	0.05% (w/v)
	Sodium azide (NaN_3)	0.01% (w/v)
	in pure H_2O	
Quenching buffer (Ova coupling)	Tris-HCl, pH 8 in pure H_2O	100 mM

Wash buffer high pH (Ova coupling)	Tris-HCl, pH 8.0 Sodium chloride (NaCl) in pure H_2O	100 mM 500 mM
Wash buffer low pH (Ova coupling)	Sodiumacetate ($C_2H_3NaO_2$), pH 4.0 Sodiumchloride (NaCl) in pure H_2O	100 mM 500 mM

2.1.5 Media

Table 2-4 List of used media and their supplement compositions

Media	Supplements	Concentration
B cell media	FCS	10% (v/v)
	β-Mercaptoethanol	100 µM
	HEPES	1 mM
	Penicillin Streptomycin	100 u/mL
	in RPMI1640 (L-Glutamine)	
Re-stimulation media	Brefeldin A	1x
	Monensin	1x
	PMA	0.5 µg/mL
	Ionomycin	1 µg/mL
	in B cell media (see above)	

2.1.6 Adjuvants

Table 2-5 List of used adjuvants

Adjuvant	Manufacturer / Vendor
Incomplete Freund's Adjuvant	Sigma-Aldrich (St, Louis, MO, USA)
M. Tuberculosis Des. H37 Ra (non-viable)	BD Bioscience (San Diego, CA, USA)
Montanide ISA 51 VG 10ST	AIR LIQUIDE Medical

AddaVax™	
Adju-Phos adjuvant	
Alhydrogel adjuvant 2% (Alum)	
Monophosphoryl Lipid A (MPLA) –SM	
VacciGrade™	InvivoGen (Toulouse, France)
Poly(I:C) HMW VacciGrade™	
R848 VacciGrade™	
TDB VacciGrade™	
TDB-HS15	

2.1.7 Antibodies

Table 2-6 List of used antibodies

Specificity	Clone	Isotype	Conjugate	Manufacturer/ Vendor
mouse IgG Fc	polyclonal	goat IgG	HRP	
mouse IgG1	polyclonal	goat IgG	HRP	
mouse IgG2b	polyclonal	goat IgG	HRP	Bethyl Laboratories (Montgomery, TX, USA)
mouse IgG2c	polyclonal	goat IgG	HRP	
mouse IgG3	polyclonal	goat IgG	HRP	
mouse IgG Fc	polyclonal	goat F(ab')2	PE	
mouse/human B220 (CD45R)	RA3-6B2	rat IgG2a	BV786	
mouse CD16/32 (Fc block)	93	rat IgG2a	/	Biolegend (San Diego, CA, USA)
mouse CD3	17A2	rat IgG2b	AF488	

mouse CD4	RM4-5	rat IgG2a	BV711	
mouse CD8	53-6.7	rat IgG2a	AF700	
mouse CXCR5 (CD185)	L138D7	rat IgG2b	Biotin	
mouse/human GL7	GL7	rat IgM	PerCP/ Cy5.5	Biolegend (San Diego, CA, USA)
mouse IFN-γ	XMG1.2	rat IgG1	AF647	
mouse IFN-γ	XMG1.2	rat IgG1	PE	
mouse IgG1	RMG1-1	rat IgG	BV421	
mouse CD138	281-2	rat IgG2a	BV711	
mouse Fas (CD95)	Jo2	hamster IgG2	BV510	BD Bioscience (San Diego, CA, USA)
mouse Foxp3	MF-23	rat IgG2b	AF647	
human St6gal1	polyclonal	goat IgG	/	R&D Systems (Minneapolis, MN, USA)
/ (goat IgG control)	polyclonal	goat IgG	/	
mouse/rat IL-17A	eBio17B7	rat IgG2a	PE	Thermo Fisher (Waltham, MA, USA)

2.1.8 Recombinant proteins

Table 2-7 List of used proteins

Protein	Manufacturer / Vendor
Recombinant murine IL-10	Peprotech
Recombinant murine IFN-γ	Peprotech
CD28 Protein, mouse, recombinant (His Tag)	Sino Biological Inc.

2.1.9 Kits

Table 2-8 List of used kits

Kit	Manufacturer /Vendor
B Cell Isolation Kit, Mouse	Miltenyi Biotec (Bergisch Gladbach, Germany)
True-Nuclear™ Transcription Factor Buffer Set	Biolegend, (San Diego, CA, USA)
AlexaFluor 488 Abs labeling kit	Thermo Fisher (Waltham, MA, USA)

2.1.10 Instruments

Table 2-9 List of used instruments

Instrument	Manufacturer / Vendor
Attune NxT Flow Cytometer	Thermo Fisher (Waltham, MA, USA)
Autoclave VX-75	Systec (Linden, Germany)
Barnstead GenePure Pro (Ultrapure water)	Thermo Fisher (Waltham, MA, USA)
BioGARD Hood	The Baker Company, Inc. (Sanford, ME, USA)
Centrifuge 5424R	Eppendorf (Hamburg, Germany)
Centrifuge Mega Star 3.0R	VWR
Electronic balance	Kern & Sohn (Balingen-Frommern, Germany)
ELISA-Reader Spectra Max iD3	Molecular Devices, LLC. (San Jose, CA, USA)
Incubator AutoFlow NU-5510	NuAire (Plymouth, MN, USA)
Magnet, MACS MultiStand	Miltenyi Biotec (Bergisch Gladbach, Germany)

Magnet, QuadroMACS™Seperator	Miltenyi Biotec (Bergisch Gladbach, Germany)
Microscope Primovert	Zeiss
NanoDrop-2000C	peqlab Biotechnologie GmbH (Erlangen, Germany)
pH Meter FiveEasy F20	Mettler-Toledo (Columbus, OH, USA)
Pipetboy Accu 2	IntegraBioscience (Zizers, Switzerland)
Pipette (eight- multichannel)	VWR (Radnor, PA, USA)
Pipette (twelve- multichannel)	Eppendorf (Hamburg, Germany)
Pipette (single-channel)	Eppendorf (Hamburg, Germany)
Pipette Multi-channel Eppendorf Xplorer® plus	Eppendorf (Hamburg, Germany)
Tube Rotator „end-over-end“ shaker	VWR (Radnor, PA, USA)
Vortex-Genie 2	Scientific Industries (Bohemia, NY, USA)
Vortex ZX3	VELP Scientifica (UsmateVelate, Italy)
Waterbath SW-20C	Julabo

2.1.11 Software

Table 2-10 List of used software

Software	Company
Excel	Microsoft (Redmond, WA, USA)
FlowJo	BD Bioscience (San Diego, CA, USA)
Prism v. 6.04	GraphPad Software (San Diego, CA, USA)

2.2 Methods

2.2.1 Mouse handling

2.2.1.1 Immunization

Mice were immunized intraperitoneally (i.p.) with 100 µg Ova in 200 µL. Therefore 100 µL of an Ova dissolved in PBS (1 mg/mL) were mixed with 100 µL of the appropriate adjuvant. The boost injection contained no adjuvants; Ova was mixed in PBS resulting in 100 µg Ova in 200 µL.

2.2.1.1.1 Oil-based adjuvants (IFA, eCFA, Montanide)

Oil-based adjuvants are not soluble in the watery Ova solution. Hence, emulsions were prepared.

IFA and Montanide are ready-to-use Adjuvants. For the preparation of enriched CFA (eCFA), 20 mL of IFA were mixed with 100 mg *Mtb*.H37 RA to reach a final concentration of 5 mg *Mtb*/mL. The eCFA was vortexted before every use so that the *Mtb* was homogenously distributed, yet not too much air was captured in the oily IFA. The Ova-Adjuvant mixtures were prepared, as freshly as possible, on the day of injection. The same volumes of Ova and adjuvant were filled in individual syringes and connected by a 3-way stopcock after removing air bubbles. The two phases were emulsified by fast transferring the solutions from one to the other syringe, starting with the input of the watery Ova phase into the oily adjuvant phase. After mixing for approximately 5 min, the emulsion was pressed into one syringe. The empty syringe was removed, and 1 mL syringes locked onto the 3-way stopcock and fully filled (>1 mL).

2.2.1.1.2 Adjuvants in watery solution

Alum, Adju-Phos and Addavax were purchased as ready-to-use adjuvants. The adjuvants MPLA-SM, Poly(I:C), R848, TDB and TDB-HS15 were reconstituted following the manufacturer's instructions to stock concentration of 1 mg/mL.

Equal Volumes of Ova in PBS and adjuvants were mixed. Alum and Adju-Phos were added dropwise to the Ova solution during vortexing, subsequently pipetted up and down for 5 min and incubated for 1 h at 4°C. The other adjuvants were added directly to the Ova solution in equal volumes and mixed by pipetting up and down a few times. Eventually,

200 µL of the Ova-Adjuvant mixtures contained 100 µg Ova plus Alum, Adju-Phos, Addavax, MPLA (30 µg, diluted in PBS), Poly(I:C) (100µg), R848 (100 µg), TDB (100 µg) or TDB-HS15 (100 µg).

2.2.1.2 Organ sampling

During the experiment, blood was sampled from the *vena facialis* on conscious mice. One drop of blood was collected into MiniCollect tubes. The puncture site was altered over the experiment time. On the final day, mice were narcotized with 200 µL Ketamin/Xylazin per mouse. Up to 1 mL blood was sampled via heart punction. Spleens were taken after cervical dislocation and kept in cold PBS on ice for further preparation (2.2.5.2).

Blood was collected in MiniCollect tubes. After centrifugation at 4,000xg for 5 min the separated sera were transferred into a new 1.5 mL reaction tube and stored at 4°C or -20°C until usage.

2.2.2 Antigen-specific ELISA

For the detection of Ova-specific antibodies and their subclasses in the serum 50 µL of a 10 µg/mL solution of Ova in coating buffer were coated onto 96-well costar assay plates and incubated over night at 4°C. The antigen solution was removed, and the plate blocked with 100 µL blocking solution for 1h at RT. The blocking solution was removed, and the plate was washed four times with 150 µL of PBS-T. Serum samples were diluted, as indicated, in blocking solution using 8-well tube stripes and 50 µL of the appropriate dilution were applied per well. Binding of sera antibodies to the Ova antigen was performed for 1h at RT. The serum dilutions were discarded, and the wells washed three times with 150 µL PBS-T. HRP-coupled anti-murine IgG Fc, IgG1, IgG2b, IgG2c or IgG3 detection antibodies were diluted 1:10,000 in blocking solution and 50 µL per well incubated for 1h at RT. The plates were washed four times with PBS-T. For the detection 50 µL per well of freshly prepared TMB substrate (1:1 mix) were applied. The color reaction was stopped with 25 µL of 4.2% sulfuric acid and the optical density (OD) at 450 nm was measured.

2.2.3 IgG Fc glycan analysis by LC-MS

The IgG subclass LC-MS analysis was performed as described elsewhere (de Haan et al., 2017) In brief, the Fc glycan analysis by Liquid Chromatography-Mass Spectrometry (LC-MS) allows the determination of glycosylation patterns of individual IgG subclasses. IgG antibodies are purified from serum by the use of an affinity column. In this thesis Ova-specific serum IgG was purified using an Ova-coupled sepharose (2.2.3.1) column. After trypsin-digestion, the resulting glycopeptides consist of different amino acid sequences of the CH2 domain corresponding to their IgG subclass plus the corresponding glycan attached to the Asn-297. In the LC part of this method, glycopeptides get separated from non-glycosylated peptides. The eluted glycopeptides are subsequently analyzed in MS. For murine IgG from C57BL/6 mice, IgG1, IgG2(b and c) and IgG3 can be discriminated.

Glycopeptides containing agalacotosylated glycans (G0), galactosylated glycans (G1, G2), sialylated glycans (sialylation, S), bisected glycans (bisection) and/or fucosylated glycans (fucosylation, F) can be differentiated. For the analysis, the relative fractions were summed for each individual subclass. Afucosylated glycans were mostly under the detection limit. Bisecting and occurring afucosylated glycans were assigned to their corresponding fraction of galactosylation and sialylation. Not all subclasses could be identified in all samples; in general, the best signals were observed for IgG1.

2.2.3.1 Ova-Sepharose Coupling

The coupling of Ova to sepharose was performed using the CNBr-activated Sepharose 4 Fast Flow. The coupling principle is based on the high reactivity and binding of cyanate ester on the surface of the sepharose beads to primary amino groups of proteins or other molecules.

In the first step, freeze-dried sepharose beads were reconstituted. 0.25 g freeze-dried beads were esed for 1 mL swollen resin. The dried sepharose beads were transferred to a 50 ml falcon and reconstituted in the 5x column volume activation buffer (1 mM HCl) for 2h at 4°C on an end-over-end shaker. During that time Ova was dissolved in coupling buffer to a final concentration of approx. 10 mg/mL. The concentration was verified via Nanodrop and noted.

The swollen beads were centrifuged at 1,000xg for 5 min and washed once more with activation buffer. After centrifugation at 1,000xg for 5 min the supernatant was discarded. The Ova solution was added to the swollen sepharose in a 1:1 volume ratio. The coupling of Ova to the sepharose beads was performed over night at 4°C whilst end-over-end rotation.

The beads were centrifuged at 1,000xg for 5 min, the supernatant removed and saved. The concentration of the supernatant was measured via Nanodrop to compare the Ova concentration before and after Ova coupling – the concentration should have reduced markedly. The beads were washed for 30 min at RT rotating with the 5x column volume coupling buffer to remove remaining, unbound Ova. Unoccupied binding sites of the CNBr-Sepharose were blocked in quenching buffer (5x column volume) for 2 h at RT on the end-over-end shaker. The beads were transferred to a Maxi column and washed three times with the high pH wash buffer and three times with the low pH wash buffer, these washing steps were repeated twice. Finally, buffer was exchanged to 20% EtOH in PBS (5x column volume) and Ova-coupled sepharose beads were stored in 20% EtOH in PBS (1x column volume) at 4°C until usage.

2.2.3.2 LC-MS measurement

The LC-MS measurement was conducted by Sander Wagt, a PhD student from our lab, at the Center for Proteomics and Metabolomics, under the direction of and in cooperation with Prof. M. Wuhrer, Leiden University Medical Center, Leiden, the Netherlands and are described in detail elsewhere (de Haan et al., 2017; Selman et al., 2012).

2.2.4 B cell culture

The here performed B cell culture is a primary cell culture. For the isolation of naïve B cells, a negative selection was performed using the B cell isolation kit for mouse from Miltenyi Biotec. Spleens were harvested from untreated mice. After organ sampling (2.2.1.2), all further steps were performed under the clean bench, under sterile conditions; all buffers and reagents were kept cold.

2.2.4.1 B cell isolation

One freshly harvested spleen was meshed through a 70 µm cell strainer. The cells were washed by adding MACS buffer up to 25 mL, following centrifugation at 300xg, 4°C for 6 min and discarding the supernatant. The addition of MACS buffer was used to simultaneously wash the strainer. The cell pellet was resuspended in 2 mL MACS buffer by pipetting and filtered through a new cell strainer into a new falcon tube. The filter was washed with 1 mL MACS buffer. For the following cell count, a 1:50 pre-dilution of the cell suspension in MACS buffer was prepared and again mixed with trypan blue 1:2. The cells were counted under the microscope using a Neubauer chamber. The cell concentration was calculated by the equation 2-1.

$$x = \frac{n_{count}}{4} \cdot 100\ (final\ dilution\ factor) \cdot 10^4 (chamber\ const) \qquad (2.1)$$

x = *cells/mL*

n_{count} = *number of counted cells*

The volume of 8 x 10^7 cells was transferred to a new 50 mL tube and brought to a final volume of 2 mL with MACS buffer. The cells were mixed with 50 µL of the biotin-antibody cocktail and incubated for 20 min on ice. Cells were washed with 25 mL MACS buffer and pelleted for 6 min at 300xg, 4°C and the supernatant was discarded. The cell pellet was resuspended in 3 mL MACS buffer and incubated with 100 µL anti-biotin microbeads for 20 min on ice. The cells were washed once more with 25 mL MACS buffer, spun down (300xg, 4°C, 6 min) and the supernatant was discarded. During the centrifugation, a LS column was placed in the corresponding magnet and equilibrated with 3 mL MACS buffer. The cell pellet was resuspended in 2 mL MACS buffer and applied to the column; the flow through (containing the B cells) was collected in a new 50 mL tube. For the B cell count, a 1:20 pre-dilution in MACS buffer was prepared and mixed 1:2 with trypan blue. The concentration was determined as described before (eq. 2.1) using a final dilution factor of 40.

2.2.4.2 Purity check

The purity check was performed on the day 0 to confirm the proper isolation of B cells. For comparison, from both cell suspensions, splenic cells and isolated B cells, 60 µL were transferred to a new reaction tube and the volume brought to 100 µL with FACS buffer. 0.5 µL of fixable viability dye (eFluor780) as well as a B220-BV786 and CD3-AF488 antibody were added, and cells stained for 20 min on ice int the dark. The cells were washed with 200-400 µL FACS buffer, spun down (300xg, 4°C, 6 min) and resuspended in 200 µL FACS buffer for measuring at the flow cytometer.

2.2.4.3 Culture of B cells

For the cultivation, B cells were added to B cell culture media to a final concentration of 8 x 10^4 cells/mL and supplemented with 3 µg/mL LPS. Based on this stock, master mixes for each condition were prepared for duplicates or quadruplicates. Dependent of the culture conditions IL-10 (10 ng/mL), IFN-γ (20 ng/mL) or soluble CD28 (0.2-10 ng/mL) were optionally added. The cells were transferred onto a 12-well culture plate (2.5 mL/well) and incubated for 4 days at 37°C and 5% CO_2.

On day 4 the cells from each well were transferred to a new 15 mL falcon, 10 µL were mixed with 190 µL of trypan blue (1:100 in PBS) and the cell concentration was determined using the flow cytometer.

2.2.5 Flow Cytometry

2.2.5.1 Antibody labeling

The anti-St6gal1 antibody and the goat isotype control antibody were labeled inhouse using the AlexaFluor 488 Abs labeling kit. 100 µg of lyophilized antibody were dissolved in 100 µL 0.1 M ammonium bicarbonate (1 mg/mL). The antibody solution was transferred to the activated AF488 dye. The tube was firmly converted for mixture and incubated for 1h at RT in the absence of light. The reaction was quenched using 50 µL of 1 M Tris (pH8) for 20 min at RT in the dark. Finally, 350 µL of FACS buffer were added, reaching an antibody concentration of 0.2 mg/mL.

2.2.5.2 Preparation of splenic cells from *in vivo* experiments

Freshly harvested spleens were meshed through a 70 µm cell strainer; the strainer was rinsed with cold PBS to gain a final cell suspension of 15 mL. The cells were kept on ice. The cell suspensions were centrifuged at 300xg and 4°C for 6 min, the supernatant was discarded. The cells were resuspended, and lysis of erythrocytes was performed in 5 mL red blood cell lysis buffer for 5 min at RT. Lysis was stopped by adding 20 mL of cold PBS. Cells were centrifuged at 300xg, 4°C for 6 min and the supernatants discarded. 1 mL of cold FACS buffer was added to the cell pellet, clotted dead cell debris were removed and the remaining cells resuspended by pipetting. For the cell count, the cell suspension was diluted 1:20 in Trypan blue (1:100 prediluted in PBS) and the concentration was measured at the Attune NxT.

2.2.5.3 B cell staining

B cell staining was performed to identify plasma cells ($CD138^+$) and GC B cells ($B220^+$, $GL7^+$, FAS^+). Furthermore, these subpopulations were characterized by staining for IgG, IgG1, as well as for St6gal1 and the specificity for Ova.

The volume of 5×10^6 splenic cells of the prepared cell suspensions (2.2.5.2) was transferred to a conical 96-well plate. For isotype controls or FMOs, cells from different conditions were pooled. The cells were pelleted at 300xg for 6 min at 4°C and the supernatant was discarded inverting the plate and clapping onto a tissue. The cells were washed with 200 µL cold FACS buffer, centrifuged (300xg, 4°C, 6 min) again and the supernatant discarded. For the staining of extracellular makers, the cells were resuspended in 100 µL of a master mix containing the following antibodies and reagents diluted in FACS buffer (Table 2.11).

Table 2-11 Staining panel for extracellular B cell staining from *in vivo* experiments

Marker	Fluorescence	Dilution
fixable viability dye	eFluor 780	1:1,000
B220	BV786	1:200
CD138	BV711	1:200
GL7	PerCP-Cy5.5	1:200
FAS	BV510	1:200
IgG Fc*	PE	1:200
IgG1	BV421	1:200
Ova	AF647	1:500

* optional

The cells were incubated for 30 min on ice in the dark and afterwards washed with 200 µL of FACS buffer (300xg, 4°C, 6 min). For the fixation and permeabilization 200 µL of Cytofix/Cytoperm was applied to the cells for 30 min at RT in the dark. Afterwards, cells were washed twice with PermWash buffer, first in 150 µL then in 200 µL, centrifuged and the supernatant was discarded. For the intracellular staining, the cell pellets were resuspended in 100 µL staining solution containing the following antibodies and reagents in PermWash buffer (Table 2.12). In one isotype control sample, the anti-St6gal1 antibody was substituted with normal, polyclonal goat IgG.

Table 2-12 Staining panel for intracellular B cell staining from *in vivo* experiments

Marker	Fluorescence	Dilution
IgG Fc*	PE	1:200
IgG1	BV421	1:200
Ova	AF647	1:500
St6gal1 / Goat isotype ctrl.**	AF488	1:50

* optional, ** in isotype control

The cells were stained for 45 min on ice in the dark, afterwards washed three times with 200 µL PermWash buffer (300xg, 4°C, 6 min) and resuspended in 200 µL FACS buffer. Before measuring, 400 µL of focusing fluid was added to each sample. The cells were measured at a flow rate of 200 µL/min. A stop option was set at 2.5 x 10^6 events.

2.2.5.4 Staining for Foxp3$^-$ T follicular helper and Foxp3$^+$ T follicular regulatory cells

T cells were stained for CXCR5 and ICOS to characterize T follicular cells as well as for Foxp3 to determine T follicular helper (Foxp3$^-$) or T follicular regulatory (Foxp3$^+$) cells.

T cell staining was performed using 2.5 x 10^6 splenic cells. The corresponding volume of the prepared cell suspensions (2.2.5.2.) was transferred onto a conical 96-well plate and centrifuged at 300xg for 6 min at 4°C. For isotype controls or FMOs, cells from different conditions were pooled. The supernatant was discarded by inverting the plate and clapping onto a tissue. The cells were additionally washed with 200 µL FACS buffer (300xg, 4°C, 6 min). For the extracellular staining the pellets were resolved in 100 µL mastermix containing antibodies/reagents against the following makers in FACS buffer (Table 2.13).

Table 2-13 Staining panel for extracellular T cell staining from *in vivo* experiments

Marker	Fluorescence	Dilution
fixable viability dye	eFluor 780	1:1,000
B220	BV786	1:200
CD4	BV711	1:200
CD8*	AF700	1:200
ICOS	PE-Cy7	1:200
CXCR5	Biotin	1:200

* optional

The cells were stained for 45 min on ice in the absence of light and washed with 200 µL FACS buffer (300xg, 4°C, 6 min). Afterwards, 100 µL of Streptavidin-BV605, diluted 1:100 in FACS buffer, were added, the cell pellets resolved and incubated for 20 min on ice in the dark. Cells were washed with 200 µL FACS buffer, centrifuged and the supernatant discarded.

In case of the IL-10 reporter mice, an additional pre-fixation was performed: A 2% phosphate buffered formaldehyde fixation solution was prepared diluting the 4.5% formaldehyde stock solution in PBS, 200 µL were added and incubated for 1 h at RT in the dark, after which the cells were spun down at 300xg, 4°C for 6 min and the fixation solution was discarded.

For regular fixation, True Nuclear™ fixation solution was freshly prepared by diluting the True Nuclear™ 4x fix concentrate in the appropriate diluents, 200 µL were added and the cells were fixed for 1h at RT in the dark. The cells were centrifuged (300xg, 4°C, 6 min) and the fixation solution discarded, followed by three washings steps with 200 µL of 1x eBioscience™ Foxp3 Perm buffer. The cell pellets were resuspended in 100 µL Foxp3 Perm buffer containing a Foxp3-AF647 antibody (1:200) for intranuclear staining. The cells were stained for 45 min at RT in the dark and subsequently washed three times with 200 µL Foxp3 Perm buffer (300xg, 4°C, 6 min), the supernatant was discarded, and the cell pellets resuspended in 200 µL FACS buffer. For measuring, 200 µL focusing fluid were added to each sample and cells were measured at a flow rate of 200 µL/min.

2.2.5.5 Cytokine staining in T cells

The cytokine staining in T cells was performed to determine varying cytokine expressions in different T cell subsets. For a better detection of the cytokines, cells were re-stimulated for at least four up to five hours in re-stimulation media before staining.

For re-stimulation, 3 mL/well of freshly prepared re-stimulation media were transferred onto a 6-well culture plate and, if possible, kept warm in advance. The volume corresponding to 1 x 10^7 cells of the prepared cell suspension (2.2.5.2) was added to the media and cells were incubated for approx. 4.5 h at 37°C and 5% CO_2.

Afterwards the cells were transferred to a 15 mL tube, kept on ice and pelleted at 300xg at 4°C for 6 min. The supernatant was discarded by inverting the tube and removing drops with a tissue. The cells were resuspended in the remaining liquid and transferred onto a conical 96-well plate. The wells were three-quarter filled with FACS buffer, the cells spun down (300xg, 4°C, 6 min) and the supernatant discarded by inverting the plate and clapping onto a tissue. For extracellular staining, the cells were resuspended in 100 µL of a master mix containing the below listed antibodies and reagents (Table 2.14) diluted in FACS buffer.

Table 2-14 Staining panel for extracellular cytokine staining in T cells from *in vivo* experiments

Marker	Fluorescence	Dilution
fixable viability dye	eFluor 780	1:1,000
B220	BV786	1:200
CD4	BV711	1:200
CD8*	AF700	1:200
ICOS	PE-Cy7	1:200
CXCR5	Biotin	1:200

* optional

The cells were stained for 45 min on ice in the dark and washed with 200 µL FACS buffer (300xg, 4°C, 6 min). After removing the supernatant, the cells were resuspended in 100 µL Streptavidin-BV421 diluted 1:100 in FACS buffer and incubated for 20 min on ice in the dark.

Different fixation protocols were used for the cytokine staining. Cells with the IL-10-GFP signal were pre-fixed (additional fixation) in 200 µL of a 2% phosphate buffered formaldehyde fixation solution, which was prepared from a 4.5% formaldehyde stock solution in PBS, for 1h at RT in the dark. The cells were centrifuged at 300xg, 4°C for 6 min and the fixation solution was discarded.

In this thesis two different regular fixation and intracellular staining combinations were used, depending on the Foxp3 staining. In case of Foxp3 staining, a fixation allowing subsequent intranuclear staining was necessary and combination II was performed. Otherwise, combination I was performed.

I. For the regular fixation 200 µL of Cytofix/Cytoperm were added directly on the cell pellet, the cells resuspended and incubated for 30 min at RT in the dark. To remove the fixation solution, the cells were washed twice, first with 150 µL later with 200 µL of PermWash buffer (300xg and 4°C for 6 min). The supernatant was discarded. For the intracellular staining 100 µL of a master mix in PermWash buffer containing the following antibodies (Table 2.15) were applied for 30 min on ice in the dark. Afterwards, the cells were washed twice with 200 µL PermWash buffer.

Table 2-15 Staining panel for intracellular cytokine staining in T cells from *in vivo* experiments after Cytofix/Cytoperm fixation

Marker	Fluorescence	Dilution
CD4	BV711	1:200
IFN-γ	AF647	1:200
IL-17A	PE	1:200

II. For the regular fixation, including Foxp3 staining, 200 µL of a freshly prepared True Nuclear™ fixation (True Nuclear™ 4x fix concentrate diluted in the appropriate diluents) were added directly to the cell pellet and the resuspended cells incubated for 1 h at RT in the dark. The fixation solution was discarded after centrifugation at 300xg and 4°C for 6 min. The cells were additionally washed twice with 200 µL Foxp3 Perm buffer (300xg, 4°C, 6 min). Intracellular and – nuclear staining was performed in 100 µL Foxp3 Perm buffer of a master mix containing the following antibodies (Table 2.16). The cells were stained for 45 min at RT in the dark and thereafter washed twice with 200 µL Foxp3 Perm buffer (300xg, 4°C, 6 min).

Table 2-16 Staining panel for intracellular and -nuclear cytokine staining in T cells from *in vivo* experiments after True Nuclear™ fixation

Marker	Fluorescence	Dilution
Foxp3	AF647	1:200
IFN-γ	PE	1:200

After the staining was completed, the pellets were resuspended in 200 µL FACS buffer and mixed with additional 200 µL focusing fluid. The measurement was conducted at the Attune NxT using a flow rate of 200 µL/min.

2.2.5.6 Staining of cultured B cells

The volume corresponding to 2.5 – 5 x 10^5 cells of the collected cell suspensions (2.2.4.2) was transferred into in new 15 mL tube. For isotype controls or FMOs, cells from different conditions were pooled. The cells were pelleted (300xg, 4°C, 6 min) and the supernatant discarded by inverting the falcon and remove drops with a tissue. The cells were resuspended in the remaining liquid and transferred onto a conical 96-well plate. The wells were filled up three-quarter with FACS buffer and the plate centrifuged at 300xg, 4°C for 6 min. The supernatant was removed by inverting the plate and clapping onto a tissue. The cells were washed with 200 µL FACS buffer (300xg, 4°C, 6 min) and the supernatant discarded. To block the Fc receptors on the B cell surface to avoid unwanted signals, the cells were resuspended in 50 µL of a master mix containing a mouse CD16/32 antibody (2 µg/mL) and incubated for 15 min on ice. For the staining of extracellular makers, 50 µL of a master mix containing the following antibodies and reagents (Table 2.17) were added to the Fc block solution and further incubated for 30 min on ice in the dark.

Table 2-17 Staining panel for extracellular B cell staining after B cell culture

Marker	Fluorescence	Dilution
fixable viability dye	eFluor 780	1:500
B220	BV786	1:100
CD138	BV711	1:100

The cells were washed with 200 µL FACS buffer, spun down (300xg, 4°C, 6 min) and the supernatant discarded. Fixation was performed in 100 µL Cytofix/Cytoperm for 30 min at RT in the dark, after which 200 µL of PermWash buffer was added and the cells pelleted at 300xg, 4°C for 6 min. The supernatant was discarded. For the detection of the St6gal1 expression, the cells were stained in 100 µL of a master mix containing the St6gal1-AF488 antibody (1:50) in PermWash buffer for 45 min on ice in the dark. Simultaneously, one isotype control sample was incubated with a goat-IgG control antibody diluted 1:50 in PermWash buffer. The cells were washed twice in 200 µL PermWash buffer (300xg, 4°C, 6 min) and the cell pellets were resuspended in 200 µL FACS buffer. Before measuring 200 µL focusing fluid were added.

2.2.6 Statistical analysis

The statistical analysis was calculated in Prism v. 6.04. A normal distribution was assumed. Two normally distributed groups were analyzed by an unpaired two-tailed t-test, multi-comparison of >2 groups were analyzed by one-way Analysis of Variance (ANOVA). Significant differences were considered starting at P< 0.05 (*P< 0.05; **P<0.01; ***P< 0.001; ****P< 0.0001). Data are shown as mean values, the error bars indicate the standard error of the mean (± SEM). If not otherwise stated, results represent one of two to three independent experiments. For the St6gal1 expression levels, the median fluorescence intensity (MFI) in the St6gal1-AF488 channel of the according cell population was calculated in FlowJo for each individual sample. The mean values ± SEM of the individual MFIs of one group are presented in the figures.

3 Results

3.1 Different adjuvants have distinct effects on the immune response and antibody production upon immunization.

Adjuvants are reagents used in vaccination to initiate, direct and/or enhance the immune response to the applied foreign antigen. Adjuvants have distinct potentials to induce and influence the immune response, granting each adjuvant a unique immunological signature. It has been shown for a few adjuvants that the serum antibody titer, the type of IgG Fc *N*-glycosylation, the St6gal1 expression level in plasma cells (PCs), as well as T cell differentiation is influenced by the choice of adjuvant and a subsequent assertion of the inflammatory potential of the respective adjuvant has been suggested (Bartsch, 2019; Hess et al., 2013; Oefner et al., 2012). To understand the potential of different adjuvants on the induced type of IgG Fc glycosylation might help to improve vaccination protocols.

Here, a broad panel of adjuvants was tested in a mouse immunization model with the soluble T cell-dependent foreign protein antigen Ovalbumin (Ova) to investigate their inflammatory potential and the IgG Fc *N*-glycosylation programming. The applied adjuvants were the preclinical used water-in-oil adjuvants incomplete Freund adjuvant (IFA) and enriched complete Freund adjuvant (eCFA, containing 5 mg/mL *Mtb* in IFA), the clinically used water-in-oil adjuvant Montanide (water-in-oil adjuvant), Alum (aluminium hydroxide), Adju-Phos (aluminium phosphate) and the squalene-based water-in-oil adjuvant AddaVax, that are presently used in human vaccination and the TLR agonists MPLA, R848 and Poly(I:C) (Tab. 3-1).
Furthermore, different influence factors and molecular mechanisms were investigated more precisely for a better understanding of the immune response and IgG Fc *N*-glycosylation programming on a cellular level after immunization.

Table 3-1 List of adjuvants with their type classification and targets

List of tested adjuvants with their type, target and concentrations used in the experiments. *isoelectric point of Ova is 4.5 → at pH 7.2 Ova is negatively charged

	Type	Adjuvant Conc.	Adjuvant/mouse	Clinical stage
eCFA	Water-in-oil emulsion	5 mg/mL *Mtb* in IFA	100 µL, 500 µg *Mtb*	pre-clinical
IFA	Water-in-oil emulsion	-	100 µL	pre-clinical
Montanide	Water-in-oil emulsion	-	100 µL	licensed
Alum	Aluminium-based (anion-binder)*	2%	1%	licensed
Adju-Phos	Aluminium-based (cation-binder)*	2%	1%	licensed
AddaVax	Squalene emulsion (similar formulation to MF59)	-	100 µL	licensed
R848	TLR agonist	1 mg/mL	100 µg	Clinical trials
MPLA-SM	TLR agonist	1 mg/mL	10 µg	licensed (in combination)
Poly(I:C)	TLR agonist	1 mg/mL	100 µg	pre-clinical
TDB	Cord factor of *Mtb* (C-type lectin agonist)	1 mg/mL	100 µg	pre-clinical

3.1.1 Different adjuvants have a distinct effect on the distribution and titers of serum IgG subclasses as well as their Fc *N*-glycosylation

First, the potential of the different adjuvants on the induction of IgG antibody production and inflammatory glycosylation patterns was investigated. Therefore, mice were immunized intraperitoneally (i.p.) with Ova in combination with the different adjuvants on day 0. The immune response was boosted on day 28 with a second i.p. injection of Ova (without antigen). Serum was taken weekly, except for day 33. Here, serum was taken 5 days, instead of 7 days, after the boost due to the faster immune response after a second antigen contact. The Ova^+ IgG subclass titer and Fc *N*-glycosylation patterns were analyzed by ELISA or LC-MS, respectively (Fig 3-1).

The water-in-oil adjuvants eCFA and IFA had the strongest induction of anti-Ova IgG antibodies followed by the water-in-oil adjuvant Montanide and the aluminium-based adjuvants Alum and Adju-Phos. The squalene-based adjuvant AddaVax as well as the TLR-agonists only showed moderate induction of total IgG antibodies after the first immunization, yet strong increases were detected after the boost. A similar trend, as seen for anti-Ova total IgG, was obtained for the anti-Ova IgG1 subclass. The highest IgG1 induction was reached by the water-in-oil co-stimuli followed by Alum and Adju-Phos. The other adjuvants only showed moderate increases of IgG1 antibodies. For all IgG subclasses eCFA showed a dominant effect. Anti-Ova IgG2 antibodies were in addition to IFA and eCFA promoted by MPLA and Poly(I:C). Especially the IgG2c subclass showed a strong induction following Poly(I:C) immunization, with an augmented increase after the boost. The Ova-specific IgG3 antibody titers were generally low, with only slight induction through eCFA and IFA. No effect of the boost on day 28 was detected for the IgG3 subclass (Fig 3-1 A-B).

The Fc *N*-glycosylation patterns of anti-Ova subclass antibodies induced after immunization with the different adjuvants were analyzed by LC-MS. In this method, anti-Ova antibodies were purified from the serum samples using an Ova-coupled sepharose. Purified anti-Ova antibodies were enzymatically digested by trypsin, resulting in glycopeptides of a specific amino acid sequence plus the attached glycan. These glycopeptides get further separated from non-glycosylated peptides by LC and subsequently analyzed in MS. The obtained mass to charge (m/z) values are subclass-specific, dependent on the amino acid sequence of the CH2 part. IgG2c and IgG2b cannot

be distinguished in this method; therefore, IgG2c and IgG2b were analyzed together as IgG2. The measured glycosylation patterns were assigned to one of the nine glycopeptide groups (G0, G1, G2, G3, G4, G1S1, G2S1, G3S1 and G2S2). Bisecting glycopeptides were not detected. Glycopeptides lacking fucose were detected with peak intensities <2% and therefore added to their corresponding group out of the mentioned 9 groups. In this experiment, all IgG3 and some IgG2 signals were too low and had to be excluded from the analysis. For a better overview, all groups containing at least one sialic acid residue were merged to one "sialylation" group and compared with the agalactosylated "G0" glycans.

In the comparison of the two subclasses, IgG1 and IgG2, IgG2 had higher sialylation levels and less G0 than IgG1 (Fig 3-1 C-D). This is in line with previous publications, in which C57BL/6 mice had higher sialylation and galactosylation levels in the IgG2 subclass compared with IgG1 (de Haan et al., 2017; Kao et al., 2017; Pfeifle et al., 2017) and is probably caused by a better accessibility of the transferases to the CH2 domain of the IgG2 subclass.

On day 7, all immunization groups revealed high IgG1 and IgG2 galactosylation (low agalactosylation; G0) and sialylation levels exceeding the sialylation status of untreated mice in the bulk IgG1 and IgG2 subclass fraction (Fig. 3-1 C-D). Because all immune responses were dominated by the anti-Ova IgG1 subclass, the anti-Ova IgG2 subclass glycopeptide analysis did not result in valuable data for all samples or time points (Fig. 3-1 D). These early produced galactosylated and sialylated antibodies might be generated in a fast immune response of extrafollicular PCs (Wang et al., 2015).

Starting at day 14 the decisive effect of the adjuvants on the antigen-specific Fc *N*-glycosylation becomes distinct. The IgG sialylation decreases for all adjuvants, which could be shown for all anti-Ova IgG1 and several IgG2 data. However, the decrease is differently strong, and the adjuvants can be divided into three groups. The first group is represented by the water-in-oil adjuvants IFA and Montanide, showing a highly inflammatory effect promoting a switch to less galactoslyated (enhanced agalactosylation; G0) and less sialylated anti-Ova IgG1 and IgG2 antibodies. The inflammatory potential of IFA could even be enhanced by the addition of *Mtb*, which is reflected in the even more decreased galactosylation and more decreased sialylation of anti-Ova IgG1 and IgG2 caused by eCFA (second group). On the contrary, the remaining adjuvants, forming the third group, induced a higher galactosylated and sialylated antibody response. Due to the

distinct effects in the later immune response (from day 14 on), it can be assumed that the inflammatory potential of the adjuvants to program the Fc *N*-glycosylation in particular accounts for increased long-lived PC responses from probably GC-derived PCs. Furthermore, the comparable trends between the IgG1 and IgG2 subclasses suggest a common regulatory mechanism working for both, IgG1 and IgG2, subclasses.

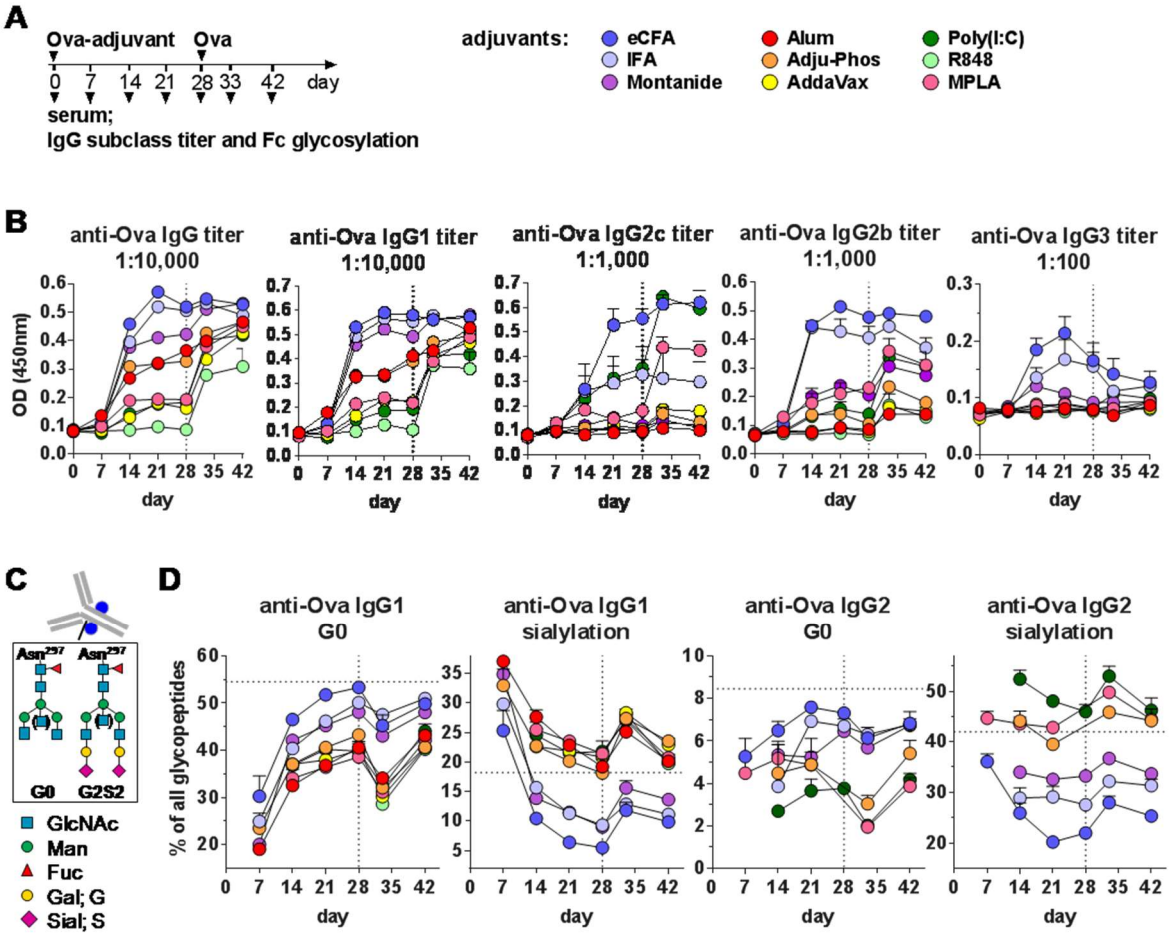

Figure 3-1: Different adjuvants induce distinct IgG subclass titer and Fc glycosylation patterns after immunization with soluble foreign protein antigen.

(A) The experimental design: C57BL/6 WT female mice were immunized with Ova plus adjuvant and boosted with Ova without adjuvant on day 28 (n=5 / group), and the investigated adjuvants with their color code. **(B)** Serum titers of anti-Ova total IgG and IgG subclasses on the indicated time points, used serum dilution are shown. **(C)** Schematic structure of two possible IgG Fc *N*-glycans (G0 and G2S2) coupled to asparagine-297 (Asn^{297}). **(D)** Percentages of serum anti-Ova IgG1 and IgG2 (IgG2c + IgG2b) Fc agalactosylation (corresponding glycopeptides G0) and sialylation (G1S1 + G2S1 + G3S1 + G2S2) at the indicated time points. Several IgG2 signals were too low for a reliable analysis, because of lower titers, and therefore excluded. Horizontal dashed lines indicate average bulk serum IgG1 or IgG2 glycosylation traits before immunization; vertical dashed lines represent the Ova boost on day 28. The here presented results were published in Bartsch et al., 2020 (Bartsch et al., 2020).

After re-exposure to the antigen (without adjuvant) on day 28, similar dynamics as before were determined. Increasing sialylation was detected for each immunization group on day 33, implying a fast, extrafollicular response by newly activated B cells and/or reactivated memory B cells. A following decrease of the sialylation on day 42 showed similar differences between the groups as detected before the boost, which reinforces the theory that the inflammatory effect of the different adjuvants was mainly exerted in longer-lived PC responses, probably in GC-derived PCs. During the time course, immunizations with adjuvants from group three had higher IgG sialylation levels than untreated mice, eventually reaching the untreated baseline levels on around day 28 and after day 42 in both, the IgG1 and IgG2 subclass.

In summary, upon day 14 after the first immunization and upon day 42 after the second immunization, the inflammatory potential of the adjuvants seemed to determine a corresponding IgG1 as well as IgG2 galalytosylation and sialylation level.

This experiment was performed in cooperation with Yannic Bartsch, who conducted anti-Ova IgG subclass the ELISA. The LC-MS analysis of the anti-Ova IgG subclass Fc *N*-glycosylation was performed by Sander Wagt in collaboration with the laboratory of Prof. Manfred Wuhrer in Leiden, Netherlands.

The here presented results have been successfully published in Yannic C. Bartsch*, Simon Eschweiler*, Alexei Leliavski*, Hanna Lunding*, Sander Wagt*, …., Christoph Hölscher, Manfred Wuhrer, and Marc Ehlers. IgG Fc sialylation is regulated during the germinal center reaction with different adjuvants. *The Journal of Allergy and Clinical Immunology, 2020* (*these authors contributed equally) (Bartsch et al., 2020).

3.1.2 IgG Fc glycosylation correlates with St6gal1 expression level in antigen-specific IgG$^+$ plasma cells and germinal center B cells

The α2,6-sialyltransferase (St6gal1) is the enzyme responsible for the transfer of sialic acid to galactose and hence necessary for the IgG Fc alpha2,6-sialylation, the connection identified for Igg Fc sialylation. The Fc *N*-glycosylation patterns of IgG antibodies have been correlated with the expression level of the St6gal1 in antigen-specific PCs (Bartsch et al., 2018; Oefner et al., 2012; Ohmi et al., 2016; Pfeifle et al., 2017). In accordance with the agalactosylation and sialylation levels (Fig. 3-1), it has been shown recently that the distinct Fc *N*-glycosylation patterns of IgG antibodies induced by Ova-eCFA and Ova-

Alum upon day 14 correlated with the expression level of the St6gal1 in antigen-specific PCs on day 14 (late response), but not on day 8 (early response)(Bartsch, 2019), reinforcing the idea of a GC-dependent Fc glycosylation programming.

To determine the St6gal1 expression level under the influence of different co-stimuli and its dependency on the GC reaction, mice were immunized i.p. with Ova in combination with eCFA, IFA, Montanide, Alum, MPLA or AddaVax (all three adjuvant groups described above have been included) and splenic $CD138^+$ PCs as well as $GL7^+$ Fas^+ GC B cells were investigated by flow cytometry on day 12 (Fig. 3-2). Splenocytes were additionally stained extra- and intracellularly with anti-IgG1 and Ova as well as intracellularly with anti-St6gal1.

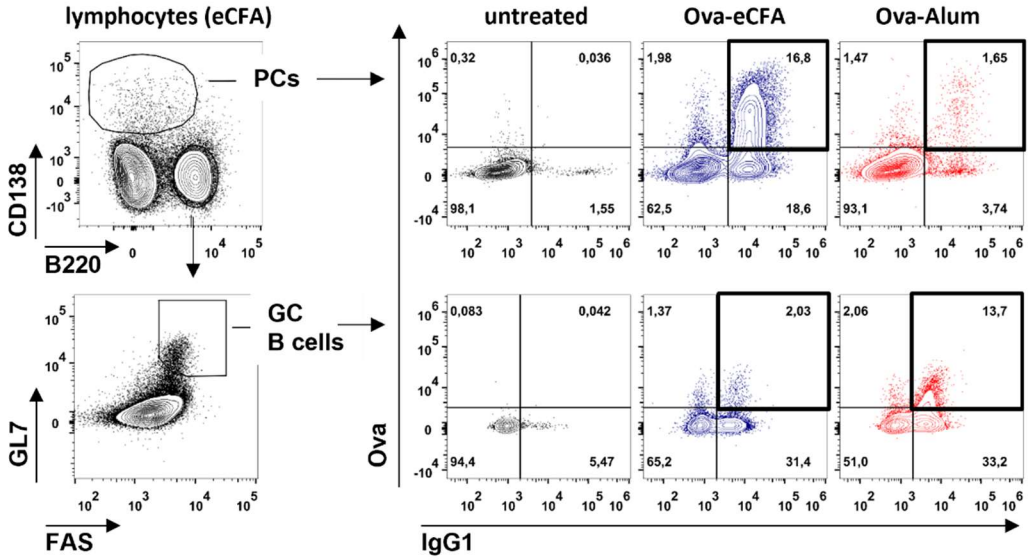

Figure 3-2: Gating strategy to identify antigen-specific (Ova^+) $IgG1^+$ PCs and GC B cells

Cell populations were defined on pre-gated viable single lymphocytes after Ova-eCFA and Ova-Alum immunization on day 12 compared with untreated control. The here presented gating scheme was part of Bartsch et al., 2020 (Bartsch et al., 2020).

The differences of the induced Fc *N*-glycosylation patterns between the adjuvants (Fig. 3-1) were reflected in the respective St6gal1 protein expression levels in Ova-specific IgG1 as well as IgG2/3 (IgG1−IgG1) PCs and GCs (Fig. 3-3 and Fig. S-1 + S-2). Not all samples showed enough anti-Ova IgG2/3 PCs and GCs for a sufficient analysis. Montanide and particularly IFA tend to down-regulate the St6gal1 level in $IgG1^+$ and $IgG2/3^+$ Ova^+ $CD138^+$ PCs as well as in $IgG1^+$ and $IgG2/3^+$ Ova^+ $GL7^+$ Fas^+ GC B cells compared to St6gal1 expression levels in IgG1 and IgG2/3 PCs as well as GC B cells of untreated mice (Fig. 3-3 and Fig. S1 + S2). Intriguingly, the addition of *Mtb* to IFA (eCFA) further enhanced the pro-inflammatory effect, leading to a significant reduction of the St6gal1 level induced by eCFA compared to IFA and Montanide. The adjuvants Alum, MPLA and AddaVax showed no significant downregulation of the St6gal1 level in comparison to levels in corresponding PCs and GC B cells of untreated mice. These findings highly suggest that an adjuvant-dependent IgG Fc *N*-glycosylation programming takes (at least partially) place during the GC reaction.

In the following, experiments were mainly performed with IFA, eCFA and Alum to further investigate the influence of water-in-oil adjuvants and *Mtb* on the IgG Fc glycosylation. Alum was used as a mild inflammatory adjuvant for comparison. Using these three Adjuvants each of the before assigned adjuvant groups was represented.

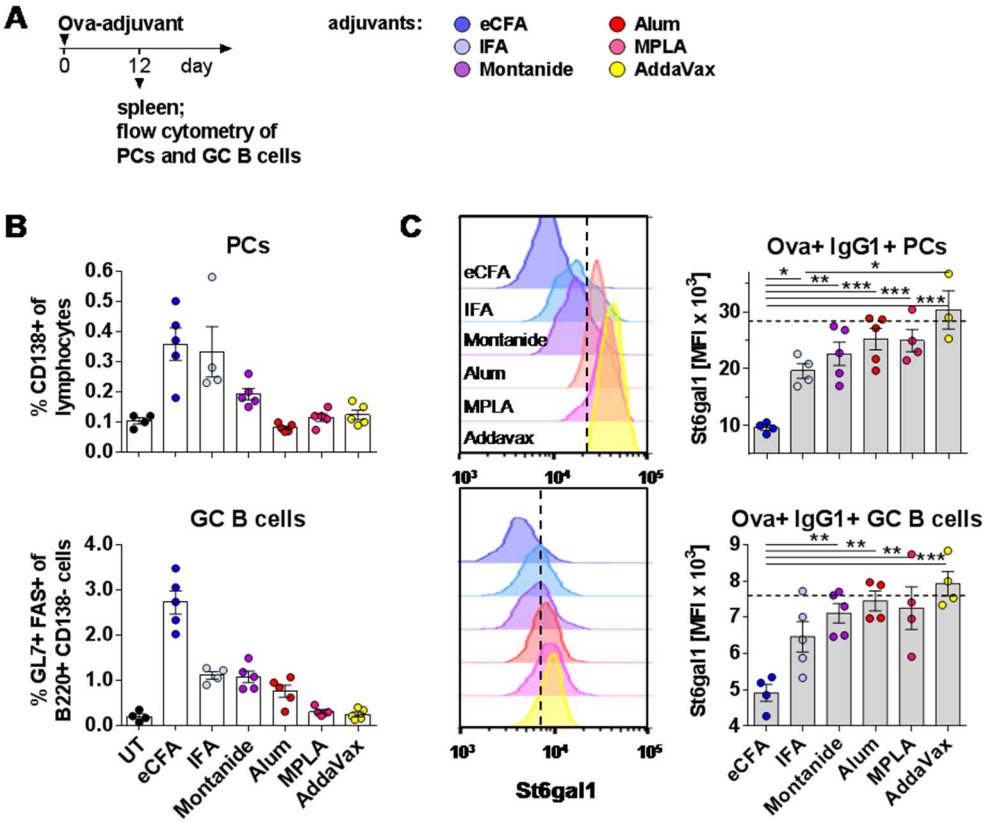

Figure 3-3: Different adjuvants induce distinct St6gal1 protein expression levels in splenic antigen-specific IgG1$^+$ PCs as well as GC B cells

(A) Experimental design: C57BL/6 WT female mice were immunized with Ova plus distinct adjuvants (incl. color code) and spleens were taken on day 12 for analysis by flow cytometry (n=4-5/group). **(B)** Frequencies of splenic PCs and GC B cells on day 12 **(C)** Intracellular St6gal1 protein expression (median fluorescence intensity [MFI]), including overlay histograms of representative mice of Ova-specific (Ova$^+$) IgG1$^+$ PCs and GC B cells on day 12. Graph points indicate individual mice. Horizontal dashed lines indicate the average St6gal1 expression level in IgG1$^+$ PCs or GC B cells of untreated mice. Vertical dashed lines are orientation guides. One of two independent experiments is shown. The data presented in this figure were published in Bartsch et al., 2020 (Bartsch et al., 2020).

The above-described experiment was accomplished in a team effort with Yannic Bartsch and Vanessa Krémer. The results were successfully published in Yannic C. Bartsch*, Simon Eschweiler*, Alexei Leliavski*, Hanna Lunding*, Sander Wagt*, … Christoph Hölscher, Manfred Wuhrer,.and Marc Ehlers. IgG Fc sialylation is regulated during the germinal center reaction with different adjuvants. *The Journal of Allergy and Clinical Immunology, 2020* (*these authors contributed equally) (Bartsch et al., 2020).

3.1.3 Strong co-stimuli enhance T follicular cell differentiation and the T_{FH}/T_{FR} cell ratio

Different immune cells stand in close cell-cell contact and mutual dependency during the GC reaction. After the B cell activation through antigen-presenting cells (APCs), $CXCR5^+$ $ICOS^+$ T follicular cells engage with follicular B cells regulating its B cell response. T follicular cells can be further subdivided into $Foxp3^-$ T_{FH} cells, favoring a strong B cell response, and their counterpart $Foxp3^+$ T_{FR} cells, responsible for self-regulation. Based on the previous experiments, an investigation of the influence of different adjuvants on the T follicular cell response was conducted for a better understanding of the GC reaction.

To investigate the T follicular cell status during the GC reaction upon immunization with different adjuvants, C57BL/6 wild type mice were immunized with Ova in combination with eCFA, IFA and Alum. Splenic $CXCR5^+$ $ICOS^+$ T follicular cells were analyzed by flow cytometry on day 12 (Fig. 3-4).

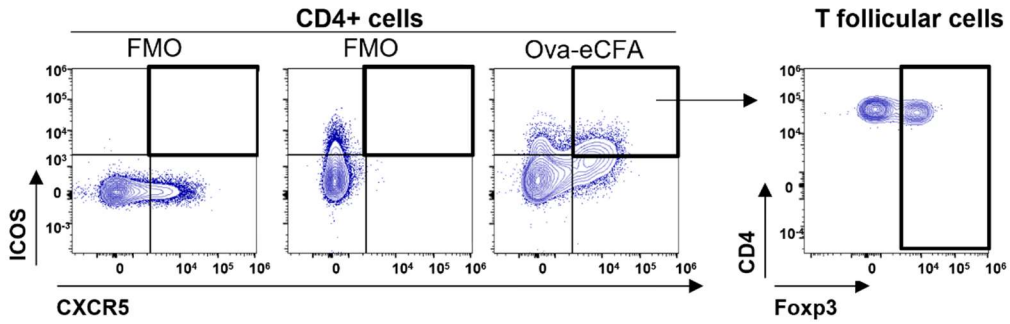

Figure 3-4: Gating strategy to identify splenic $CXCR5^+$ $ICOS^+$ T follicular, $Foxp3^-$ T_{FH} and $Foxp3^+$ T_{FR} cells

Cell populations were defined on pre-gated viable single lymphocytes after Ova-eCFA immunization. CXCR5 and ICOS FMOs (fluorescence minus one) are shown. This gating scheme was published similarly in Bartsch et al., 2020 (Bartsch et al., 2020).

The immunization with the water-in-oil adjuvant IFA strongly induced T follicular and T_{FH} cell differentiation (Fig. 3-5). This effect was even enhanced by additional *Mtb* in T follicular cells and significantly enhanced in T_{FH} cell responses. Lower amounts of T follicular and T_{FH} cells were induced by the Alum immunization (Fig. 3-5). Intriguingly, the T_{FH} cell frequencies showed a moderate correlation to the frequencies of GC B cells and a reverse correlation to the St6gal1 expression level in Ova^+ IgG^+ GC B cells and PCs

as well as to the antigen-specific IgG subclass Fc *N*-glycosylation patterns (Fig. 3-3 + Fig. S1 + S2 and 3-1, respectively). These data support a recently reported study demonstrating that water-in-oil adjuvants induce a strong T follicular cell response (Batten et al., 2010). Surprisingly, the frequencies for T_{FR} cells were highest for IFA with significant differences to Alum. However, regarding the T_{FH}/T_{FR} ratio, IFA and Alum were comparable, whereas eCFA induced a T_{FH}/T_{FR} ratio more than twice as high (Fig. 3-5).

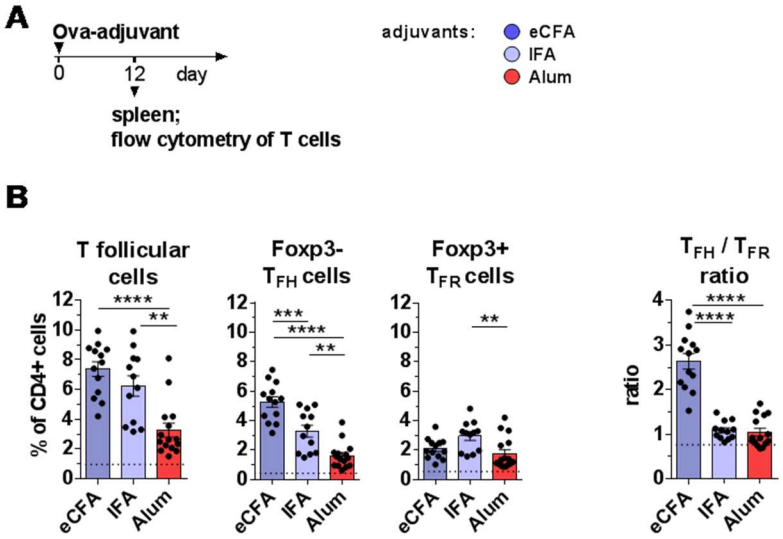

Figure 3-5: Adjuvants induce distinct T follicular cell responses and T_{FH}/T_{FR} ratios

(A) Experimental design: C57BL/6 WT female mice were immunized with Ova plus the indicated distinct adjuvants (incl. color code) and spleens were taken on day 12 for analysis by flow cytometry (n=4-5/group). **(B)** Frequencies of splenic T follicular, T_{FH} and T_{FR} cells and the T_{FH}/T_{FR} cell ratio. Horizontal dashed lines indicate average cell population frequencies of untreated mice. The graph shows pooled data of four independent experiments. The here presented data were partially published in Bartsch et al., 2020 (Bartsch et al., 2020).

These findings suggest that the downregulation of the St6gal1 protein expression level induced by immunizations with the water-in-oil adjuvant IFA depends on the T follicular response that can be further enhanced by the addition of *Mtb*.

The pooled experiments were performed together with Yannic Bartsch. These data were partially published in Yannic C. Bartsch*, Simon Eschweiler*, Alexei Leliavski*, Hanna Lunding*, Sander Wagt*, …. Christoph Hölscher, Manfred Wuhrer, and Marc Ehlers. IgG Fc sialylation is regulated during the germinal center reaction with different adjuvants. *The Journal of Allergy and Clinical Immunology, 2020* (*these authors contributed equally) (Bartsch et al., 2020).

3.2 Adjuvants containing *Mtb* or its cord factor promote T follicular cell differentiation and enhance T_{FH}/T_{FR} ratios correlating with strong germinal center reactions and reduced IgG Fc glycosylation programming

In section 3.1 it was clearly displayed, that addition of *Mtb* to IFA had a strong pro-inflammatory effect on the GC reaction and IgG Fc glycosylation. Further previous investigations have shown that the *Mtb* effect also enhances the T_{FH17} response (Bartsch et al., 2020; Hess et al., 2013). Anyhow, it was not clear if these effects were additive effects particularly depending on the water-in-oil adjuvant.

To study the effect of *Mtb* on the GC reaction independently of water-in-oil adjuvants and whether this effect can be restricted to a single *Mtb* molecule, *Mtb* and TDB were used in combination with Alum for immunization. TDB is a synthetic analog of the cord factor trehalose 6,6'-dimycolate, which is a major component of the bacterial outer membrane binding to the Mincle receptor.

C57BL/6 wild type mice were immunized with Ova mixed with Alum containing 5 mg/mL *Mtb* (Alum + *Mtb*), Alum with TDB, or Alum alone for comparison. Splenic T follicular and GC B cells were analyzed via flow cytometry and serum IgG subclass glycosylation via LC-MS on day 12.

Both co-stimuli, *Mtb* and TDB, significantly enhanced T follicular and T_{FH} cell responses compared to only Alum, but *Mtb* with a higher extent. T_{FR} cell responses were nearly unchanged compared to immunizations with only Alum. Consequently, also the T_{FH}/T_{FR} ratios were enhanced, when Alum was combined with *Mtb* or TDB, with an almost 3-fold higher ratio of Alum + *Mtb* compared to Alum. Furthermore, an increase of T_{FH17} cells was detected after immunization with Alum in combination with *Mtb* as well as with TDB compared to only Alum (Fig. 3-6 A-C). A trend, similar to the T_{FH} cells, was detected in the frequencies of the GC B cells. Reduced St6gal1 expression levels in Ova^+ $IgG1^+$ GC B cells, significantly for Alum + *Mtb* and a trend for Alum + TDB, indicated a strong GC reaction induced by *Mtb* and TDB, the latter to a lesser, only tending extent (Fig 3-6 D, E).

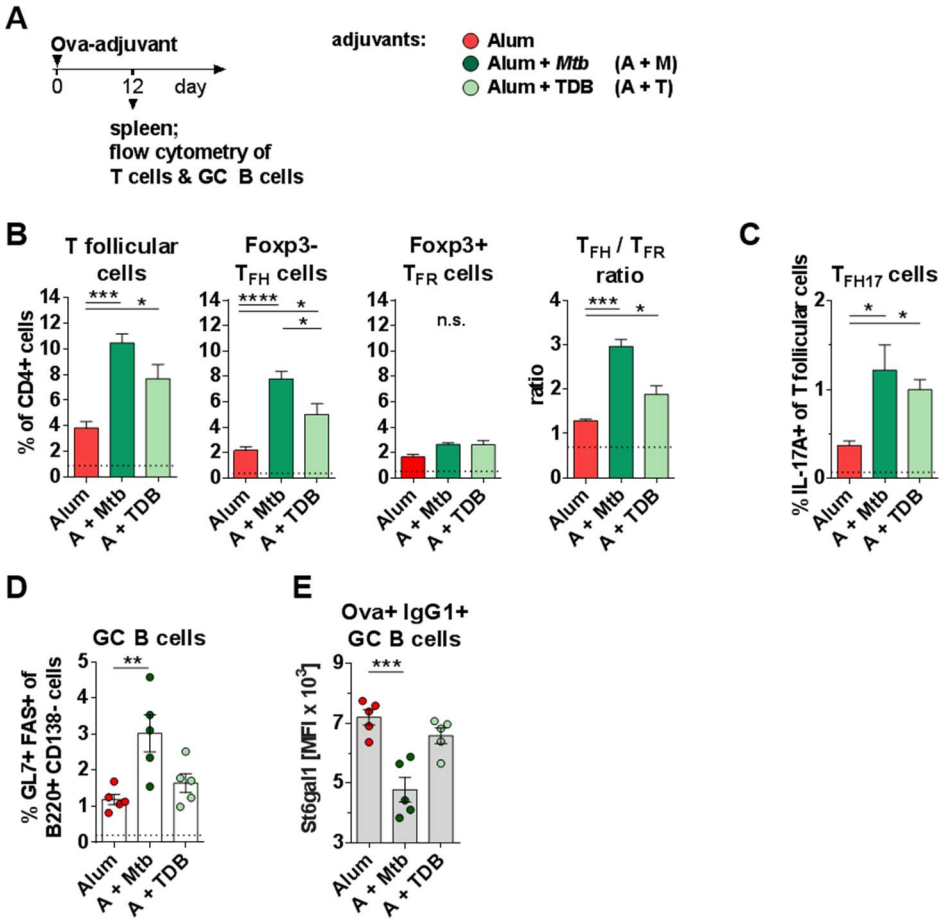

Figure 3-6: *Mtb* or TDB combined with Alum induce T follicular and T_{FH17} cell differentiation, increase T_{FH}/T_{FR} ratios and down-regulate St6gal1 expression in GC B cells

(A) Experimental design: C57BL/6 WT female mice were immunized with Ova in combination with the indicated distinct adjuvants (Alum, Alum+ *Mtb*, Alum+TDB, incl. color code) and spleens were taken on day 12 for analysis by flow cytometry (n=4-5/group). **(B)** Frequencies of splenic T follicular, T_{FH} and T_{FR} cells and the T_{FH}/T_{FR} cell ratio. **(C)** Frequencies of T_{FH17} cells. **(D)** Frequencies of splenic GC B cells. **(E)** Intracellular St6gal1 protein expression (median fluorescence intensity [MFI]) in Ova-specific (Ova^+) $IgG1^+$ PCs and GC B cells on day 12. Graph points indicate individual mice. Horizontal dashed lines indicate average cell population frequencies of untreated mice. These results were published in Bartsch et al., 2020 (Bartsch et al., 2020).

In accordance with the St6gal1 protein expression, the anti-Ova IgG1 subclass glycosylation levels shift to a more inflammatory pattern after immunization with Alum + *Mtb* and Alum + TDB compared to only Alum on day 12 (Fig. 3-7). In particular, eCFA (IFA + *Mtb*) and Alum + *Mtb* showed a significantly reduced anti-Ova IgG1 Fc galactosylation and sialylation compared to IFA or Alum. The reduction in sialylation was moderate for TDB, yet still significant compared to Alum. An analysis of the IgG2 Fc glycosylation could not be performed due to insufficient IgG2 induction by Alum and Alum combinations.

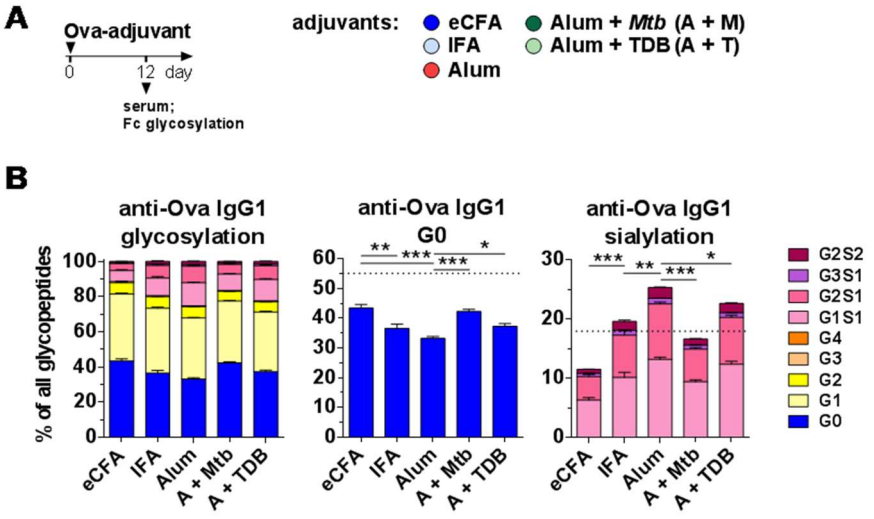

Figure 3-7: *Mtb* or TDB combined with IFA or Alum induce a pro-inflammatory shift in the IgG1 glycosylation pattern

(A) Experimental design: C57BL/6 WT female mice were immunized with Ova plus the indicated distinct adjuvants (eCFA, IFA, Alum, Alum + *Mtb*, Alum + TDB). Sera were taken on day 12 for glycan analysis via LC-MS. **(B)** Percentages of serum anti-Ova IgG1 Fc *N*-glycans, agalactosylation (G0) and sialylation (G1S1 + G2S1 + G3S1 + G2S2) at day 12. The data presented in this figure were published in Bartsch et al., 2020 (Bartsch et al., 2020).

In a further experiment, testing the effect of TDB alone on the anti-Ova Fc *N*-glycosylation in comparison to Alum, Alum + TDB and eCFA on day 12 or 14, only TDB and only Alum showed similar anti-Ova IgG1 Fc sialylation levels, whereas the combination of Alum and TDB further decreased sialylation, indicating an additive effect (Fig. 3-8). IgG2 levels, induced by Alum, TDB and Alum + TDB, were too low for a sufficient Fc glycosylation analysis.

In total, these data revealed that the *Mtb* effect in IFA on the differentiation of T_{FH} and T_{FH17} cells, the T_{FH}/T_{FR} ratio and the downregulation of the St6gal1 expression level, as well as the anti-Ova IgG1 Fc galactosylation and sialylation is not restricted to water-in-oil adjuvants, but also exhibited when *Mtb* or its cord factor homolog were added to Alum. Since the effect of Alum with *Mtb* was still not as strong as the effect of *Mtb* in IFA, and TDB alone was not as potent as *Mtb* mixed with Alum, a stronger effect of IFA compared to Alum and of *Mtb* compared to TDB were visible.

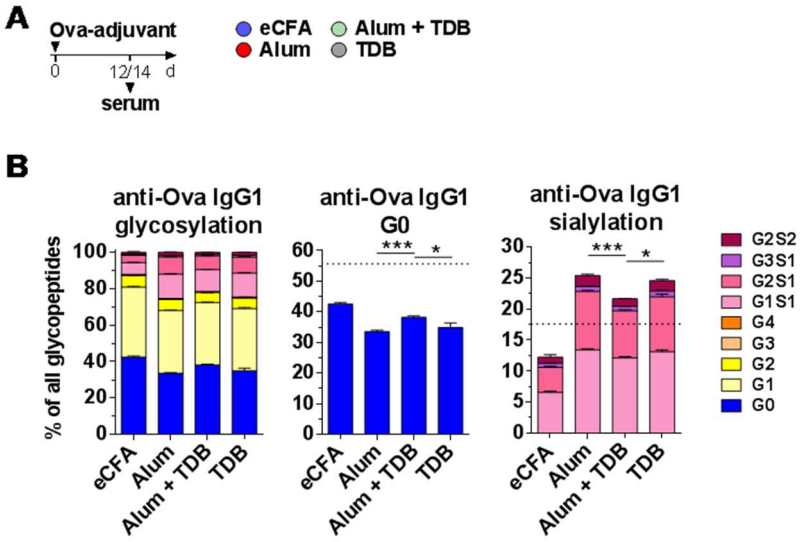

Figure 3-8: Combination of Alum and TDB increases their potential to down-regulate the IgG1 galactosylation and sialylation

(A) Experimental design: C57BL/6 WT female mice were immunized with Ova plus the indicated distinct adjuvants (eCFA, Alum, Alum + TDB, TDB). Sera were taken on day 12 or 14 for glycan analysis via LC-MS. **(B)** Percentages of serum anti-Ova IgG1 Fc *N*-glycans, agalactosylation (G0) and sialylation (G1S1 + G2S1 + G3S1 + G2S2). The horizontal dashed lines represent average bulk IgG1 agalactosylation and sialylation before immunization. Results of two independent experiments were pooled. The here presented results were published in Bartsch et al., 2020 (Bartsch et al., 2020).

The experiments from section 3.2 were published in Yannic C. Bartsch*, Simon Eschweiler*, Alexei Leliavski*, Hanna Lunding*, Sander Wagt*, …. Christoph Hölscher, Manfred Wuhrer, and Marc Ehlers. IgG Fc sialylation is regulated during the germinal center reaction with different adjuvants. *The Journal of Allergy and Clinical Immunology, 2020* (*these authors contributed equally).

3.3 The role of the interleukin-27 – interferon-γ axis on the germinal center reaction and IgG Fc *N*-glycosylation

After discovering the importance of T follicular, T_{FH} and T_{FH17} cells as well as the T_{FH}/T_{FR} ratio on the downregulation of the St6gal1 and IgG glycosylation levels, the attention was drawn to the identification of other T_{FH} subsets. Therefore, the role of the IL-27 receptor (IL-27R) and the IFN-γ cytokine were investigated, due to reports stating IL-27 to contribute to the differentiation of T follicular cells and induction of the T_H1 response (Yoshida et al., 2001).

3.3.1 The inflammatory potential of the adjuvants eCFA, IFA and Alum is mediated by interleukin-27 receptor signaling

To determine the influence of the IL-27R, wild type and IL-27R KO mice on the C75BL/6 background were immunized with Ova in combination with eCFA, IFA and Alum. On day 12 splenic B and T cells were analyzed via flow cytometry and serum IgG subclass Fc *N*-glycosylation was measured by LC-MS.

The frequencies of T follicular, T_{FH} and T_{FR} cells, and subsequently the T_{FH}/T_{FR} ratio, as well as the frequencies of GC B cells and PCs from the IL-27R KO mice showed no differences compared to wild type mice (Fig. 3-9 A-C). Yet, the St6gal1 expression was gradually higher in IL-27R KO mice, with significant differences detected after immunization with the water-in-oil adjuvants eCFA and IFA in Ova^+ $IgG1^+$ GC B cells and PCs. For Alum only a trend was detected in Ova^+ $IgG1^+$ PCs (Fig. 3-9 D). In accordance, a similar pattern was obtained for the Ova-specific IgG1 galactosylation and sialylation (Fig. 3-10). The IL-27R KO mice showed significantly higher anti-Ova IgG1 galactosylation and sialylation levels compared to the wild type after immunization with the same adjuvant (Fig. 3-10). No reliable IgG2 Fc glycosylation analysis could be performed for the IL-27R KO mice, due to weak IgG2 titers.

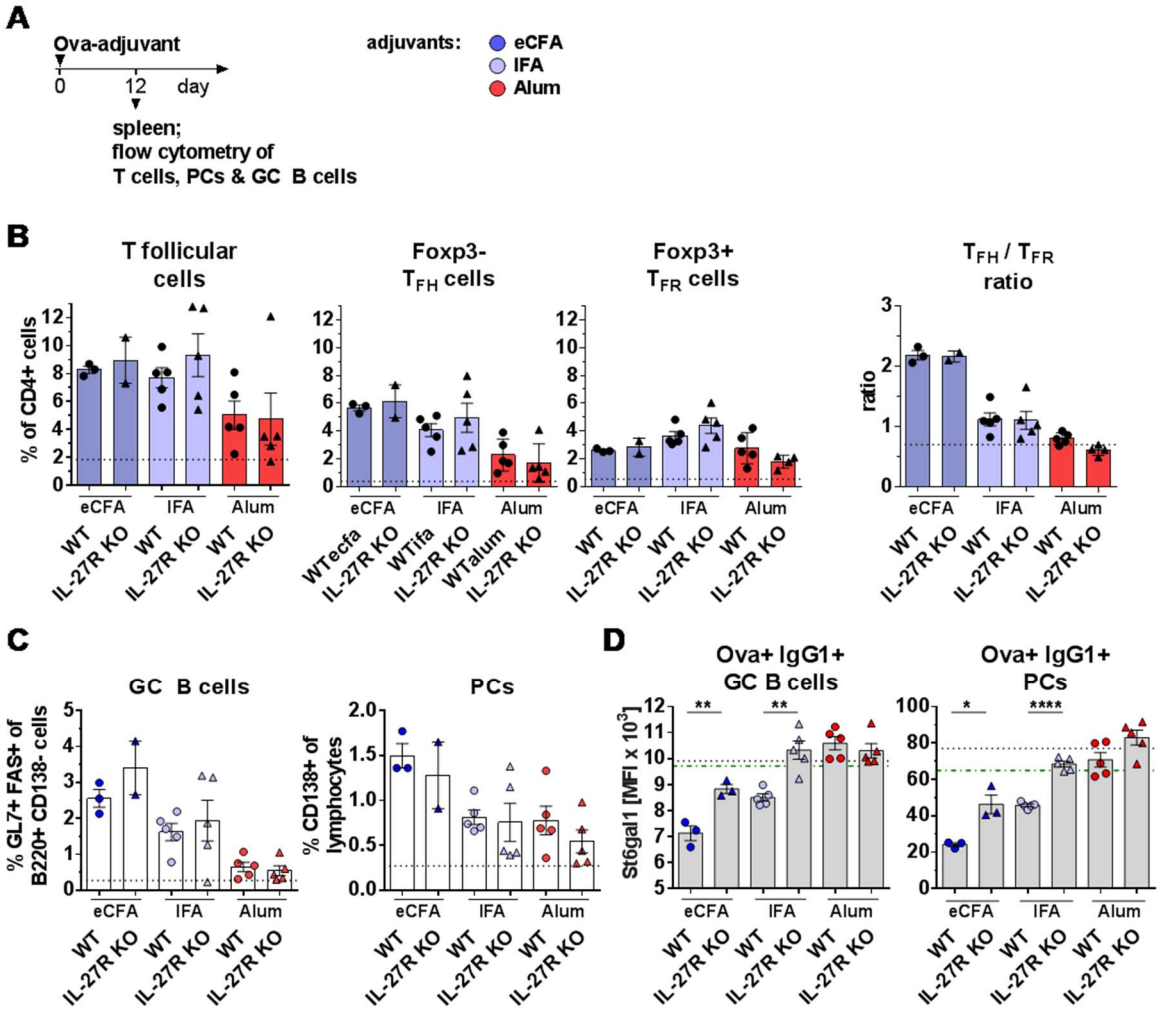

Figure 3-9: IL-27R signaling is necessary to down-regulate St6gal1 expression in GC B cells and PCs upon immunization with inflammatory adjuvants

(A) Experimental design: female WT and IL27R-KO (wsx-1) mice on C57BL/6 background were immunized with Ova plus the indicated adjuvants (eCFA, IFA, Alum, incl. color code) and cells were analyzed on day 12 by flow cytometry (n=2-5/group). **(B)** Frequencies of splenic T follicular, T_{FH} and T_{FR} cells and the T_{FH}/T_{FR} cell ratio. **(C)** Frequencies of GC B cells and PCs. Horizontal dashed lines indicate average cell population frequencies of untreated mice. **(D)** Intracellular St6gal1 protein expression (median fluorescence intensity [MFI]) in Ova-specific (Ova^+) $IgG1^+$ GC B cells and PCs on day 12. Graph points indicate individual mice. Horizontal dashed lines indicate average MFI St6gal1 expression levels in $IgG1^+$ GC B cells or PCs of untreated mice (black for WT mice, green for IL27R KO mice). Parts of the data presented in this figure were published in Bartsch et al., 2020 (Bartsch et al., 2020).

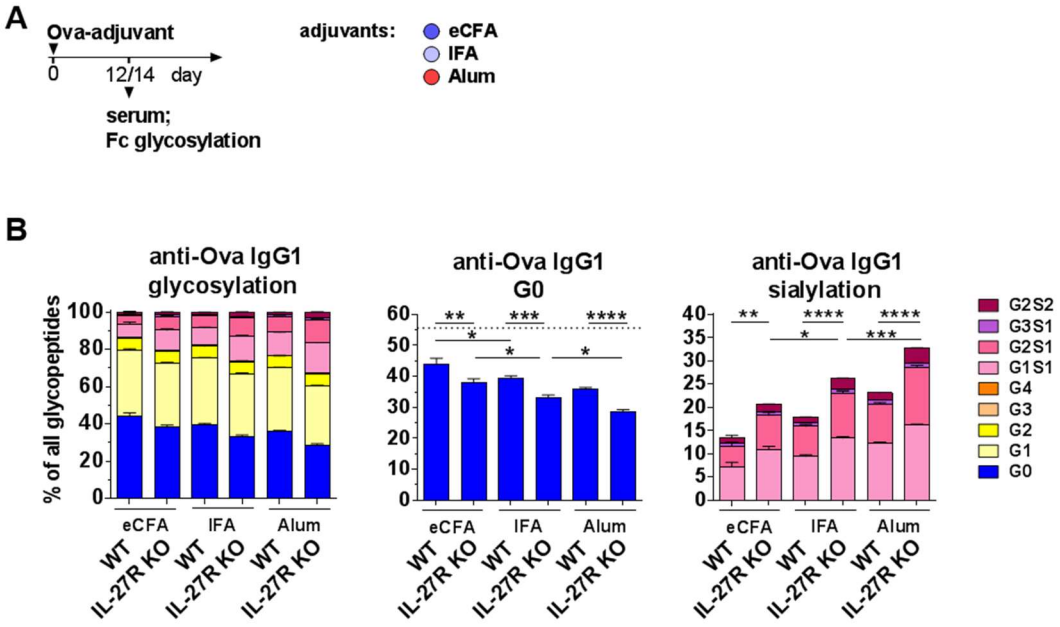

Figure 3-10: IL-27R signaling is necessary to down-regulate the IgG Fc galactosylation and sialylation upon immunization with inflammatory adjuvants

(A) Experimental design: female WT and IL27R-KO (wsx-1) mice on C57BL/6 background were immunized with Ova plus the indicated adjuvants and sera were analyzed on day 12 in LC-MS (n=3-5/group). (B) Serum anti-Ova IgG1 agalagtosylation (G0) and sialylation (G1S1 + G2S1 + G3S1 + G2S2). Horizontal dashed lines represent average bulk IgG1 G0 and sialylation before immunization. Results of three independent experiments were pooled. The here presented data were partially published in Bartsch et al., 2020.

These results were partially published in Yannic C. Bartsch*, Simon Eschweiler*, Alexei Leliavski*, Hanna Lunding*, Sander Wagt*, …. Christoph Hölscher, Manfred Wuhrer, and Marc Ehlers. IgG Fc sialylation is regulated during the germinal center reaction with different adjuvants. *The Journal of Allergy and Clinical Immunology, 2020* (*these authors contributed equally).

So far, the results pointed out an effect of the IL-27R signaling on the regulation of the St6gal1 and IgG glycosylation that neither influenced the total T follicular cell responses nor the T_{FH}/T_{FR} ratio. Therefore, the influence of IL-27R signaling on the induction of the certain T_{FH} cell subset was analyzed in the following.

3.3.2 Interleukin-27 receptor signaling induces inflammatory GC reactions through the induction of IFN-γ-producing T_{FH1} cells

To further investigate a potential influence of IFN-γ-producing T_H1 cells as well as T_{FH1} cells induced by the water-in-oil adjuvants eCFA and IFA, T cells were analyzed for IFN-γ-producing T_H1 and T_{FH1} subset cells. This analysis was conducted from the data of the same experiment stated in section 3.3.1; wild type and IL-27R KO mice were immunized with Ova in combination with eCFA, IFA and Alum and splenic T cells were analyzed on day 12 by flow cytometry.

Interestingly, the frequencies of T_H1 cells were comparable in wild type and IL-27R KO mice after immunization with eCFA, IFA and Alum, whereas the frequencies of T_{FH1} cells were intensely reduced in the IL-27R KO compared to the wild type (Fig. 3-11).

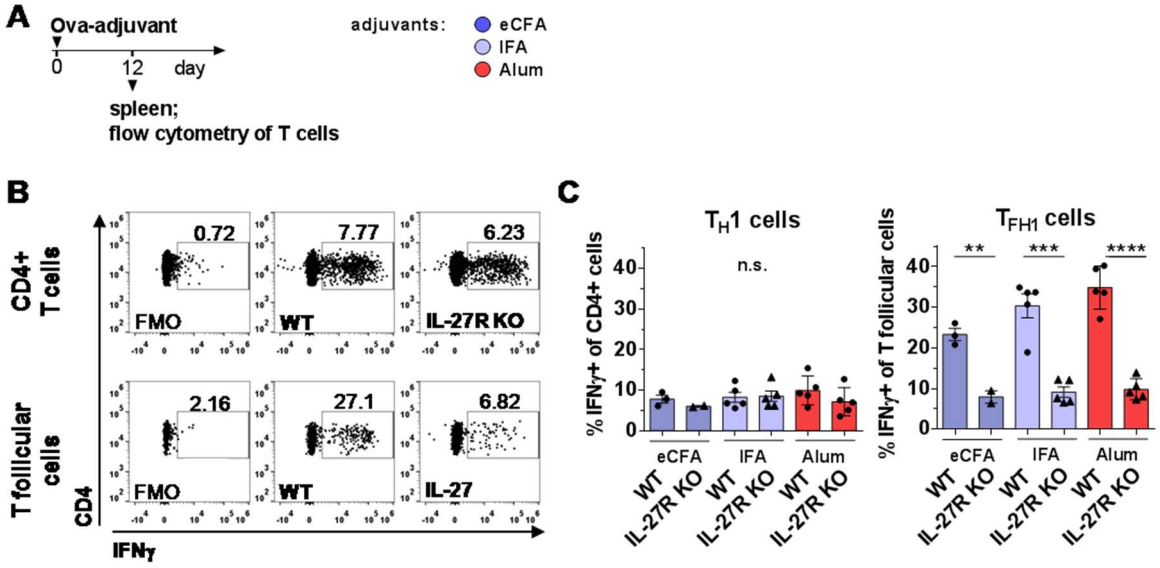

Figure 3-11: IL27R-signaling induces IFN-γ-producing T_{FH1} cells

(A) Experimental design: female WT and IL27R-KO (wsx-1) mice on C57BL/6 background were immunized with Ova plus the indicated adjuvants (eCFA, IFA, Alum, incl. color code) and cells were analyzed on day 12 by flow cytometry (N=2-5/group). **(B)** Representing flow cytometry IFN-γ staining (including IFN-γ FMOs) of splenic $CD4^+$ (upper row) or $CXC5^+$ $ICOS^+$ $CD4^+$ (lower row) T follicular cells after immunization with eCFA. **(C)** Frequencies of splenic IFN-γ^+ T_H1 and T_{FH1} cells. The data of this figure were partially published in Bartsch et al., 2020 (Bartsch et al., 2020).

In total, the data revealed an effect of the IL-27R on the St6gal1 expression and IgG Fc *N*-glycosylation through the induction of IFN-γ-producing T_{FH1} cells. The substantial role of IFN-γ producing T follicular cells, but not IFN-γ-producing $CD4^+$ T cells, confirms that the regulation of the IgG glycosylation programming takes place during the GC reaction.

Parts of the here presented data were published in Yannic C. Bartsch*, Simon Eschweiler*, Alexei Leliavski*, Hanna Lunding*, Sander Wagt*, ….Christoph Hölscher, Manfred Wuhrer and Marc Ehlers. IgG Fc sialylation is regulated during the germinal center reaction with different adjuvants. *The Journal of Allergy and Clinical Immunology, 2020* (*these authors contributed equally).

Rather unexpectedly, there was not only a high number of eCFA- and IFA- induced T_{FH1} cells, but also a high number of T_{FH1} cells induced by Alum.

Strikingly, Alum-immunized wild type mice showed the highest frequencies of IFN-γ-producing T follicular cells and the largest difference and highest significance between the wild type and the IL-27R KO. Since IFN-γ is a potent inflammatory cytokine, this observation leads to the question, why immunization with Alum does not reduce the St6gal1 expression as well as IgG galactosylation and sialylation as much as eCFA, IFA and Montanide (adjuvant groups 1 and 2 in Fig. 3-1 & 3-2).

The issue of the high frequencies of IFN-γ^+ cells in Alum was attended to in the following investigation.

3.3.3 The pro-inflammatory effect of IFN-γ is reduced by the regulatory cytokine Interleukin-10

IFN-γ is known to be a strong pro-inflammatory cytokine, in great extent produced by T_H1 cells. Nevertheless, its potential to down-regulate the St6gal1 expression and IgG galactosylation and sialylation is somehow diminished after immunization with Alum. Even though Alum-immunized mice had high frequencies of IFN-γ-producing T follicular cells (Fig. 3-11), the St6gal1 protein level and IgG glycosylation exhibit only a mild pro-inflammatory effect (Fig. 3-1 & 3-2). Thus, there must be components with additive reverse effects. One possibility for reverse effects might be the presence of IFN-γ^+ IL-10^+ T regulatory type 1 (Tr1) cells (Awasthi et al., 2007; Fitzgerald et al., 2007). Besides

inducing T_H1 responses, IL-27 was also reported to induce the differentiation of Tr1 cells (Awasthi et al., 2007; Fitzgerald et al., 2007; Iwasaki et al., 2015; Pot et al., 2009). Tr1 cells are $CD4^+$ $Foxp3^-$ T cells featuring the production of the regulatory cytokine IL-10. Thus, they have a strong ability to suppress inflammation and promote immune tolerance (Awasthi et al., 2007; Fitzgerald et al., 2007). The immunosuppressive properties of these cells might be substantial for the reduced inflammation after Alum immunizations.

To determine this idea, IFN-γ and IL-10 production was studied *in vivo*. IL-10 reporter mice were immunized with Ova in combination with eCFA, IFA and Alum. On day 12 IFN-γ and IL-10 production in splenic $CD4^+$ T helper, $CD4^+$ $CXCR5^+$ $ICOS^+$ T follicular cells and their $Foxp3^-$ T_{FH} and $Foxp3^+$ T_{FR} subsets were measured. The focus was set on the IFN-γ and IL-10 single positive populations as well as on the IFN-γ and IL-10 double positive population.

As seen before, no significant differences in the IFN-γ levels were detected in $CD4^+$ T helper cells, which was true for each cell population (IFN-γ^+ IL-10^-, IFN-γ^- IL-10^+, IFN-γ^+ IL-10^+) (Fig. 3-12). In T follicular cells in turn, the IFN-γ level increased significantly from eCFA over IFA to Alum. However, the same pattern was seen for IFN-γ^+ IL-10^+ double positive cells. No difference was seen in the IFN-γ^- IL-10^+ single positive cell population (Fig. 3-13). These gradually increased level of IFN-γ^+ IL-10^- single and IFN-γ^+ IL-10^+ double positive cells was further associated with the $Foxp3^-$ T_{FH} cell subset, showing significant differences between eCFA and Alum. This was not the case for the $Foxp3^+$ T_{FR} subpopulation, displaying similar frequencies of IFN-γ or IL-10 producing cells; double positive cells were too rare to analyze (Fig. 3-13). The fact that differences of IFN-γ^+ IL-10^+ double positive cells were seen in $Foxp3^-$ T_{FH} cells indicated a gradual increase of follicular Tr1 cells from eCFA over IFA to Alum. Thus, even though Alum induced the highest frequencies of single positive IFN-γ^+ $Foxp3^-$ T_{FH1} cells, also the frequency of IFN-γ^+ IL-10^+ follicular Tr1 cells was highest upon Alum immunization, suggesting that several IFN-γ+ TFH cells exist as follicular Tr1 cells and counter regulate the effect of IFN-γ on the IgG Fc glycosylation.

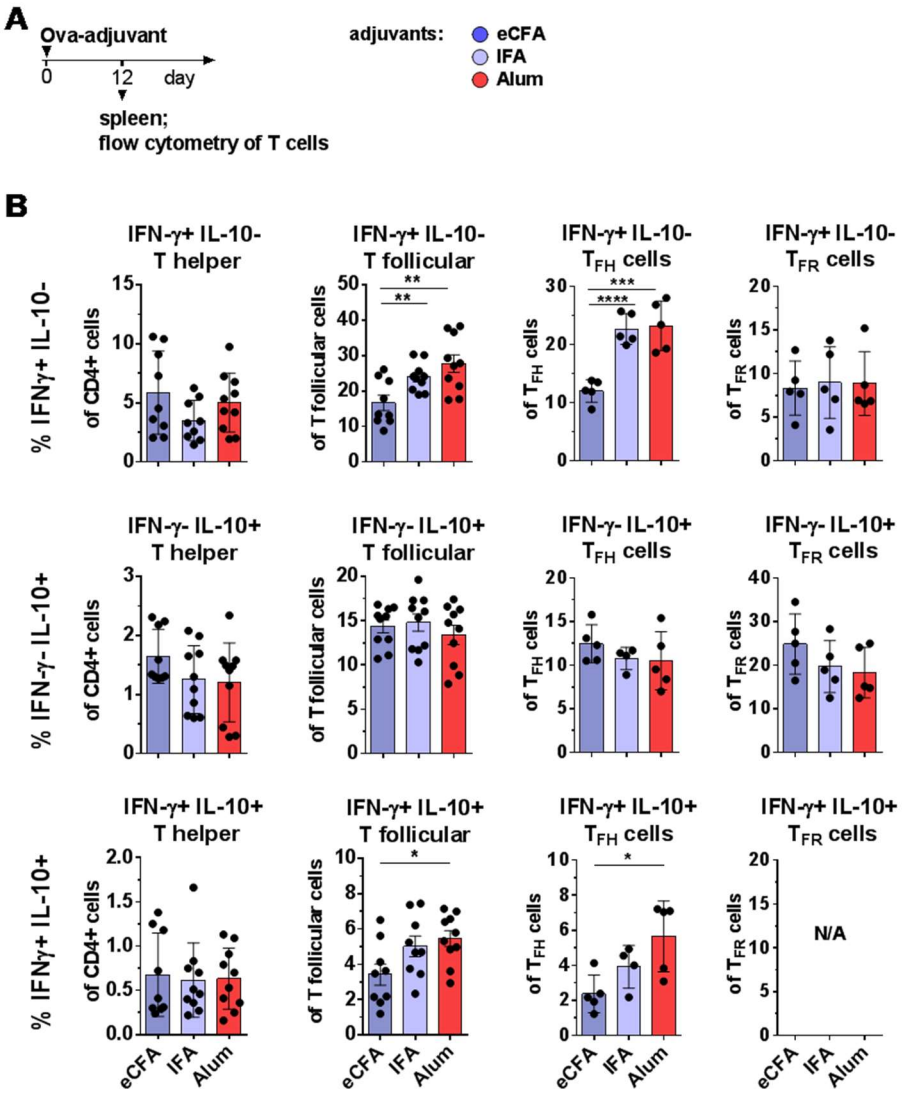

Figure 3-12: The mild adjuvant Alum strongly induces IFN-γ and IL-10 double positive T follicular cells

(A) Experimental design: C57BL/6 WT female mice were immunized with Ova plus the indicated distinct adjuvants (incl. color code) and spleens were taken on day 12 for T cell analysis by flow cytometry (n=4-5/group). **(B)** Frequencies of IFN-γ^+ IL-10^-, IFN-γ^- IL-10^+ and IFN-γ^+ IL-10^+ cells of splenic $CD4^+$ T helper, $CXCR5^+$ $ICOS^+$ $CD4^+$ T follicular, $Foxp3^-$ T_{FH} and $Foxp3^+$ T_{FR} cells.

Next, the effect of IFN-γ alone or in combination with IL-10 on B cells was tested in a B cell culture. Naïve B cells were isolated from a spleen of an untreated wild type mouse and cultured for 4 days with LPS, as B cell stimulus, and optional with IFN-γ or IFN-γ plus IL-10. The intracellular expression level of the St6gal1 was detected by flow cytometry.

As expected, IFN-γ was able to down-regulate the St6gal1 protein expression significantly in B cells. In combination with IL-10 however this effect was strongly reduced (Fig. 3-12), revealing the reverse effect of the two cytokines on the B cell programming.

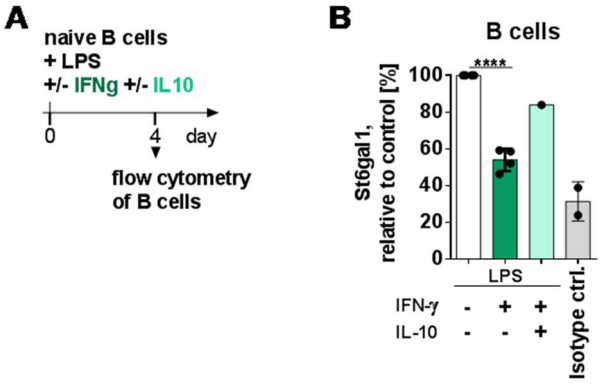

Figure 3-13: Reduction of St6gal1 expression in B cells induced by IFN-γ can be inhibited by IL-10
(A) Experimental design: Naïve B cells were isolated from untreated WT mice and cultured with LPS and optionally with IFN-γ and IL-10 for four days at 37°C and 5% CO_2. **(B)** Relative St6gal1 expression normalized to the LPS control.

Taken together, all three adjuvants induced equal frequencies of IL-10 single positive cells, but Alum induced the highest amount of IL-10 and IFN-γ double positive follicular Tr1 cells compared with eCFA and IFA. The data suggests that these cells probably operate by reversing the down-regulating effect of INF-γ on the St6gal1 through IL-10 production, as shown in the B cell culture. Since these observations were made in follicular T cells, an impact on the germinal center reaction can be assumed.

3.4 The pro-inflammatory cytokines interferon-γ and IL-17 augment each other to induce low glycosylated IgG antibodies

The previous section revealed that the B cell programming and IgG glycosylation are influenced by the T_H1 cytokine IFN-γ. First, an IFN-γ dependent effect of the IL-27R was demonstrated. Next, the potential of IFN-γ to down-regulate the St6gal1 expression level in naïve B cells, which could be impaired by the anti-inflammatory cytokine IL-10, was proven. Additionally, the effect of *Mtb* (section 3.2) could be associated with an increase in T_{FH17} cells, indicating an influence of the T_H17 cytokine IL-17. A substantial effect of IL-17 on the B cell programming and antigen-specific IgG subclass glycosylation was already demonstrated (Bartsch, 2019; Hess et al., 2013; Pfeifle et al., 2017). Also, former studies showed an impact of INF-γ in IFNgRI KO mice and IL-17 in IL-17R KO mice as well as an additive effect of IFN-γ and IL-17 in IFNgRI x IL-17R double KO (dKO) mice after immunization with CFA on the glycosylation level of antigen-specific total serum IgG. Yet so far, these effects were not investigated for the IgG subclasses or in B cell FACS analysis after eCFA immunization (Hess et al., 2013). Based on these results, here, the effects of IFN-γ signaling and IFN-γ signaling in combination with IL-17 signaling were additionally tested on the B cell differentiation at its St6gal1 expression levels as well as on the Ova-specific IgG1 subclass Fc *N*-glycosylation after immunization with the strong and *Mtb*-dependent adjuvant eCFA.

To investigate the influence on the B cell programming in GC B cells and PCs, as well as on the antigen-specific IgG subclass glycosylation after immunization with a strong adjuvant, IFNgRI KO mice, IFNgRI x IL-17R dKO mice, alongside with IL-17R KO, and WT mice were immunized i.p. with Ova in eCFA. As a control for a moderate immunization effect, an additional WT group was immunized with Ova plus Alum. On day 12 splenic B and T cells and antigen-specific serum IgG subclass glycosylation were measured by flow cytometry or LC-MS, respectively.

All KO strains showed a distinct reduction in T follicular cell frequencies compared to the eCFA-immunized WT mice, yet still higher frequencies than WT mice immunized with Alum. The induction of GC B cell was rather undefined. The IFNgRI KO had less GC B cells than the other strains immunized with eCFA, which were comparable among each

other (Fig. 3-14 A-B). Accordingly, a reduced potential of the IFNgRI KO strain to down-regulate the St6gal1 expression was detected in $Ova^{+}IgG1^{+}$ PCs. In the double KO strain, this potential was strongly diminished, leading to St6gal1 expression levels comparable to Alum-induced expression levels. The same effect was seen as a trend in Ova^{+} $IgG1^{+}$ GC B cells for the IFNgRI single KO strain and significantly for the dKO strain (Fig. 3-14 C). In a comparison of all three KO strains, the two single KOs showed a similar effect, whereas the double KO showed increased St6gal1 levels compared to both single KOs.

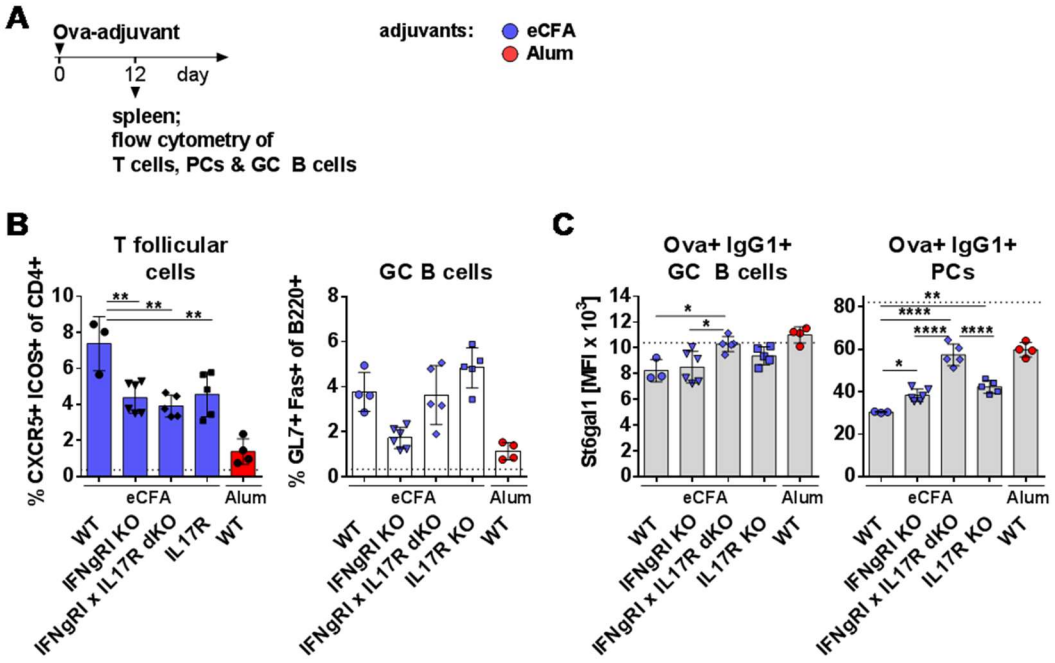

Figure 3-14: T_H1 cytokine IFN-γ- and T_H17 cytokine IL-17-signaling enhance T follicular cell differentiation and downregulate St6gal1 expression

(A) Experimental design: female WT IFNgRI KO, IL-17R KO and IFNgRI x IL-17R double KO mice on C57BL/6 background were immunized with Ova plus the indicated adjuvants. Splenic T and B cells were analyzed on day 12 by flow cytometry (N=3-5/group). **(B)** Frequencies of splenic T follicular cells and GC B cells. **(C)** Intracellular St6gal1 protein expression (median fluorescence intensity [MFI]) in Ova-specific (Ova^{+}) $IgG1^{+}$ GC B cells and PCs on day 12. Graph points indicate individual mice. Horizontal dashed lines indicate average St6gal1 expression levels in $IgG1^{+}$ GC B cells or PCs of untreated WT mice.

In line with the B and T cell analysis, anti-Ova IgG1 galactosylation increased in the IFNgRI KO and the IFNgRI x IL-17R dKO strain compared to the WT after the same immunization. The Ova^+ $IgG1^+$ sialylation increased in the IFNgRI KO and in an even greater content in the IFNgRI x IL-17R dKO strain compared to the eCFA-immunized WT (Fig. 3-15). Similar shifts were observed in a trend in serum anti-Ova IgG2 antibodies (Fig. S-3) containing the IgG2c isotype, which IFN-γ induces dominantly (Huang et al., 1993; Snapper and Paul, 1987).

Since the two single KO strains showed comparable St6gal1 expression and Ova^+ $IgG1^+$ sialylation levels, but significantly lower St6gal1 levels and in a trend lower Ova^+ $IgG1^+$ sialylation compared to the dKO strain, an additive effect of IFN-γ and IL-17 can be suggested.

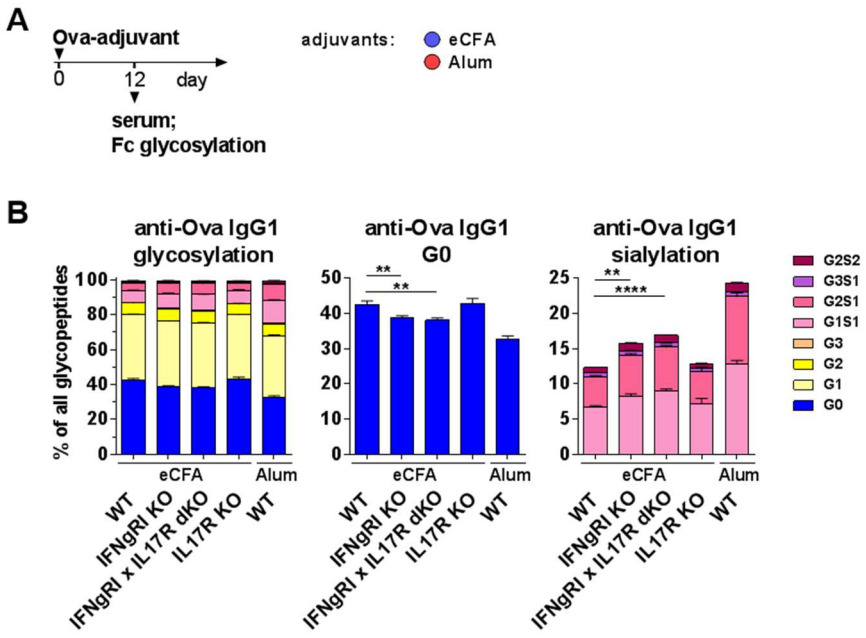

Figure 3-15: T_H1 cytokine IFN-γ- and T_H17 cytokine IL-17-signaling decrease antigen-specific IgG1 galactosylation and sialylation

(A) Experimental design: female WT, IFNgRI KO, IL-17R KO and IFNgRI x IL-17R double KO mice on C57BL/6 background were immunized with Ova plus the indicated adjuvants. Serum was analyzed on day 12 in LC-MS (N=3-5/group). **(B)** Serum anti-Ova IgG1 Fc *N*-glycans, agalagtosylation (G0) and sialylation (G1S1 + G2S1 + G3S1 + G2S2). The results from three independent experiments were pooled.

These data support the finding of a T_H1-dependent effect. Furthermore, an additive effect of the T_H1 cytokine IFN-γ and the T_H17 cytokine IL-17 on the expression level of the St6gal1 and the following antigen-specific IgG subclass glycosylation was determined. The impact of different adjuvants on the B cell programming is highly dependent on the induction of these two pro-inflammatory cytokines.

4 Discussion

4.1 The type of IgG Fc *N*-glycosylation pattern correlates with the adjuvant-induced GC reaction

The here presented data showed that a soluble protein antigen (here Ova) together with different adjuvants induce distinct GC responses, resulting in distinct antigen-specific IgG antibody titers, St6gal1 expression levels and corresponding IgG Fc glycosylation patterns. The adjuvant effects could be linked to an IL-27-dependent induction of T_{FH1} cells, an induction of T_{FH17} cells and a T_{FH}/T_{FR} cell ratio dependency.

4.1.1 The IgG Fc *N*-glycosylation programming takes place in the GC

Ova together with the water-in-oil adjuvants IFA and Montanide induced high antigen-specific IgG titers as well as strongly reduced galactosylation and sialylation upon day 14 after immunization which was reflected in reduced St6gal1 expression levels in antigen-specific IgG^+ PCs. These effects were even stronger under the influence of *Mtb*. The immunization with Alum, Adju-Phos and AddaVax as well as the TLR agonist Poly(I:C), R848 and MPLA resulted in milder immune responses with lower IgG titers as well as moderate downregulations of the St6gal1 expression and IgG Fc galactosylation and sialylation. The presented data further linked the observed effects to distinct GC-dependent programming of IgG Ab glycosylation patterns following immunization with different adjuvants. This indication is based on several observations:

Firstly, the early highly galactosylated and sialylated anti-Ova IgG antibodies at day 7 indicate a fast extrafollicular response. At this time point, the IgG Fc glycosylation was comparable for all adjuvants. In the later response starting at day 14, during which time most IgG^+ PCs were very likely GC-derived (Ise et al., 2018), IgG galactosylation and sialylation patterns became distinct dependent on the type of adjuvant. Furthermore, similar dynamics of the anti-Ova serum IgG Fc glycosylation were observed after re-exposure to the antigen at day 28. The repeated increase of anti-Ova IgG galactosylation and sialylation at day 33 equaled the one at day 7 and indicated a fast response of probably extrafollicular newly induced PCs or extrafollicular reactivated memory B cells (Inoue et al., 2018). On day 42, the anti-Ova serum IgG Fc galactosylation and sialylation decreased again, showing

similar galactosylation and sialylation patterns as seen after the first immunization between day 14 and day 28. Immune complexes with sialylated early IgGs were recently linked to the induction of high affinity IgG antibodies, by influencing the threshold for BCR activation in the GC (Wang et al., 2015). The high levels of sialylated IgG Abs at day 7 can be assumed valuable for a proper delivery of the antigen to the GC (Lofano et al., 2018; Wang et al., 2015) and thus for the GC reaction. The here suggested programming of the IgG Fc glycosylation during the GC reaction, additional to the occurring affinity maturation, would result in PCs producing highly antigen-specific IgG Abs with specific effector functions according to their glycosylation structures.

A second observation, supporting the theory of a GC-dependent IgG Fc glycosylation programming, are the differences in the St6gal1 protein expression in PCs and GC B cells. Distinct St6gal1 expression levels induced by different adjuvants were not only detected in Ova-specific IgG^+ PCs, but also, yet in a lesser extent, in Ova-specific $IgG1^+$ GC B cells. This adjuvant-dependent effect on the St6gal1 expression was demonstrated throughout all $IgG1^+$ as well as, when investigated, $IgG2/3^+$ PC and GC B cell analyses in this thesis. Even though GC-derived PCs and non-GC-derived PCs could not be distinguished, so that the analyzed IgG^+ PCs consist of both cell types, a recent study pointed out that on day 12 after immunization with a foreign protein antigen plus CFA over 80% of $CD138^+$ PCs were GC-derived (Ise et al., 2018). Hence, the majority of the Ova-specific IgG^+ PCs analyzed can be assumed to be GC-derived.

Thirdly, the St6gal1 expression as well as the IgG Fc glycosylation showed reverse patterns to the frequencies of the follicular B and T cells. Especially, high frequencies of T_{FH} cells and a high T_{FH}/T_{FR} cell ratio could be linked to a strong inflammatory reaction. The water-in-oil adjuvant IFA showed significantly higher frequencies of T_{FH} cells compared to Alum, which was even enhanced by *Mtb* in eCFA immunization. Also, the IL-27-induced IFN-γ effect was only exhibited in follicular T_{FH1} cells, not in T_H1 cells. This impact of follicular B and T cells additionally supports the categorization of the three adjuvant groups that were primarily assigned after investigation of the IgG Fc glycosylation patterns.

Considering the changes in the IgG Fc glycosylation and the IgG titers over time, the St6gal1 expression within GC B cells and PCs as well as the frequencies of follicular cells, the data strongly indicate a GC-dependent IgG Fc glycosylation programming. Furthermore, the data indicate that GC-mediated regulation of murine IgG1 and IgG2 Fc glycosylation is based on similar stimuli and mechanisms.

4.1.2 *Mtb* induces inflammatory T_{FH}/T_{FR} ratios as well as strong IL-17 and IFN-γ responses of T follicular cells

Furthermore, an additive impact of *Mtb* in both IFA as well as Alum on the induction of GC B cells and reduction of St6gal1 expression in Ova-specific IgG^+ GC B cells was identified. Changes in reduced St6gal1 expression levels and reduced IgG Fc sialylation by *Mtb* in Alum were accompanied by the induction of $IL17A^+$ T_{FH17} cells and, as discussed before for *Mtb* in IFA, by an enhanced T_{FH}/T_{FR} cell ratio. At least a partial effect of *Mtb* in Alum could be further restricted to the synthetic analog of the *Mtb* cord factor TDB. In accordance to these findings, the effect of *Mtb* in IFA (as CFA or eCFA) on the IgG Fc glycosylation was shown to be dependent on the IL-17-signaling axis (Bartsch, 2019; Hess et al., 2013). Furthermore, a newly designed adjuvant in phase I clinical trial, constituted of TDB packed in liposomes, was identified to induce T_H17 cell responses (Knudsen et al., 2016). TDB has been described to bind the mincle receptor on APCs. Mincle associates with the FcRγ-chain leading to intracellular signaling through the kinase Syk to induce APC activation and eventually influence the priming of naïve $CD4^+$ T cells (Ostrop et al., 2015; Shenderov et al., 2013).

Mtb, broadly applied as CFA in pre-clinical research, is known for a strong induction of T_H1/T_H17 immune responses (Ostrop et al., 2015; Shenderov et al., 2013). Moreover, T_H1 and T_H17 cells, especially IL23-dependent T_H17 cells, have been shown to induce IgG Abs with low galactosylation and sialylation (Hess et al., 2013; Pfeifle et al., 2017). Accordingly, the here presented study revealed that the induction of low sialylated antigen-specific IgG Abs after immunization with eCFA depends on the IFNγRI signaling. An equal effect was exhibited for IL-17 signaling (Bartsch, 2019). Intriguingly, the parallel absence of the T_H1- and T_H17-mediated immune responses, in IFNgRI x IL17R dKO mice, led to a strong suppression of the anti-inflammatory effect of eCFA with an explicit higher St6gal1 expression and augmented content of sialylated antigen-specific IgG Abs. Similar results have been suggested in an immunization model with CFA without investigating GC B cells or IgG subclass responses (Hess et al., 2013).

In contrast to strong T_H1 and T_H17 immune responses, T_H2 immune responses induce only partial IgG desialylation (Hess et al., 2013). Taking in account, that IFN-γ prominently induces IgG2a, or in C57BL/6 mice IgG2c, antibodies (Huang et al., 1993; Snapper and Paul, 1987), the diminished reduction of galactosylation and sialylation of IgG2 as well as

IgG1 antibodies indicates the importance of IFN-γ signaling on the Fc glycosylation of both IgG subclasses. Interestingly, protection against different pathogens following vaccination with new adjuvants has been associated with T_H1 and T_H17 cell, but not T_H2 cell, immune responses (Knudsen et al., 2016). These observations elucidate the superior effect of eCFA to induce high anti-Ova IgG titer with pro-inflammatory glycosylation profiles and diminished St6gal1 activity in antigen-specific IgG^+ PCs and GC B cells, compared to the T_H2 cell adjuvants Alum, Adju-Phos and AddaVax (Knudsen et al., 2016) as well as to the TLR agonists Poly(I:C), MPLA and R848.

The new data further suggest that low IgG fc galactosylationa and sialylation programming is mediated by T_{FH1} and T_{FH17} cells in the GC reaction.

4.1.3 IL-27R signaling effects the IFN-γ-producing T_{FH1} cell response

In the past, the IL-27R was identified to be essential for induction of IFN-γ^+ $CD4^+$ T cells in early phases of the immune response (Iwasaki et al., 2015; Yoshida et al., 2001). Therefore, a closer investigation of the IL-27R in context of IFN-γ production, GC formation and IgG Fc glycosylation programming was carried out. The abrogation of IL-27 signaling in IL-27R KO mice led to significantly higher IgG Fc sialylation and galactosylation as well as partially increased St6gal1 expression levels after immunization with the foreign protein antigen Ova compared to the wildtype. The IL-27R signaling effect was further linked to the induction of T_{FH1} cells, but not T_H1 cells. Also, no differences between the frequencies of GC B cells or T follicular cells and its subpopulations were detected in IL-27R KO compared to the wild type mice. This suggests that the differences between the IL-27R KO and the wild type depend on a direct effect of the pro-inflammatory cytokine IFN-γ itself on the B cells within the GC rather than an IL-27R-linked enhanced GC formation. This idea could be confirmed by the IFN-γ induced downregulation of the St6gal1 expression level in *in vitro* B cell culture.

Different from the IL-27R KO, the abrogation of the IFN-γ signaling in IFNgRI KO mice, which affected all cell types and not just diminished the IFN-γ production in T follicular cells, led to decreased frequencies of T follicular cells and GC B cells, indicating that there is an IFN-γ-dependent expansion of follicular B and T cells. In former studies, IFN-γ receptor signaling was described to expedite inflammatory autoimmune GC B cell responses by accumulation of T_{FH} cells and GC B cells, leading to spontaneous GC

formations and eventual autoimmunity (Domeier et al., 2016; Jackson et al., 2016; Lee et al., 2012). Targeting IFN-γ signaling as a treatment of autoimmunity in patients with overreactive T_{FH} or GC pathways was proposed (Lee et al., 2012). Noteworthy, this effect was only reported for GC formation to endogenous or self-antigen, but not foreign protein antigen, (Domeier et al., 2016; Lee et al., 2012), contrasting the here observed reduced frequency of T follicular cells in IFNγRI-deficient mice after Ova immunization. These contraries might be attributed to the differing experimental approaches, comparing an autoimmune model with a vaccination model. Nevertheless, the fact that IFN-γ does directly impair St6gal1 activity in B cells and that the IL-27R-dependent lack of T_{FH1} cells has an essential effect on the GC IgG Fc programming suggests targeting of the IFN-γ pathway as a powerful treatment not only for patients with abnormal GC formation but also for patients with inflammatory IgG glycosylation profiles.

In conclusion, signaling via the IL-27R induced strong T_{FH1} immune responses leading to inflammatory glycosylation patterns of the generated Abs. The protective effect of T_{FH1} immune responses following immunization (Knudsen et al., 2016), might be at least partially mediated by IL-27R signaling. The mode of action of new adjuvants inducing T_{FH1} responses could depend on this mechanism.

4.1.4 The reverse effects of IFN-γ and IL-10

Unexpectedly, the IL27-R-dependent high induction of T_{FH1} cells was not exclusively related to the strong adjuvants eCFA and IFA but was also seen after Alum immunization. Moreover, the immunization with Alum had, with almost up to 40%, the highest frequency of IFN-γ-producing T_{FH1} cells. Surely, this observation was redeemed partially by the fact, that Alum immunization induces lower frequencies of T follicular cells, so in total the presence of T_{FH1} cells might be not that distinct. Yet, a further and even more decisive effect to explain the contradiction between the induction of IFN-γ producing T_{FH1} cells and the moderate immune response, mirrored in relatively high IgG Fc galactosylation and sialylation, induced by Alum, is the simultaneous expression of the anti-inflammatory cytokine IL-10.

Besides the induction of T_H1 cells in the early phase, IL-27 was reported to have immunosuppressive effects in later phase of the immune response by the upregulation of IL-10 in naïve $CD4^+$ T cells differentiating to $Foxp3^-$ type 1 regulatory T cells (Tr1 cells).

Tr1 cells are antigen-specific, FoxP3$^-$ and Tbet$^+$, produce large amounts of IL-10 and various amounts of IFN-γ. Their differentiation is substantially promoted by IL-27R signaling (Awasthi et al., 2007; Fitzgerald et al., 2007). These cells might be responsible for the reversion of the pro-inflammatory potential of IFN-γ after immunization with Alum. Furthermore, IL-27 induced IL-10 has been linked to the suppression of IL-17 (Fitzgerald et al., 2007).

Interestingly, the increasing frequencies of IFN-γ$^+$ IL-10$^+$ double positive cells from eCFA over IFA to Alum was seen particularly in Foxp3$^-$ T_{FH} cells likewise to the detected high IFN-γ production with the unexpected intensities. The restriction to the T follicular cells supports the assumption of a GC-dependent Fc glycosylation programming, the restriction to the FoxP3$^-$ cells suggests Tr1 cells.

The potent anti-inflammatory effect of IL-10 produced by Tr1 cells leads to an inhibited development of T_H1, T_H2 and T_H17 cells (Awasthi et al., 2007; Fitzgerald et al., 2007). Their regulatory function is distinct from CD4$^+$ Foxp3$^+$ T reg cells, depends mainly on the immunosuppressive function of IL-10 and was reported to downregulate inflammation and autoimmunity (Awasthi et al., 2007; Fitzgerald et al., 2007; Iwasaki et al., 2015).

In other studies, IL-10-producing IFN-γ$^+$ Foxp3$^-$ Tbet$^+$ cells were described to develop under strong inflammatory conditions. These cells play a major role in the immune regulation during infection with intracellular pathogens and were sufficient in repressing host protection. Nevertheless, these cells were also discussed to differ from Tr1 cells in their differentiation, as IL-27 was verified not to be a major differentiation factor (Anderson et al., 2007; Jankovic et al., 2007).

Which cell type the here detected cells represent, could not be determined exactly. Yet, due to the IL-27R dependency, the IL-10$^+$ IFN-γ$^+$ double positive cells in the here tested vaccination model were most likely follicular Tr1 cells. Nevertheless, most certainly, the T_H1 response was suppressed in an IL-10-dependent manner. If IL-10 has a direct effect or if further cell-mediated mechanisms are included, needs to be investigated. In B cell culture, IL-10 was shown to at least partially reverse the IFN-γ effect. Still, the diminished B cell growth under IL-10 condition needs to be considered. A closer investigation of the described IL-10$^+$ IFN-γ$^+$ cells could lead to a better discrimination between (vaccination-induced) T_{FH1} and follicular Tr1 cell responses.

In terms of vaccination development, it might be of advantage to consider the control mechanisms for IL-27 to on the one hand induce T_{FH1} immune responses in the early phase and on the other hand induce immune suppressive follicular Tr1 cells in the later phase. A main producer of IL-27 are APCs after TLR stimulation (Iwasaki et al., 2015). A prolonged high expression of IL-27 might lead to a shift from a T_{FH1} cell to follicular Tr1 cell induction and following immunosuppressive effects. According to this mechanism, the TLR agonists Poly(I:C), MPLA and R848 induced much lower down-regulation of the St6gal1 expression and IgG Fc galactosylation and sialylation compared to the water-on-oil adjuvants. Similar mechanism might be induced by Alum that was designated to the same adjuvant group as the TLR agonists (group 3) and showed similar results on the St6gal1 expression and the IgG Fc galactosylation and sialylation.

4.2 Conclusion and Outlook

Taken together, the data of this thesis revealed that different adjuvants lead to distinct GC responses accompanied by distinct St6gal1 activities and following corresponding IgG Fc *N*-glycosylation patterns. This IgG glycosylation programming was found to take place in the GC. *Mtb*, as an adjuvant supplement, was exhibited to be a strong inducer of pro-inflammatory glycosylation profiles, that were associated with the induction of T_{FH1} and T_{H17} cells. The pro-inflammatory cytokines IL-17 and IFN-γ possess a strong effect on the regulation of the IgG glycosylation with a shift to agalactosylated IgG Abs. The induction of IFN-γ-producing T_{FH1} cells could be linked to IL-27R signaling. Besides T_{FH1} cells, the IL-27R also induced follicular Tr1 cells with an anti-inflammatory function. These follicular Tr1 cells produced IFN-γ as well as IL-10, that was identified to reverse the pro-inflammatory effect of IFN-γ.

Currently, the success of vaccination is measured by the induction and persistence of serum IgG Abs and their neutralizing capacity. It would be wise to further discover regulating mechanisms that include not only the amount but also the Fc mediated functional properties of Abs.

The early produced IgG antibodies were shown to carry high sialylated glycans. These sialylated IgG Abs might be efficient in delivering the antigen to the GC (Lofano et al., 2018) and therefore can be assumed to be essential for a proper GC-dependent Fc glycosylation programming. In addition, sialylated ICs in the GC enhance the threshold of the required BCR affinity for positive selection (Wang et al., 2015). The resulting GC-derived antigen-specific IgG antibodies are highly affine and obtained an enhanced neutralizing function in HIV patients (Lofano et al., 2018; Wang et al., 2015).

In the later phase, IgG Abs showed galactosylation and sialylation levels that are very likely determined during the GC reaction and dependent on the kind of adjuvant. These late Abs have and might need equal properties (low sialylation and low galactosylation) as the pathogenic autoantibodies in inflammatory autoimmune diseases (Bartsch et al., 2018; Ercan et al., 2010; Parekh et al., 1985; Pfeifle et al., 2017), to effectively fight pathogens. Accordingly, low levels of galactosylation and sialylation correlated with enhanced protection against simian immunodeficiency virus in rhesus macaques after immunization (Vaccari et al., 2016) and the protection in HIV controllers (infected individuals without HIV enrichment)(Ackerman et al., 2013).

Currently, the role of antigen-specific IgG galactosylation and sialylation is highly discussed. Different roles of galactosylated and sialylated IgG Abs might mediated at distinct time points upon infection or vaccination (Lofano et al., 2018; Wang et al., 2015).

Interestingly, the before mentioned HIV controllers, with enhanced levels of agalactosylated IgG Abs, showed an additional loss of fucosylation that probably helps to control the disease by enhanced ADCC (Ackerman et al., 2013). Elevated afucosylation was also detected in and correlated with latent tuberculosis (TB) infections compared to acute infections (Lu et al., 2016). Experiments on the IgG Fc fucosylation were not possible with the here performed immunization model using a soluble protein antigen. Further experiments on regulatory mechanism on the IgG Fc fucosylation could be performed using a membrane-bound protein antigen (Larsen et al., 2021).

These observations indicate that different IgG Fc glycosylations can support pathogen elimination. As different pathogens induce different glycan structures of antigen-specific IgG, as it is seen for the HIV-specific and influenza-specific IgG glycosylation (Irvine and Alter, 2020), the most effective IgG glycan structures seems to be pathogen-dependent.

In the future, to verify that the late Abs originate from GC-dependent PCs, our group planned to investigate the amount of GC-derived PCs and the St6gal1 protein expression in these cells using a mouse model, in which a fluorescence gene can be conditionally induced in GC B cells (Shinnakasu et al., 2016).

Furthermore, it would be relevant to investigate the role of the molecular signaling axis of IL-17, IL-27 and IFN-γ in terms of generating potentially pathogenic Abs. For the investigation of the IL-27 signaling TLR agonistic adjuvants, such as Poly(I:C), MPLA and R848 that are supposed to induce APC-dependent IL-27 production (Iwasaki et al., 2015), could be tested alongside with Alum in future studies using the vaccination model. The induction of T_H1 and T_H17 responses was already proven to correlate with vaccination success (Knudsen et al., 2016). Here, the importance of the corresponding cell subsets T_{FH1} and T_{FH17} in the GC response after immunization was emphasized. A promising approach, to further investigate the effect of these cytokines within in GC, is the use of conditional gene targeting.

The here used immunization strategy was applied to induce IgG antibodies with distinct glycosylation patterns. Which glycosylation pattern is most potent to ensure protective immune responses needs to be further investigated, and probably depends on the pathogen of interest.

The collected results and further clarification of the mechanisms that are involved in the reduction of antigen-specific IgG galactosylation and sialylation during the immune response may contribute to the development of improved vaccination strategies in humans.

A use of adjuvants might be even interesting in combination with the newly introduced mRNA vaccines, since they basically introduce the antigen without a strong immunogenic agent, their success is generally based on the induction of high Ab titers and long-term studies still need to be validated. Certainly, the protection induced by novel adjuvants needs to be evaluated in corresponding mouse and human models.

References

Ackerman, M.E., Crispin, M., Yu, X., Baruah, K., Boesch, A.W., Harvey, D.J., Dugast, A.-S., Heizen, E.L., Ercan, A., Choi, I., Streeck, H., Nigrovic, P.A., Bailey-Kellogg, C., Scanlan, C., Alter, G., 2013. Natural variation in Fc glycosylation of HIV-specific antibodies impacts antiviral activity. J. Clin. Invest. 123, 2183–2192. https://doi.org/10.1172/JCI65708

Ada, G., 2005. Overview of Vaccines and Vaccination. Mol. Biotechnol. 29, 255–272. https://doi.org/10.1385/MB:29:3:255

Aloulou, M., Carr, E.J., Gador, M., Bignon, A., Liblau, R.S., Fazilleau, N., Linterman, M.A., 2016. Follicular regulatory T cells can be specific for the immunizing antigen and derive from naive T cells. Nat. Commun. 7, 10579. https://doi.org/10.1038/ncomms10579

Alter, G., Ottenhoff, T.H.M., Joosten, S.A., 2018. Antibody glycosylation in inflammation, disease and vaccination. Semin. Immunol. 39, 102–110. https://doi.org/10.1016/j.smim.2018.05.003

Anderson, C.F., Oukka, M., Kuchroo, V.J., Sacks, D., 2007. CD4+CD25−Foxp3− Th1 cells are the source of IL-10–mediated immune suppression in chronic cutaneous leishmaniasis. J. Exp. Med. 204, 285–297. https://doi.org/10.1084/jem.20061886

Anthony, R.M., Nimmerjahn, F., Ashline, D.J., Reinhold, V.N., Paulson, J.C., Ravetch, J.V., 2008a. Recapitulation of IVIG Anti-Inflammatory Activity with a Recombinant IgG Fc. Science 320, 373–376. https://doi.org/10.1126/science.1154315

Anthony, R.M., Wermeling, F., Karlsson, M.C.I., Ravetch, J.V., 2008b. Identification of a receptor required for the anti-inflammatory activity of IVIG. Proc. Natl. Acad. Sci. 105, 19571–19578. https://doi.org/10.1073/pnas.0810163105

Arnold, J.N., Wormald, M.R., Sim, R.B., Rudd, P.M., Dwek, R.A., 2007. The Impact of Glycosylation on the Biological Function and Structure of Human Immunoglobulins. Annu. Rev. Immunol. 25, 21–50. https://doi.org/10.1146/annurev.immunol.25.022106.141702

Awasthi, A., Carrier, Y., Peron, J.P.S., Bettelli, E., Kamanaka, M., Flavell, R.A., Kuchroo, V.K., Oukka, M., Weiner, H.L., 2007. A dominant function for interleukin 27 in generating interleukin 10–producing anti-inflammatory T cells. Nat. Immunol. 8, 1380–1389. https://doi.org/10.1038/ni1541

Bartsch, Y.C., 2019. The role of IL-6 in vaccine-induced IgG Fc glycosylation. Universität zu Lübeck.

Bartsch, Y.C., Eschweiler, S., Leliavski, A., Lunding, H.B., Wagt, S., Petry, J., Lilienthal, G.-M., Rahmöller, J., de Haan, N., Hölscher, A., Erapaneedi, R., Giannou, A.D., Aly, L., Sato, R., de Neef, L.A., Winkler, A., Braumann, D., Hobusch, J., Kuhnigk, K., Krémer, V., Steinhaus, M., Blanchard, V., Gemoll, T., Habermann, J.K., Collin, M., Salinas, G., Manz, R.A., Fukuyama, H., Korn, T., Waisman, A., Yogev, N., Huber, S., Rabe, B., Rose-John, S., Busch, H., Berberich-Siebelt, F., Hölscher, C., Wuhrer, M., Ehlers, M., 2020. IgG Fc sialylation is regulated during the germinal center reaction following immunization with different adjuvants. J. Allergy Clin. Immunol. 146, 652-666.e11. https://doi.org/10.1016/j.jaci.2020.04.059

Bartsch, Y.C., Rahmöller, J., Mertes, M.M.M., Eiglmeier, S., Lorenz, F.K.M., Stoehr, A.D., Braumann, D., Lorenz, A.K., Winkler, A., Lilienthal, G.-M., Petry, J., Hobusch, J., Steinhaus, M., Hess, C., Holecska, V., Schoen, C.T., Oefner, C.M., Leliavski, A., Blanchard, V., Ehlers, M., 2018. Sialylated Autoantigen-Reactive IgG Antibodies

Attenuate Disease Development in Autoimmune Mouse Models of Lupus Nephritis and Rheumatoid Arthritis. Front. Immunol. 9, 1183. https://doi.org/10.3389/fimmu.2018.01183

Batten, M., Ramamoorthi, N., Kljavin, N.M., Ma, C.S., Cox, J.H., Dengler, H.S., Danilenko, D.M., Caplazi, P., Wong, M., Fulcher, D.A., Cook, M.C., King, C., Tangye, S.G., de Sauvage, F.J., Ghilardi, N., 2010. IL-27 supports germinal center function by enhancing IL-21 production and the function of T follicular helper cells. J. Exp. Med. 207, 2895–2906. https://doi.org/10.1084/jem.20100064

Bonilla, F.A., 2018. Update: Vaccines in primary immunodeficiency. J. Allergy Clin. Immunol. 141, 474–481. https://doi.org/10.1016/j.jaci.2017.12.980

Bruhns, P., 2012. Properties of mouse and human IgG receptors and their contribution to disease models. Blood 119, 5640–5649. https://doi.org/10.1182/blood-2012-01-380121

Bruhns, P., Jönsson, F., 2015. Mouse and human FcR effector functions. Immunol. Rev. 268, 25–51. https://doi.org/10.1111/imr.12350

Chiang, C.L.-L., Kandalaft, L.E., Coukos, G., 2011. Adjuvants for Enhancing the Immunogenicity of Whole Tumor Cell Vaccines. Int. Rev. Immunol. 30, 150–182. https://doi.org/10.3109/08830185.2011.572210

Coffman, R.L., Sher, A., Seder, R.A., 2010. Vaccine Adjuvants: Putting Innate Immunity to Work. Immunity 33, 492–503. https://doi.org/10.1016/j.immuni.2010.10.002

Collin, M., Ehlers, M., 2013. The carbohydrate switch between pathogenic and immunosuppressive antigen-specific antibodies. Exp. Dermatol. 22, 511–514. https://doi.org/10.1111/exd.12171

Collins, E.S., Galligan, M.C., Saldova, R., Adamczyk, B., Abrahams, J.L., Campbell, M.P., Ng, C.-T., Veale, D.J., Murphy, T.B., Rudd, P.M., FitzGerald, O., 2013. Glycosylation status of serum in inflammatory arthritis in response to anti-TNF treatment. Rheumatology 52, 1572–1582. https://doi.org/10.1093/rheumatology/ket189

de Haan, N., Reiding, K.R., Krištić, J., Hipgrave Ederveen, A.L., Lauc, G., Wuhrer, M., 2017. The N-Glycosylation of Mouse Immunoglobulin G (IgG)-Fragment Crystallizable Differs Between IgG Subclasses and Strains. Front. Immunol. 8, 608. https://doi.org/10.3389/fimmu.2017.00608

Domeier, P.P., Chodisetti, S.B., Soni, C., Schell, S.L., Elias, M.J., Wong, E.B., Cooper, T.K., Kitamura, D., Rahman, Z.S.M., 2016. IFN-γ receptor and STAT1 signaling in B cells are central to spontaneous germinal center formation and autoimmunity. J. Exp. Med. 213, 715–732. https://doi.org/10.1084/jem.20151722

Endres, R.O., Kushnir, E., Kappler, J.W., Marrack, P., Kinsky, S.C., 1983. A requirement for nonspecific T cell factors in antibody responses to “T cell independent” antigens. J. Immunol. 130, 781.

Epp, A., Hobusch, J., Bartsch, Y.C., Petry, J., Lilienthal, G.-M., Koeleman, C.A.M., Eschweiler, S., Möbs, C., Hall, A., Morris, S.C., Braumann, D., Engellenner, C., Bitterling, J., Rahmöller, J., Leliavski, A., Thurmann, R., Collin, M., Moremen, K.W., Strait, R.T., Blanchard, V., Petersen, A., Gemoll, T., Habermann, J.K., Petersen, F., Nandy, A., Kahlert, H., Hertl, M., Wuhrer, M., Pfützner, W., Jappe, U., Finkelman, F.D., Ehlers, M., 2018. Sialylation of IgG antibodies inhibits IgG-mediated allergic reactions. J. Allergy Clin. Immunol. 141, 399-402.e8. https://doi.org/10.1016/j.jaci.2017.06.021

Ercan, A., Cui, J., Chatterton, D.E.W., Deane, K.D., Hazen, M.M., Brintnell, W., O’Donnell, C.I., Derber, L.A., Weinblatt, M.E., Shadick, N.A., Bell, D.A., Cairns, E., Solomon, D.H., Holers, V.M., Rudd, P.M., Lee, D.M., 2010. Aberrant IgG

galactosylation precedes disease onset, correlates with disease activity, and is prevalent in autoantibodies in rheumatoid arthritis. Arthritis Rheum. 62, 2239–2248. https://doi.org/10.1002/art.27533

Fitzgerald, D.C., Zhang, G.-X., El-Behi, M., Fonseca-Kelly, Z., Li, H., Yu, S., Saris, C.J.M., Gran, B., Ciric, B., Rostami, A., 2007. Suppression of autoimmune inflammation of the central nervous system by interleukin 10 secreted by interleukin 27–stimulated T cells. Nat. Immunol. 8, 1372–1379. https://doi.org/10.1038/ni1540

Freund, J., Casals, J., Hosmer, E.P., 1937. Sensitization and Antibody Formation after Injection of Tubercle Bacilli and Paraffin Oil. Exp. Biol. Med. 37, 509–513. https://doi.org/10.3181/00379727-37-9625

Hess, C., Winkler, A., Lorenz, A.K., Holecska, V., Blanchard, V., Eiglmeier, S., Schoen, A.-L., Bitterling, J., Stoehr, A.D., Petzold, D., Schommartz, T., Mertes, M.M.M., Schoen, C.T., Tiburzy, B., Herrmann, A., Köhl, J., Manz, R.A., Madaio, M.P., Berger, M., Wardemann, H., Ehlers, M., 2013. T cell–independent B cell activation induces immunosuppressive sialylated IgG antibodies. J. Clin. Invest. 123, 3788–3796. https://doi.org/10.1172/JCI65938

Ho, C.-H., Chien, R.-N., Cheng, P.-N., Liu, J.-H., Liu, C.-K., Su, C.-S., Wu, I.-C., Li, I.-C., Tsai, H.-W., Wu, S.-L., Liu, W.-C., Chen, S.-H., Chang, T.-T., 2015. Aberrant Serum Immunoglobulin G Glycosylation in Chronic Hepatitis B Is Associated With Histological Liver Damage and Reversible by Antiviral Therapy. J. Infect. Dis. 211, 115–124. https://doi.org/10.1093/infdis/jiu388

Howell, J.W., Hood, L., Sanders, B.G., 1967. Comparative analysis of the IgG heavy chain carbohydrate peptide. J. Mol. Biol. 30, 555–558. https://doi.org/10.1016/0022-2836(67)90369-5

Huang, S., Hendriks, W., Althage, A., Hemmi, S., Bluethmann, H., Kamijo, R., Vilcek, J., Zinkernagel, R., Aguet, M., 1993. Immune response in mice that lack the interferon-gamma receptor. Science 259, 1742–1745. https://doi.org/10.1126/science.8456301

Ichinohe, T., Lee, H.K., Ogura, Y., Flavell, R., Iwasaki, A., 2009. Inflammasome recognition of influenza virus is essential for adaptive immune responses. J. Exp. Med. 206, 79–87. https://doi.org/10.1084/jem.20081667

Inoue, T., Moran, I., Shinnakasu, R., Phan, T.G., Kurosaki, T., 2018. Generation of memory B cells and their reactivation. Immunol. Rev. 283, 138–149. https://doi.org/10.1111/imr.12640

Irvine, E.B., Alter, G., 2020. Understanding the role of antibody glycosylation through the lens of severe viral and bacterial diseases. Glycobiology 30, 241–253. https://doi.org/10.1093/glycob/cwaa018

Ise, W., Fujii, K., Shiroguchi, K., Ito, A., Kometani, K., Takeda, K., Kawakami, E., Yamashita, K., Suzuki, K., Okada, T., Kurosaki, T., 2018. T Follicular Helper Cell-Germinal Center B Cell Interaction Strength Regulates Entry into Plasma Cell or Recycling Germinal Center Cell Fate. Immunity 48, 702-715.e4. https://doi.org/10.1016/j.immuni.2018.03.027

Iwasaki, A., Medzhitov, R., 2010. Regulation of Adaptive Immunity by the Innate Immune System. Science 327, 291–295. https://doi.org/10.1126/science.1183021

Iwasaki, Y., Fujio, K., Okamura, T., Yamamoto, K., 2015. Interleukin-27 in T Cell Immunity. Int. J. Mol. Sci. 16, 2851–2863. https://doi.org/10.3390/ijms16022851

Jackson, L.A., Anderson, E.J., Rouphael, N.G., Roberts, P.C., Makhene, M., Coler, R.N., McCullough, M.P., Chappell, J.D., Denison, M.R., Stevens, L.J., Pruijssers, A.J., McDermott, A., Flach, B., Doria-Rose, N.A., Corbett, K.S., Morabito, K.M., O'Dell, S., Schmidt, S.D., Swanson, P.A., Padilla, M., Mascola, J.R., Neuzil, K.M.,

Bennett, H., Sun, W., Peters, E., Makowski, M., Albert, J., Cross, K., Buchanan, W., Pikaart-Tautges, R., Ledgerwood, J.E., Graham, B.S., Beigel, J.H., 2020. An mRNA Vaccine against SARS-CoV-2 — Preliminary Report. N. Engl. J. Med. 383, 1920–1931. https://doi.org/10.1056/NEJMoa2022483

Jackson, S.W., Jacobs, H.M., Arkatkar, T., Dam, E.M., Scharping, N.E., Kolhatkar, N.S., Hou, B., Buckner, J.H., Rawlings, D.J., 2016. B cell IFN-γ receptor signaling promotes autoimmune germinal centers via cell-intrinsic induction of BCL-6. J. Exp. Med. 213, 733–750. https://doi.org/10.1084/jem.20151724

James, L.K., Till, S.J., 2016. Potential Mechanisms for IgG4 Inhibition of Immediate Hypersensitivity Reactions. Curr. Allergy Asthma Rep. 16, 23. https://doi.org/10.1007/s11882-016-0600-2

Jankovic, D., Kullberg, M.C., Feng, C.G., Goldszmid, R.S., Collazo, C.M., Wilson, M., Wynn, T.A., Kamanaka, M., Flavell, R.A., Sher, A., 2007. Conventional T-bet+Foxp3− Th1 cells are the major source of host-protective regulatory IL-10 during intracellular protozoan infection. J. Exp. Med. 204, 273–283. https://doi.org/10.1084/jem.20062175

June, C.H., Bluestone, J.A., Nadler, L.M., Thompson, C.B., 1994. The B7 and CD28 receptor families. Immunol. Today 15, 321–331. https://doi.org/10.1016/0167-5699(94)90080-9

Kaneko, Y., 2006. Anti-Inflammatory Activity of Immunoglobulin G Resulting from Fc Sialylation. Science 313, 670–673. https://doi.org/10.1126/science.1129594

Kao, D., Lux, A., Schaffert, A., Lang, R., Altmann, F., Nimmerjahn, F., 2017. IgG subclass and vaccination stimulus determine changes in antigen specific antibody glycosylation in mice. Eur. J. Immunol. 47, 2070–2079. https://doi.org/10.1002/eji.201747208

Karsten, C.M., Pandey, M.K., Figge, J., Kilchenstein, R., Taylor, P.R., Rosas, M., McDonald, J.U., Orr, S.J., Berger, M., Petzold, D., Blanchard, V., Winkler, A., Hess, C., Reid, D.M., Majoul, I.V., Strait, R.T., Harris, N.L., Köhl, G., Wex, E., Ludwig, R., Zillikens, D., Nimmerjahn, F., Finkelman, F.D., Brown, G.D., Ehlers, M., Köhl, J., 2012. Anti-inflammatory activity of IgG1 mediated by Fc galactosylation and association of FcγRIIB and dectin-1. Nat. Med. 18, 1401–1406. https://doi.org/10.1038/nm.2862

Khabbaz, R.F., Moseley, R.R., Steiner, R.J., Levitt, A.M., Bell, B.P., 2014. Challenges of infectious diseases in the USA. The Lancet 384, 53–63. https://doi.org/10.1016/S0140-6736(14)60890-4

Knudsen, N.P.H., Olsen, A., Buonsanti, C., Follmann, F., Zhang, Y., Coler, R.N., Fox, C.B., Meinke, A., D´Oro, U., Casini, D., Bonci, A., Billeskov, R., De Gregorio, E., Rappuoli, R., Harandi, A.M., Andersen, P., Agger, E.M., 2016. Different human vaccine adjuvants promote distinct antigen-independent immunological signatures tailored to different pathogens. Sci. Rep. 6, 19570. https://doi.org/10.1038/srep19570

Kojouharova, M., Reid, K., Gadjeva, M., 2010. New insights into the molecular mechanisms of classical complement activation. Mol. Immunol. 47, 2154–2160. https://doi.org/10.1016/j.molimm.2010.05.011

Kurosaki, T., Kometani, K., Ise, W., 2015. Memory B cells. Nat. Rev. Immunol. 15, 149–159. https://doi.org/10.1038/nri3802

Larsen, M.D., de Graaf, E.L., Sonneveld, M.E., Plomp, H.R., Nouta, J., Hoepel, W., Chen, H.-J., Linty, F., Visser, R., Brinkhaus, M., Šuštić, T., de Taeye, S.W., Bentlage, A.E.H., Toivonen, S., Koeleman, C.A.M., Sainio, S., Kootstra, N.A., Brouwer, P.J.M., Geyer, C.E., Derksen, N.I.L., Wolbink, G., de Winther, M., Sanders, R.W.,

van Gils, M.J., de Bruin, S., Vlaar, A.P.J., Amsterdam UMC COVID-19, biobank study group, Rispens, T., den Dunnen, J., Zaaijer, H.L., Wuhrer, M., Ellen van der Schoot, C., Vidarsson, G., van Agtmael, M., Algera, A.G., van Baarle, F., Bax, D., van de Beek, D., Beudel, M., Bogaard, H.J., Bonta, P.I., Bomers, M., Bos, L., Botta, M., de Bree, G., Brouwer, M.C., Brabander, J., de Bruin, S., Bugiani, M., Bulle, E., Chouchane, O., Cloherty, A., Elbers, P., Fleuren, L., Geerlings, S., Geerts, B., Geijtenbeek, T., Girbes, A., Goorhuis, B., Grobusch, M.P., Hafkamp, F., Hagens, L., Hamann, J., Harris, V., Hemke, R., Hermans, S.M., Heunks, L., Hollmann, M.W., Horn, J., Hovius, J.W., de Jong, M., Koning, R., van Mourik, N., Nellen, J., Nossent, E.J., Paulus, F., Peters, E., van der Poll, T., Preckel, B., Prins, J.M., Raasveld, J., Rijnders, T., Schinkel, M., Schultz, M., Schuurmans, A.R., Sigaloff, K., Smit, M., Stijnis, C.S., Stilma, W., Teunissen, C., Thoral, P., Tsonas, A., van der Valk, M., Veelo, D., Vlaar, A.P.J., de Vries, H., van Vugt, M., Wiersinga, W.J., Wouters, D., Zwinderman, A.H. (Koos), 2021. Afucosylated IgG characterizes enveloped viral responses and correlates with COVID-19 severity. Science 371, eabc8378. https://doi.org/10.1126/science.abc8378

Lasaro, M.O., Ertl, H.C., 2009. New Insights on Adenovirus as Vaccine Vectors. Mol. Ther. 17, 1333–1339. https://doi.org/10.1038/mt.2009.130

Lauc, G., Huffman, J.E., Pučić, M., Zgaga, L., Adamczyk, B., Mužinić, A., Novokmet, M., Polašek, O., Gornik, O., Krištić, J., Keser, T., Vitart, V., Scheijen, B., Uh, H.-W., Molokhia, M., Patrick, A.L., McKeigue, P., Kolčić, I., Lukić, I.K., Swann, O., van Leeuwen, F.N., Ruhaak, L.R., Houwing-Duistermaat, J.J., Slagboom, P.E., Beekman, M., de Craen, A.J.M., Deelder, A.M., Zeng, Q., Wang, W., Hastie, N.D., Gyllensten, U., Wilson, J.F., Wuhrer, M., Wright, A.F., Rudd, P.M., Hayward, C., Aulchenko, Y., Campbell, H., Rudan, I., 2013. Loci Associated with N-Glycosylation of Human Immunoglobulin G Show Pleiotropy with Autoimmune Diseases and Haematological Cancers. PLoS Genet. 9, e1003225. https://doi.org/10.1371/journal.pgen.1003225

Lee, S.K., Silva, D.G., Martin, J.L., Pratama, A., Hu, X., Chang, P.-P., Walters, G., Vinuesa, C.G., 2012. Interferon-γ Excess Leads to Pathogenic Accumulation of Follicular Helper T Cells and Germinal Centers. Immunity 37, 880–892. https://doi.org/10.1016/j.immuni.2012.10.010

Lilienthal, G.-M., Rahmöller, J., Petry, J., Bartsch, Y.C., Leliavski, A., Ehlers, M., 2018. Potential of Murine IgG1 and Human IgG4 to Inhibit the Classical Complement and Fcγ Receptor Activation Pathways. Front. Immunol. 9, 958. https://doi.org/10.3389/fimmu.2018.00958

Lofano, G., Gorman, M.J., Yousif, A.S., Yu, W.-H., Fox, J.M., Dugast, A.-S., Ackerman, M.E., Suscovich, T.J., Weiner, J., Barouch, D., Streeck, H., Little, S., Smith, D., Richman, D., Lauffenburger, D., Walker, B.D., Diamond, M.S., Alter, G., 2018. Antigen-specific antibody Fc glycosylation enhances humoral immunity via the recruitment of complement. Sci. Immunol. 3, eaat7796. https://doi.org/10.1126/sciimmunol.aat7796

Lu, L.L., Chung, A.W., Rosebrock, T.R., Ghebremichael, M., Yu, W.H., Grace, P.S., Schoen, M.K., Tafesse, F., Martin, C., Leung, V., Mahan, A.E., Sips, M., Kumar, M.P., Tedesco, J., Robinson, H., Tkachenko, E., Draghi, M., Freedberg, K.J., Streeck, H., Suscovich, T.J., Lauffenburger, D.A., Restrepo, B.I., Day, C., Fortune, S.M., Alter, G., 2016. A Functional Role for Antibodies in Tuberculosis. Cell 167, 433-443.e14. https://doi.org/10.1016/j.cell.2016.08.072

Mahan, A.E., Jennewein, M.F., Suscovich, T., Dionne, K., Tedesco, J., Chung, A.W., Streeck, H., Pau, M., Schuitemaker, H., Francis, D., Fast, P., Laufer, D., Walker,

B.D., Baden, L., Barouch, D.H., Alter, G., 2016. Antigen-Specific Antibody Glycosylation Is Regulated via Vaccination. PLOS Pathog. 12, e1005456. https://doi.org/10.1371/journal.ppat.1005456

Manz, R., 1998. Survival of long-lived plasma cells is independent of antigen [In Process Citation]. Int. Immunol. 10, 1703–1711. https://doi.org/10.1093/intimm/10.11.1703

Manz, R.A., Thiel, A., Radbruch, A., 1997. Lifetime of plasma cells in the bone marrow. Nature 388, 133–134. https://doi.org/10.1038/40540

Marrack, P., McKee, A.S., Munks, M.W., 2009. Towards an understanding of the adjuvant action of aluminium. Nat. Rev. Immunol. 9, 287–293. https://doi.org/10.1038/nri2510

Martin, F., Oliver, A.M., Kearney, J.F., 2001. Marginal Zone and B1 B Cells Unite in the Early Response against T-Independent Blood-Borne Particulate Antigens. Immunity 14, 617–629. https://doi.org/10.1016/S1074-7613(01)00129-7

Massoud, A.H., Yona, M., Xue, D., Chouiali, F., Alturaihi, H., Ablona, A., Mourad, W., Piccirillo, C.A., Mazer, B.D., 2014. Dendritic cell immunoreceptor: A novel receptor for intravenous immunoglobulin mediates induction of regulatory T cells. J. Allergy Clin. Immunol. 133, 853-863.e5. https://doi.org/10.1016/j.jaci.2013.09.029

McHeyzer-Williams, M., Okitsu, S., Wang, N., McHeyzer-Williams, L., 2012. Molecular programming of B cell memory. Nat. Rev. Immunol. 12, 24–34. https://doi.org/10.1038/nri3128

McNeil, M.M., DeStefano, F., 2018. Vaccine-associated hypersensitivity. J. Allergy Clin. Immunol. 141, 463–472. https://doi.org/10.1016/j.jaci.2017.12.971

Mesin, L., Ersching, J., Victora, G.D., 2016. Germinal Center B Cell Dynamics. Immunity 45, 471–482. https://doi.org/10.1016/j.immuni.2016.09.001

Mond, J., 1995. T cell independent antigens. Curr. Opin. Immunol. 7, 349–354. https://doi.org/10.1016/0952-7915(95)80109-X

Moremen, K.W., Tiemeyer, M., Nairn, A.V., 2012. Vertebrate protein glycosylation: diversity, synthesis and function. Nat. Rev. Mol. Cell Biol. 13, 448–462. https://doi.org/10.1038/nrm3383

Murphy, K., Travers, P., Walport, M., Janeway, C., 2012. Janeway's Immunobiology, 8th edition. ed. Garland Science.

Neuberger, M.S., Rajewsky, K., 1981. Activation of mouse complement by monoclonal mouse antibodies. Eur. J. Immunol. 11, 1012–1016. https://doi.org/10.1002/eji.1830111212

Noor, R., 2021. Developmental Status of the Potential Vaccines for the Mitigation of the COVID-19 Pandemic and a Focus on the Effectiveness of the Pfizer-BioNTech and Moderna mRNA Vaccines. Curr. Clin. Microbiol. Rep. 8, 178–185. https://doi.org/10.1007/s40588-021-00162-y

Nose, M., Wigzell, H., 1983. Biological significance of carbohydrate chains on monoclonal antibodies. Proc. Natl. Acad. Sci. 80, 6632–6636. https://doi.org/10.1073/pnas.80.21.6632

Oefner, C.M., Winkler, A., Hess, C., Lorenz, A.K., Holecska, V., Huxdorf, M., Schommartz, T., Petzold, D., Bitterling, J., Schoen, A.-L., Stoehr, A.D., Vu Van, D., Darcan-Nikolaisen, Y., Blanchard, V., Schmudde, I., Laumonnier, Y., Ströver, H.A., Hegazy, A.N., Eiglmeier, S., Schoen, C.T., Mertes, M.M.M., Loddenkemper, C., Löhning, M., König, P., Petersen, A., Luger, E.O., Collin, M., Köhl, J., Hutloff, A., Hamelmann, E., Berger, M., Wardemann, H., Ehlers, M., 2012. Tolerance induction with T cell–dependent protein antigens induces regulatory sialylated

IgGs. J. Allergy Clin. Immunol. 129, 1647-1655.e13. https://doi.org/10.1016/j.jaci.2012.02.037

Ohmi, Y., Ise, W., Harazono, A., Takakura, D., Fukuyama, H., Baba, Y., Narazaki, M., Shoda, H., Takahashi, N., Ohkawa, Y., Ji, S., Sugiyama, F., Fujio, K., Kumanogoh, A., Yamamoto, K., Kawasaki, N., Kurosaki, T., Takahashi, Y., Furukawa, K., 2016. Sialylation converts arthritogenic IgG into inhibitors of collagen-induced arthritis. Nat. Commun. 7, 11205. https://doi.org/10.1038/ncomms11205

Ostrop, J., Jozefowski, K., Zimmermann, S., Hofmann, K., Strasser, E., Lepenies, B., Lang, R., 2015. Contribution of MINCLE–SYK Signaling to Activation of Primary Human APCs by Mycobacterial Cord Factor and the Novel Adjuvant TDB. J. Immunol. 195, 2417–2428. https://doi.org/10.4049/jimmunol.1500102

Pai, M., Stall, N.M., Schull, M., Miller, K.J., Razak, F., Chan, B., Grill, A., Ivers, N., Maltsev, A., Odutayo, A., Schwartz, B., Sholzberg, M., Steiner, R., Wilson, S., Niel, U., Juni, P., Morris, A.M., 2021. Vaccine-Induced Immune Thrombotic Thrombocytopenia (VITT) Following Adenovirus Vector COVID-19 Vaccination: Interim Guidance for Healthcare Professionals in Emergency Department and Inpatient Settings. Ontario COVID-19 Science Advisory Table. https://doi.org/10.47326/ocsat.2021.02.21.2.0

Pardoll, D.M., 1998. Cancer vaccines. Nat. Med. 4, 525–531. https://doi.org/10.1038/nm0598supp-525

Parekh, R.B., Dwek, R.A., Sutton, B.J., Fernandes, D.L., Leung, A., Stanworth, D., Rademacher, T.W., Mizuochi, T., Taniguchi, T., Matsuta, K., Takeuchi, F., Nagano, Y., Miyamoto, T., Kobata, A., 1985. Association of rheumatoid arthritis and primary osteoarthritis with changes in the glycosylation pattern of total serum IgG. Nature 316, 452–457. https://doi.org/10.1038/316452a0

Pasquale, A., Preiss, S., Silva, F., Garçon, N., 2015. Vaccine Adjuvants: from 1920 to 2015 and Beyond. Vaccines 3, 320–343. https://doi.org/10.3390/vaccines3020320

Paus, D., Phan, T.G., Chan, T.D., Gardam, S., Basten, A., Brink, R., 2006. Antigen recognition strength regulates the choice between extrafollicular plasma cell and germinal center B cell differentiation. J. Exp. Med. 203, 1081–1091. https://doi.org/10.1084/jem.20060087

Petrovsky, N., Aguilar, J.C., 2004. Vaccine adjuvants: Current state and future trends. Immunol. Cell Biol. 82, 488–496. https://doi.org/10.1111/j.0818-9641.2004.01272.x

Petrovsky, N., Silva, D., Schatz, D.A., 2003. Vaccine Therapies for the Prevention of Type 1 Diabetes Mellitus: Pediatr. Drugs 5, 575–582. https://doi.org/10.2165/00148581-200305090-00001

Petry, J., Rahmöller, J., Dühring, L., Lilienthal, G.-M., Lehrian, S., Buhre, J.S., Bartsch, Y.C., Epp, A., Lunding, H.B., Moremen, K.W., Leliavski, A., Ehlers, M., 2021. Enriched blood IgG sialylation attenuates IgG-mediated and IgG-controlled-IgE-mediated allergic reactions. J. Allergy Clin. Immunol. 147, 763–767. https://doi.org/10.1016/j.jaci.2020.05.056

Pfeifle, R., Rothe, T., Ipseiz, N., Scherer, H.U., Culemann, S., Harre, U., Ackermann, J.A., Seefried, M., Kleyer, A., Uderhardt, S., Haugg, B., Hueber, A.J., Daum, P., Heidkamp, G.F., Ge, C., Böhm, S., Lux, A., Schuh, W., Magorivska, I., Nandakumar, K.S., Lönnblom, E., Becker, C., Dudziak, D., Wuhrer, M., Rombouts, Y., Koeleman, C.A., Toes, R., Winkler, T.H., Holmdahl, R., Herrmann, M., Blüml, S., Nimmerjahn, F., Schett, G., Krönke, G., 2017. Regulation of autoantibody activity by the IL-23–TH17 axis determines the onset of autoimmune disease. Nat. Immunol. 18, 104–113. https://doi.org/10.1038/ni.3579

Pieper, K., Grimbacher, B., Eibel, H., 2013. B-cell biology and development. J. Allergy Clin. Immunol. 131, 959–971. https://doi.org/10.1016/j.jaci.2013.01.046

Pincetic, A., Bournazos, S., DiLillo, D.J., Maamary, J., Wang, T.T., Dahan, R., Fiebiger, B.-M., Ravetch, J.V., 2014. Type I and type II Fc receptors regulate innate and adaptive immunity. Nat. Immunol. 15, 707–716. https://doi.org/10.1038/ni.2939

Plotkin, S.A., 2005. Vaccines: past, present and future. Nat. Med. 11, S5–S11. https://doi.org/10.1038/nm1209

Polack, F.P., Thomas, S.J., Kitchin, N., Absalon, J., Gurtman, A., Lockhart, S., Perez, J.L., Pérez Marc, G., Moreira, E.D., Zerbini, C., Bailey, R., Swanson, K.A., Roychoudhury, S., Koury, K., Li, P., Kalina, W.V., Cooper, D., Frenck, R.W., Hammitt, L.L., Türeci, Ö., Nell, H., Schaefer, A., Ünal, S., Tresnan, D.B., Mather, S., Dormitzer, P.R., Şahin, U., Jansen, K.U., Gruber, W.C., 2020. Safety and Efficacy of the BNT162b2 mRNA Covid-19 Vaccine. N. Engl. J. Med. 383, 2603–2615. https://doi.org/10.1056/NEJMoa2034577

Porter, R.R., 1973. Structural Studies of Immunoglobulins. Science 180, 713–716.

Pot, C., Jin, H., Awasthi, A., Liu, S.M., Lai, C.-Y., Madan, R., Sharpe, A.H., Karp, C.L., Miaw, S.-C., Ho, I.-C., Kuchroo, V.K., 2009. Cutting Edge: IL-27 Induces the Transcription Factor c-Maf, Cytokine IL-21, and the Costimulatory Receptor ICOS that Coordinately Act Together to Promote Differentiation of IL-10-Producing Tr1 Cells. J. Immunol. 183, 797–801. https://doi.org/10.4049/jimmunol.0901233

Pučić, M., Knežević, A., Vidič, J., Adamczyk, B., Novokmet, M., Polašek, O., Gornik, O., Šupraha-Goreta, S., Wormald, M.R., Redžić, I., Campbell, H., Wright, A., Hastie, N.D., Wilson, J.F., Rudan, I., Wuhrer, M., Rudd, P.M., Josić, D., Lauc, G., 2011. High Throughput Isolation and Glycosylation Analysis of IgG–Variability and Heritability of the IgG Glycome in Three Isolated Human Populations. Mol. Cell. Proteomics 10, M111.010090. https://doi.org/10.1074/mcp.M111.010090

Quast, I., Peschke, B., Lünemann, J.D., 2017. Regulation of antibody effector functions through IgG Fc N-glycosylation. Cell. Mol. Life Sci. 74, 837–847. https://doi.org/10.1007/s00018-016-2366-z

Rashid, H., Khandaker, G., Booy, R., 2012. Vaccination and herd immunity: what more do we know? Curr. Opin. Infect. Dis. 25, 243–249. https://doi.org/10.1097/QCO.0b013e328352f727

Riedel, S., 2005. Edward Jenner and the History of Smallpox and Vaccination. Bayl. Univ. Med. Cent. Proc. 18, 21–25. https://doi.org/10.1080/08998280.2005.11928028

Rombouts, Y., Ewing, E., van de Stadt, L.A., Selman, M.H.J., Trouw, L.A., Deelder, A.M., Huizinga, T.W.J., Wuhrer, M., van Schaardenburg, D., Toes, R.E.M., Scherer, H.U., 2015. Anti-citrullinated protein antibodies acquire a pro-inflammatory Fc glycosylation phenotype prior to the onset of rheumatoid arthritis. Ann. Rheum. Dis. 74, 234–241. https://doi.org/10.1136/annrheumdis-2013-203565

Rook, G.A.W., Steele, J., Brealey, R., Whyte, A., Isenberg, D., Sumar, N., Nelson, J.L., Bodman, K.B., Young, A., Roitt, I.M., Williams, P., Scragg, I., Edge, C.J., Arkwright, P.D., Ashford, D., Wormald, M., Rudd, P., Redman, C.W.G., Dwek, R.A., Rademacher, T.W., 1991. Changes in IgG glycoform levels are associated with remission of arthritis during pregnancy. J. Autoimmun. 4, 779–794. https://doi.org/10.1016/0896-8411(91)90173-A

Rosales, C., Uribe-Querol, E., 2013. Fc receptors: Cell activators of antibody functions. Adv. Biosci. Biotechnol. 04, 21–33. https://doi.org/10.4236/abb.2013.44A004

Sage, P.T., Sharpe, A.H., 2016. T follicular regulatory cells. Immunol. Rev. 271, 246–259. https://doi.org/10.1111/imr.12411

Samuelsson, A., 2001. Anti-inflammatory Activity of IVIG Mediated Through the Inhibitory Fc Receptor. Science 291, 484–486. https://doi.org/10.1126/science.291.5503.484

Selman, M.H.J., Derks, R.J.E., Bondt, A., Palmblad, M., Schoenmaker, B., Koeleman, C.A.M., van de Geijn, F.E., Dolhain, R.J.E.M., Deelder, A.M., Wuhrer, M., 2012. Fc specific IgG glycosylation profiling by robust nano-reverse phase HPLC-MS using a sheath-flow ESI sprayer interface. J. Proteomics 75, 1318–1329. https://doi.org/10.1016/j.jprot.2011.11.003

Shade, K.-T., Anthony, R., 2013. Antibody Glycosylation and Inflammation. Antibodies 2, 392–414. https://doi.org/10.3390/antib2030392

Shenderov, K., Barber, D.L., Mayer-Barber, K.D., Gurcha, S.S., Jankovic, D., Feng, C.G., Oland, S., Hieny, S., Caspar, P., Yamasaki, S., Lin, X., Ting, J.P.-Y., Trinchieri, G., Besra, G.S., Cerundolo, V., Sher, A., 2013. Cord Factor and Peptidoglycan Recapitulate the Th17-Promoting Adjuvant Activity of Mycobacteria through Mincle/CARD9 Signaling and the Inflammasome. J. Immunol. 190, 5722–5730. https://doi.org/10.4049/jimmunol.1203343

Shields, R.L., Lai, J., Keck, R., O'Connell, L.Y., Hong, K., Meng, Y.G., Weikert, S.H.A., Presta, L.G., 2002. Lack of Fucose on Human IgG1 N-Linked Oligosaccharide Improves Binding to Human FcγRIII and Antibody-dependent Cellular Toxicity. J. Biol. Chem. 277, 26733–26740. https://doi.org/10.1074/jbc.M202069200

Shinnakasu, R., Inoue, T., Kometani, K., Moriyama, S., Adachi, Y., Nakayama, M., Takahashi, Y., Fukuyama, H., Okada, T., Kurosaki, T., 2016. Regulated selection of germinal-center cells into the memory B cell compartment. Nat. Immunol. 17, 861–869. https://doi.org/10.1038/ni.3460

Shlomchik, M.J., Luo, W., Weisel, F., 2019. Linking signaling and selection in the germinal center. Immunol. Rev. 288, 49–63. https://doi.org/10.1111/imr.12744

Slifka, M.K., Antia, R., Whitmire, J.K., Ahmed, R., 1998. Humoral Immunity Due to Long-Lived Plasma Cells. Immunity 8, 363–372. https://doi.org/10.1016/S1074-7613(00)80541-5

Snapper, C., Paul, W., 1987. Interferon-gamma and B cell stimulatory factor-1 reciprocally regulate Ig isotype production. Science 236, 944–947. https://doi.org/10.1126/science.3107127

Stavnezer, J., Guikema, J.E.J., Schrader, C.E., 2008. Mechanism and Regulation of Class Switch Recombination. Annu. Rev. Immunol. 26, 261–292. https://doi.org/10.1146/annurev.immunol.26.021607.090248

Steffen, U., Koeleman, C.A., Sokolova, M.V., Bang, H., Kleyer, A., Rech, J., Unterweger, H., Schicht, M., Garreis, F., Hahn, J., Andes, F.T., Hartmann, F., Hahn, M., Mahajan, A., Paulsen, F., Hoffmann, M., Lochnit, G., Muñoz, L.E., Wuhrer, M., Falck, D., Herrmann, M., Schett, G., 2020. IgA subclasses have different effector functions associated with distinct glycosylation profiles. Nat. Commun. 11, 120. https://doi.org/10.1038/s41467-019-13992-8

Tao, M.H., Smith, R.I., Morrison, S.L., 1993. Structural features of human immunoglobulin G that determine isotype-specific differences in complement activation. J. Exp. Med. 178, 661–667. https://doi.org/10.1084/jem.178.2.661

Trbojević Akmačić, I., Ventham, N.T., Theodoratou, E., Vučković, F., Kennedy, N.A., Krištić, J., Nimmo, E.R., Kalla, R., Drummond, H., Štambuk, J., Dunlop, M.G., Novokmet, M., Aulchenko, Y., Gornik, O., Campbell, H., Pučić Baković, M., Satsangi, J., Lauc, G., 2015. Inflammatory Bowel Disease Associates with Proinflammatory Potential of the Immunoglobulin G Glycome: Inflamm. Bowel Dis. 1. https://doi.org/10.1097/MIB.0000000000000372

Vaccari, M., Gordon, S.N., Fourati, S., Schifanella, L., Liyanage, N.P.M., Cameron, M., Keele, B.F., Shen, X., Tomaras, G.D., Billings, E., Rao, M., Chung, A.W., Dowell, K.G., Bailey-Kellogg, C., Brown, E.P., Ackerman, M.E., Vargas-Inchaustegui, D.A., Whitney, S., Doster, M.N., Binello, N., Pegu, P., Montefiori, D.C., Foulds, K., Quinn, D.S., Donaldson, M., Liang, F., Loré, K., Roederer, M., Koup, R.A., McDermott, A., Ma, Z.-M., Miller, C.J., Phan, T.B., Forthal, D.N., Blackburn, M., Caccuri, F., Bissa, M., Ferrari, G., Kalyanaraman, V., Ferrari, M.G., Thompson, D., Robert-Guroff, M., Ratto-Kim, S., Kim, J.H., Michael, N.L., Phogat, S., Barnett, S.W., Tartaglia, J., Venzon, D., Stablein, D.M., Alter, G., Sekaly, R.-P., Franchini, G., 2016. Adjuvant-dependent innate and adaptive immune signatures of risk of SIVmac251 acquisition. Nat. Med. 22, 762–770. https://doi.org/10.1038/nm.4105

van de Geijn, F.E., Wuhrer, M., Selman, M.H., Willemsen, S.P., de Man, Y.A., Deelder, A.M., Hazes, J.M., Dolhain, R.J., 2009. Immunoglobulin G galactosylation and sialylation are associated with pregnancy-induced improvement of rheumatoid arthritis and the postpartum flare: results from a large prospective cohort study. Arthritis Res. Ther. 11, R193. https://doi.org/10.1186/ar2892

Victora, G.D., Nussenzweig, M.C., 2012. Germinal Centers. Annu. Rev. Immunol. 30, 429–457. https://doi.org/10.1146/annurev-immunol-020711-075032

Vidarsson, G., Dekkers, G., Rispens, T., 2014. IgG Subclasses and Allotypes: From Structure to Effector Functions. Front. Immunol. 5. https://doi.org/10.3389/fimmu.2014.00520

Vinuesa, C.G., Linterman, M.A., Yu, D., MacLennan, I.C.M., 2016. Follicular Helper T Cells. Annu. Rev. Immunol. 34, 335–368. https://doi.org/10.1146/annurev-immunol-041015-055605

von Behring, E., Kitasato, S., 1890. Ueber das Zustandekommen der Diphtherie-Immunität und der Tetanus-Immunität bei Thieren. Deutsche Medizinische Wochenschrift 16, 1113–1114. https://doi.org/doi.org/10.17192/eb2013.0164

Vučković, F., Krištić, J., Gudelj, I., Teruel, M., Keser, T., Pezer, M., Pučić-Baković, M., Štambuk, J., Trbojević-Akmačić, I., Barrios, C., Pavić, T., Menni, C., Wang, Y., Zhou, Y., Cui, L., Song, H., Zeng, Q., Guo, X., Pons-Estel, B.A., McKeigue, P., Leslie Patrick, A., Gornik, O., Spector, T.D., Harjaček, M., Alarcon-Riquelme, M., Molokhia, M., Wang, W., Lauc, G., 2015. Association of Systemic Lupus Erythematosus With Decreased Immunosuppressive Potential of the IgG Glycome. Arthritis Rheumatol. 67, 2978–2989. https://doi.org/10.1002/art.39273

Wahl, A., van den Akker, E., Klaric, L., Štambuk, J., Benedetti, E., Plomp, R., Razdorov, G., Trbojević-Akmačić, I., Deelen, J., van Heemst, D., Slagboom, P.E., Vučković, F., Grallert, H., Krumsiek, J., Strauch, K., Peters, A., Meitinger, T., Hayward, C., Wuhrer, M., Beekman, M., Lauc, G., Gieger, C., 2018. Genome-Wide Association Study on Immunoglobulin G Glycosylation Patterns. Front. Immunol. 9, 277. https://doi.org/10.3389/fimmu.2018.00277

Wang, T.T., Maamary, J., Tan, G.S., Bournazos, S., Davis, C.W., Krammer, F., Schlesinger, S.J., Palese, P., Ahmed, R., Ravetch, J.V., 2015. Anti-HA Glycoforms Drive B Cell Affinity Selection and Determine Influenza Vaccine Efficacy. Cell 162, 160–169. https://doi.org/10.1016/j.cell.2015.06.026

WHO, 1980. World Health Organization. The global eradication of smallpox: final report of the Global Commission for the Certification of Smallpox Eradication, Geneva, December 1979.

WHO, W.H.O., 2021. Vaccine-Preventable Diseases (including pipeline vaccines).

Wuhrer, M., Selman, M.H.J., McDonnell, L.A., Kümpfel, T., Derfuss, T., Khademi, M., Olsson, T., Hohlfeld, R., Meinl, E., Krumbholz, M., 2015. Pro-inflammatory pattern

of IgG1 Fc glycosylation in multiple sclerosis cerebrospinal fluid. J. Neuroinflammation 12, 235. https://doi.org/10.1186/s12974-015-0450-1

Ye, P., Rodriguez, F.H., Kanaly, S., Stocking, K.L., Schurr, J., Schwarzenberger, P., Oliver, P., Huang, W., Zhang, P., Zhang, J., Shellito, J.E., Bagby, G.J., Nelson, S., Charrier, K., Peschon, J.J., Kolls, J.K., 2001. Requirement of Interleukin 17 Receptor Signaling for Lung Cxc Chemokine and Granulocyte Colony-Stimulating Factor Expression, Neutrophil Recruitment, and Host Defense. J. Exp. Med. 194, 519–528. https://doi.org/10.1084/jem.194.4.519

Yoshida, H., Hamano, S., Senaldi, G., Covey, T., Faggioni, R., Mu, S., Xia, M., Wakeham, A.C., Nishina, H., Potter, J., Saris, C.J.M., Mak, T.W., 2001. WSX-1 Is Required for the Initiation of Th1 Responses and Resistance to L. major Infection. Immunity 15, 569–578. https://doi.org/10.1016/S1074-7613(01)00206-0

Supplements

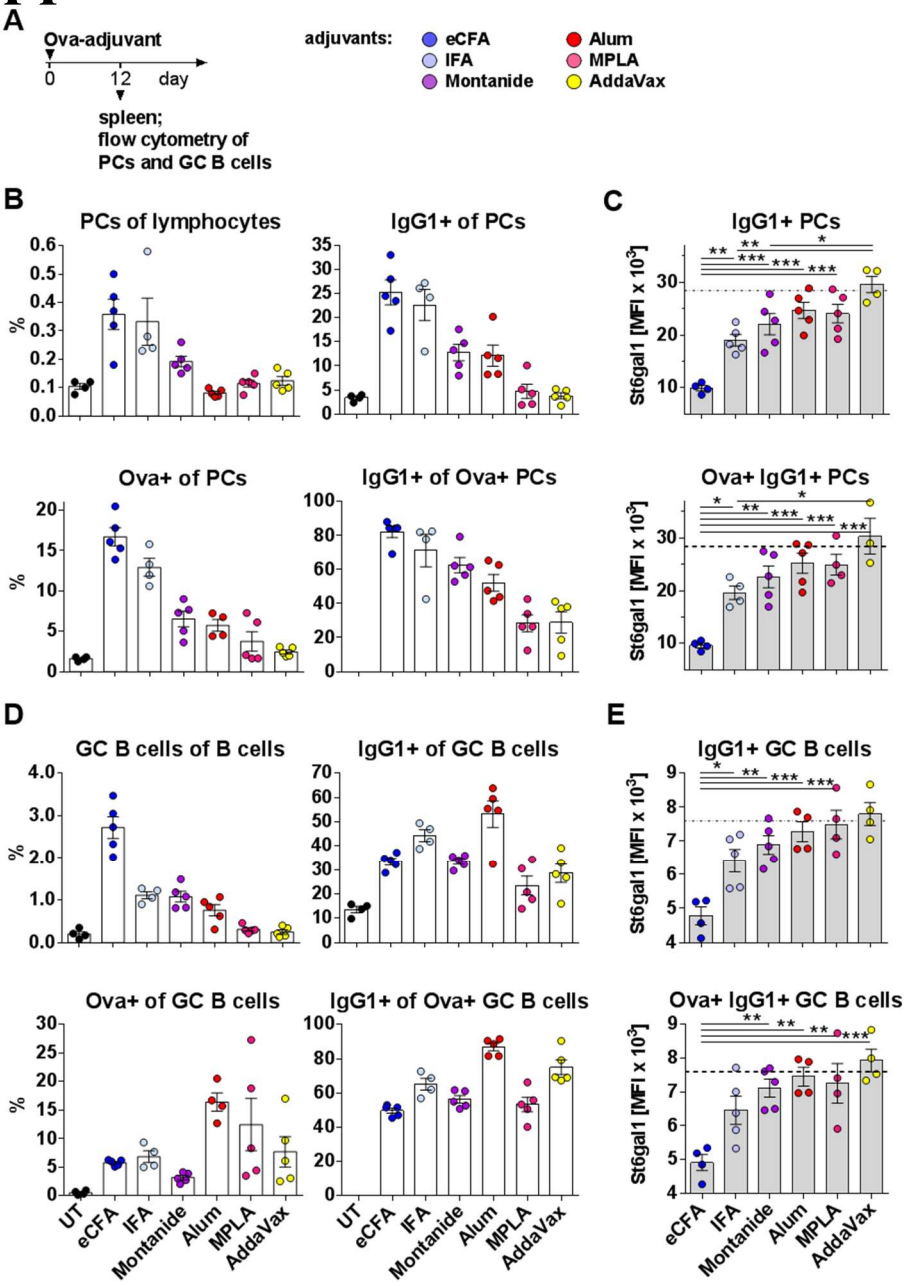

Figure S-1: Different adjuvants induce distinct St6gal1 protein expression levels in splenic antigen-specific IgG1$^+$ PCs as well as GC B cells

(A) Experimental design: C57BL/6 WT female mice were immunized with Ova plus distinct adjuvants and spleens were taken on day 12 for analysis in flow cytometry (n=4-5/group), and the investigated adjuvants with their color code **(B)** Frequencies of splenic PCs, IgG1$^+$ PCs, Ova-specific (Ova$^+$) PCs and Ova$^+$ IgG1$^+$ PCs **(C)** Intracellular St6gal1 protein expression (median fluorescence intensity [MFI]) of IgG1$^+$ PCs and Ova$^+$ IgG1$^+$ PCs. **(D)** Frequencies of splenic GCs, IgG1$^+$ GCs, Ova$^+$ GCs and Ova$^+$ IgG1$^+$ GCs **(C)** Intracellular St6gal1 protein expression (median fluorescence intensity [MFI]) of IgG1$^+$ GCs and Ova$^+$ IgG1$^+$ GCs. Graph points indicate individual mice. Horizontal dashed lines indicate average St6gal1 expression level in IgG1$^+$ PCs or GC B cells of untreated mice. One of two independent experiments is shown. The data presented in this figure were published in Bartsch et al., 2020 (Bartsch et al., 2020).

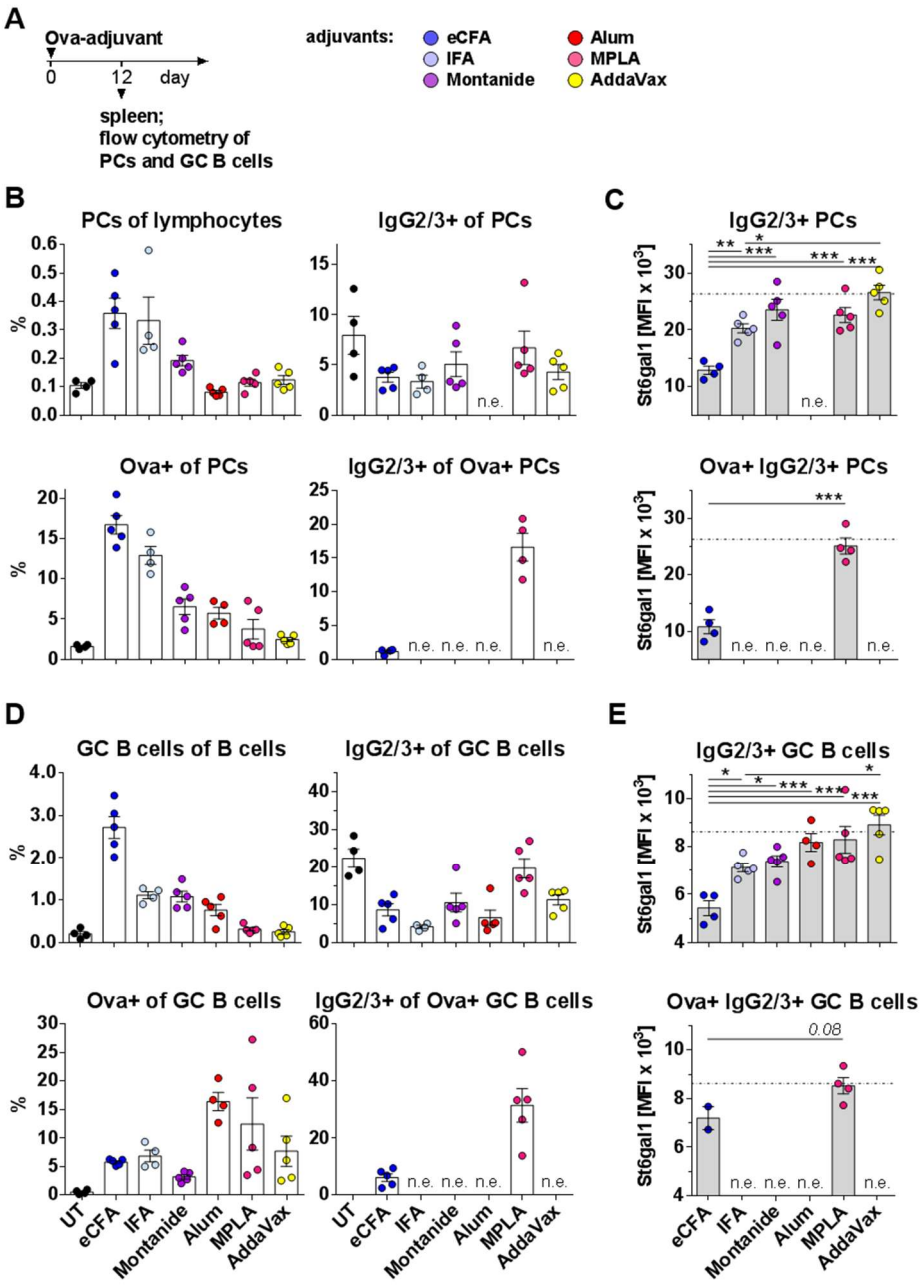

Figure S-2: Different adjuvants induce distinct St6gal1 protein expression levels in splenic antigen-specific IgG2/3$^+$ PCs and GC B cells

(A) Experimental design: C57BL/6 WT female mice were immunized with Ova plus distinct adjuvants and spleens were taken on day 12 for analysis in flow cytometry (n=4-5/group), and the investigated adjuvants with their color code **(B)** Frequencies of splenic PCs, IgG2/3$^+$ PCs, Ova-specific (Ova$^+$) PCs and Ova$^+$ IgG2/3$^+$ PCs **(C)** Intracellular St6gal1 protein expression (median fluorescence intensity [MFI]) of IgG2/3$^+$ PCs and Ova$^+$ IgG2/3$^+$ PCs. **(D)** Frequencies of splenic GCs, IgG2/3$^+$ GCs, Ova$^+$ GCs and Ova$^+$ IgG2/3$^+$ GCs **(C)** Intracellular St6gal1 protein expression (median fluorescence intensity [MFI]) of IgG2/3$^+$ GCs and Ova$^+$ IgG2/3$^+$ GCs. Graph points indicate individual mice. Horizontal dashed lines indicate average St6gal1 expression level in IgG2/3$^+$ PCs or GC B cells of untreated mice. One of two independent experiments is shown. The data presented in this figure were published in Bartsch et al., 2020 (Bartsch et al., 2020).

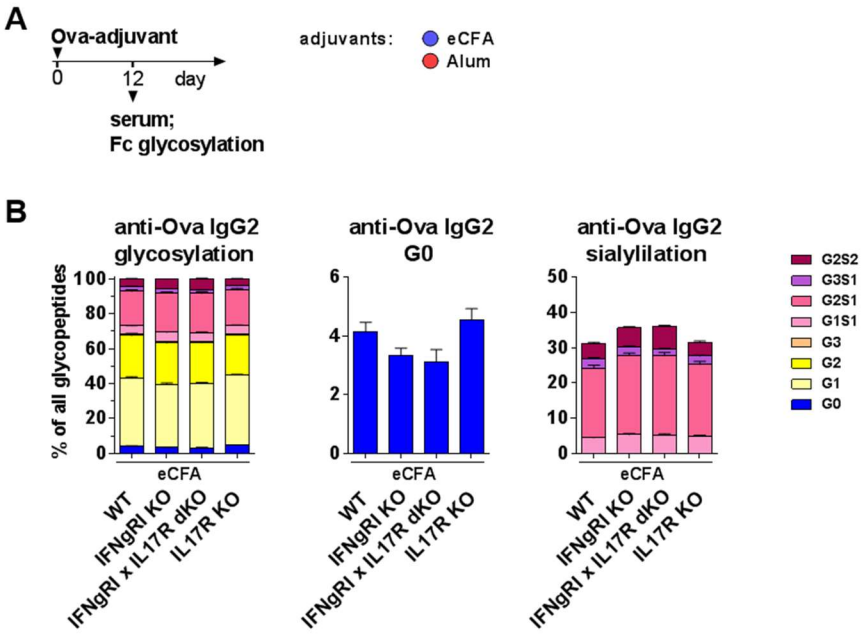

Figure S-3: T_H1 cytokine IFN-γ- and TH17 cytokine IL-17-signaling reduce antigen-specific IgG2 galactosylation and sialylation by tendency

(A) Experimental design: female WT, IFNgRI KO, IL-17R KO and IFNgRI x IL-17R double KO mice on C57BL/6 background were immunized with Ova plus the indicated adjuvants. Serum was analyzed on day 12 in LC-MS (n=3-5/group). **(B)** Serum anti-Ova IgG2 Fc *N*-glycans, agalagtosylation (G0) and sialylation (G1S1 + G2S1 + G3S1 + G2S2). The results from three independent experiments were pooled.

Danksagung

An dieser Stelle möchte ich den Personen danken, die mich auf meinem Weg zur Promotion auf unterschiedliche Weise unterstützt haben.

Ein besonderer Dank geht an meinen Betreuer Marc Ehlers, der es mir ermöglicht hat in seinem Labor zu forschen und meine Doktorarbeit zu absolvieren. Viele Diskussionen über Experimente und deren Ergebnisse, neue Erkenntnisse und neue Ideen haben mich auf Trab gehalten, gefordert, viel gelehrt und wissenschaftlich weitergebracht.

Ein Dank geht an alle Leute, die die für die Experimente notwendigen Mittel, Reagenzien oder Mäuse zur Verfügung gestellt haben, oder mir mit ihren Erfahrungswerten und wissenschaftlichem Rat zur Seite gestanden haben. Dazu gehören Sander Wagt und Manfred Wuhrer von der LUMC, die die Glykoanalysen der Seren durchgeführt haben und somit stark zu dieser Arbeit beigetragen haben. Ebenfalls danke ich meinen Mentoren aus dem GRK1727, besonders Rudolf Manz, für die zusätzlichen Unterstützung.

Ein großer Dank geht an meine ersten Kollegen Yannic Bartsch, Gina Lilienthal und Janina Petry, die mich herzlich aufgenommen haben und geduldig, jedoch immer für einen Spaß zu haben, eingearbeitet haben In diesem Zuge danke ich auch Vanessa Krémer, die neben ihrem Praktikum fleißig bei Experimenten geholfen und so zu dieser Arbeit beigetragen hat.

Ich möchte mich herzlichst bei meinen Kolleginnen Lara Dühring, Selina Lehrian und Jana Buhre bedanken, mit denen ich Frust und Ärger, aber vor allem Erfolg, Fortschritte, interessante Diskussionen, lustige Gespräche, Sonne, Eis und viel Spaß teilen konnte. In diesem Sinne möchte ich auch Bandik Föh danken, der mir im Notfall tatkräftig und mit guter Laune zur Seite stand.

Zum Schluss möchte ich mich bei meinen Freunden und meiner Familie bedanken: Meinen Freunden, die mich von fern oder nah begleiten; meinen Eltern, die mir immer ein sicherer Rückhalt sind und ganz besonders meinen Geschwistern, die mich so stark geprägt haben, gut kennen und auf die ich immer zählen kann.